

PCCP

Accepted Manuscript



This article can be cited before page numbers have been issued, to do this please use: S. Maity, R. I. Kaiser and B. M. Jones, *Phys. Chem. Chem. Phys.*, 2014, DOI: 10.1039/C4CP04149F.



This is an *Accepted Manuscript*, which has been through the Royal Society of Chemistry peer review process and has been accepted for publication.

Accepted Manuscripts are published online shortly after acceptance, before technical editing, formatting and proof reading. Using this free service, authors can make their results available to the community, in citable form, before we publish the edited article. We will replace this *Accepted Manuscript* with the edited and formatted *Advance Article* as soon as it is available.

You can find more information about *Accepted Manuscripts* in the [Information for Authors](#).

Please note that technical editing may introduce minor changes to the text and/or graphics, which may alter content. The journal's standard [Terms & Conditions](#) and the [Ethical guidelines](#) still apply. In no event shall the Royal Society of Chemistry be held responsible for any errors or omissions in this *Accepted Manuscript* or any consequences arising from the use of any information it contains.

**Formation of Complex Organic Molecules in Methanol and Methanol - Carbon Monoxide
Ices Exposed to Ionizing Radiation - A Combined FTIR and Reflectron Time-of-Flight
Mass Spectrometry Study**

Surajit Maity, Ralf I. Kaiser* and Brant M. Jones*

Department of Chemistry

W.M. Keck Research Laboratory in Astrochemistry

University of Hawai'i at Manoa

Honolulu, HI 96822, USA

Abstract

The radiation induced chemical processing of methanol and methanol-carbon monoxide ices at 5.5 K exposed to ionizing radiation in the form energetic electrons and subsequent temperature programmed desorption is reported in this study. The endogenous formation of complex organic molecules was monitored *online* and *in situ* via infrared spectroscopy in the solid state and post irradiation with temperature programmed desorption (TPD) using highly sensitive reflectron time-of-flight (ReTOF) mass spectrometry coupled with single photoionization at 10.49 eV. Following infrared spectroscopic analysis of the processed ice systems resulted in the identification of simple molecules including the hydroxymethyl radical (CH₂OH), formyl radical (HCO), methane (CH₄), formaldehyde (H₂CO), carbon dioxide (CO₂), ethylene glycol (HOCH₂CH₂OH), glycolaldehyde (HOCH₂CHO), methyl formate (HCOOCH₃), and ketene (H₂CCO). In addition, ReTOF mass spectrometry of subliming molecules following temperature program desorption definitely identified several closed shell C/H/O bearing organics including ketene (H₂CCO), acetaldehyde (CH₃COH), ethanol (C₂H₅OH), dimethyl ether (CH₃OCH₃), glyoxal (HCOCOH), glycolaldehyde (HOCH₂CHO), ethene-1,2-diol (HOCHCHOH), ethylene glycol (HOCH₂CH₂OH), methoxy methanol (CH₃OCH₂OH) and glycerol (CH₂OHCHOHCH₂OH) in the processed ice systems. Additionally, an abundant amount of molecules yet to be specifically identified were observed sublimating from the irradiated ices including isomers with formulae: C₃H_(x=4,6,8)O, C₄H_(x=8,10)O, C₃H_(x=4,6,8)O₂, C₄H_(x=6,8)O₂, C₃H_(x=4,6)O₃, C₄H₈O₃, C₄H_(x=4,6,8)O₄, C₅H_(x=6,8)O₄ and C₅H_(x=6,8)O₅. The last groups of molecules containing four to five oxygen atoms observed sublimating from the processed ice samples include astrobiologically important class of sugars; relevant in RNA, phospholipids and energy storage. Experiments are currently being designed to elucidate their chemical structure. In addition, several reaction pathways were identified in the irradiated ices of mixed isotopes based upon the results of both *in situ* FTIR analysis and TPD ReTOF gas phase analysis. In general, the results of this study provide crucial information on the formation of a variety of classes of organics including alcohols, ketones, aldehydes, esters, ethers, and sugars within the bulk ices upon exposure to ionizing radiation that are relevant to the molecular clouds within the interstellar medium.

1. Introduction

During the last decades, cold molecular clouds and star forming regions have been extensively explored for complex organic molecules as these species serve as a 'molecular clock' and thereby aid in an understanding of the chemical evolution of the interstellar medium. In these extreme environments, approximately 60 amongst the currently detected 180 molecules¹ contain six or more atoms with at least one carbon atom and are labelled as complex organic molecules (COMs).^{2, 3} Furthermore, those molecules containing oxygen such as acetaldehyde (CH₃CHO), acetic acid (CH₃COOH), glycolaldehyde (HOCH₂CHO), formamide (HCONH₂), and acetamide (CH₃CONH₂) have received considerable interest from the astrochemistry and astrobiology communities⁴⁻⁶ as these are considered as key precursors and building blocks of biologically important molecules like carbohydrates,⁷ amino acids,⁸ and polypeptides.^{6, 9} The discoveries of several sugar related molecules such as dihydroxyacetone (simple sugar), glycerol (sugar alcohol), and glyceric acid (sugar acid)⁹ along with amino acids^{10, 11} in carbonaceous meteorites such as Murchison encouraged the search for their interstellar origin as is hinted by their isotope ratios.^{12, 13} In addition, glycolaldehyde (the simplest form of a sugar, HOCH₂CHO)¹⁴⁻¹⁸ and ethylene glycol (a sugar alcohol, HOCH₂CH₂OH)^{17, 19, 20} have been detected in distinct astrophysical environments ranging from hot cores to the galactic center molecular clouds. Although searches for higher mass sugars such as glyceraldehyde (HOCH₂CH(OH)CHO)²¹ and 1,3-dihydroxyacetone ((HOCH₂)₂CO)²²⁻²⁴ have been carried out, these molecules have still remained elusive to date.

A current catalogue of observed oxygen bearing complex organic molecules is listed in the supporting information Table S1 along with the locations of their detection and molecular abundances with most of these molecules detected in the Sgr B2(N) hot core. Recently however, Requena-Toress et al. detected several of these molecules in the cold molecular clouds (MC G-0.11-0.08, MC G-0.02-0.07, and MC G+0.69-0.03) within the Galactic Center.^{17, 25} Despite well-established detections of these interstellar molecules, a detailed understanding of the formation pathways has remained elusive. Often, the abundances of complex organics observed toward protostellar cores at temperatures of up to 100 K cannot be explained by networks of gas phase processes via neutral-neutral and/or ion-molecule reactions.^{2, 3, 26} For example, the formation of

complex organic molecules in the gas phase often requires the involvement of an internally (rovibrationally) excited intermediate, which is highly short lived on the picosecond timescale without a third body for collision induced relaxation.² Subsequent models have attempted to boost the production rates of COMs by incorporating grain-surface chemistry, often involving the use of radical-radical reactions on interstellar grains.^{27, 28} In addition, chemical network models attempting to explain the observed abundances of complex organics in the hot molecular core have acknowledged the requirement to include induced suprathermal chemical reactions within icy mantles via UV photons and galactic cosmic rays.²⁹⁻³³ The significance of non-traditional chemistry within the bulk ice is again emphasized based on the relative abundances of COMs in the *cold* Central Molecular Zone and the Galactic Disk, where observations strongly suggest that the COMs are formed in the icy mantles followed by ejection to the gas phase by shock waves.^{17, 25} Further, the fractional abundances of molecules such as methyl formate (HCOOCH₃) and ethanol (C₂H₅OH) in the outflow of L1157 suggest that the time scale for the gas phase synthesis is too short, i.e. less than 2,000 years are required for the formation of these COMs following the proposed reaction network and that these complex molecules were therefore most probably formed in the icy mantles followed with desorption due to outflow shocks.³⁴

Of the many successes from the Infrared Space Observatory^{35, 36} and the Spitzer c2d ice survey,³⁷⁻⁴¹ was the confirmation that interstellar grains are coated with an icy mantle consisting mainly of water (H₂O) followed by methanol (CH₃OH), carbon monoxide (CO), carbon dioxide (CO₂), methane (CH₄) ammonia (NH₃), and formaldehyde (H₂CO) holding a thicknesses of up to a few hundreds of nanometers. The interaction of these ices with energetic ions simulating galactic cosmic rays (GCRs) and with ultraviolet photons (UV) simulating the internal ultraviolet field inside cold molecular clouds has repeatedly been demonstrated to chemically modify ices via non-thermal, non-equilibrium chemistry involving radical reactants such as hydrogen, oxygen, nitrogen, and carbon atoms, which are not in thermal equilibrium with the 10 K ices.⁴²⁻⁴⁷ Therefore, in cold molecular clouds, the interaction of ionizing radiation with ice coated nanoparticles is expected to lead to the synthesis of complex organic molecules, which cannot be explained by classical thermal chemistry.^{2, 3} Once the molecular cloud collapses and transforms to a star-forming region, the elevated temperatures result in a sublimation of these newly formed organic molecules from the grains into the gas phase thereby explaining the abundances of these molecules in the hot cores and corinos. In addition, non-thermal desorption via cosmic ray

particles, grain-grain collisions, and/or shocks may result in the ejection of COMs into the gas phase of the cold cloud cores.^{2,3}

Previous laboratory experiments mimicking interstellar ices exposed to ionizing radiation have provided compelling evidence on the formation of complex organic molecules in the ices at temperatures as low as 5 K. Acetaldehyde for instance has been shown to be formed in methane (CH₄) - carbon monoxide (CO)⁴⁸ and ethylene (C₂H₄) - carbon dioxide (CO₂) ices upon electron irradiation at 10 K thus simulating the effects of secondary electrons within the track of GCRs once penetrating the ice coated interstellar grains.⁴⁹ The thermodynamically less stable C₂H₄O isomers, vinyl alcohol (CH₂CHOH) and ethylene oxide (c-C₂H₄O), were found as well in the ethylene (C₂H₄) - carbon dioxide (CO₂) irradiated ice.⁴⁹ Structural isomers propynal (HCCCHO) and cyclopropenone (c-C₃H₂O) were formed in an icy mixture of acetylene (C₂H₂) and carbon monoxide (CO) at 10 K upon radiolysis.⁵⁰ Additionally, formic acid (HCOOH) and acetic acid (CH₃COOH) were found to be endogenous products in a water (H₂O) – carbon monoxide (CO)⁵¹ and methane (CH₄) – carbon dioxide (CO₂) ices upon exposure to ionizing radiation, respectively.⁵² Following the first detection of glycolaldehyde (HOCH₂CHO) in the galactic center,¹⁴ irradiation experiments with ices consisting of methanol (CH₃OH) and methanol (CH₃OH) - carbon monoxide (CO) were conducted in hopes of explaining the origin of this sugar together with observed isomers i.e., methyl formate (HCOOCH₃) and acetic acid (CH₃COOH) as both methanol (CH₃OH) and carbon monoxide (CO) are the two most abundant species (relative to water) in the interstellar ices.³⁵⁻⁴¹ Indeed, experiments on methanol⁵³ ice and a binary ices of methanol and carbon monoxide⁵⁴ exposed to ionizing radiation resulted in the identification of glycolaldehyde (HOCH₂CHO), methyl formate (HCOOCH₃), and ethylene glycol (HOCH₂CH₂OH) in addition to the formyl radical (HCO), hydroxyl radical (OH), methane (CH₄), carbon dioxide (CO₂), and formaldehyde (H₂CO) at 10 K. Similar work was conducted utilizing broad band UV photons produced via a hydrogen microwave discharge lamp and found evidence of methyl formate (HCOOCH₃) and glycolaldehyde (HOCH₂CHO) as a potential products post photolysis of methanol (CH₃OH) and mixtures with carbon monoxide (CO);⁵⁵ a subsequent study on UV processed methanol and methanol-carbon monoxide ices identified methyl formate (HCOOCH₃), ethylene glycol (HOCH₂CH₂OH), ethanol (C₂H₅OH), and dimethyl ether (CH₃OCH₃)⁵⁶ Methoxymethanol (CH₃OCH₂OH) was first identified in the exposure of methanol (CH₃OH) ices to low energy electron and later confirmed along with other

COMs such as ethylene glycol (HOCH₂CH₂OH), glycolaldehyde (HOCH₂CHO), and possibly glycolic acid (HOCOCH₂OH).⁵⁷ Additional experiments via 200 keV proton bombardment upon frozen methanol (CH₃OH) and mixtures with carbon monoxide (CO) resulted once again in the identification of glycolaldehyde (HOCH₂CHO),^{58, 59} methyl formate (HCOOCH₃)^{58, 59} and ethylene glycol (HOCH₂CH₂OH).⁵⁹ Chen et al. reported formation of diemthylether (CH₃OCH₃) glycolaldehyde (HOCH₂CHO), methyl formate (HCOOCH₃), acetic acid (CH₃COOH), and ethylene glycol (HOCH₂CH₂OH) in irradiated methanol ices using soft X-rays containing peak energies of 300 eV and 550 eV over a broad band spectrum (250-1200 eV).⁶⁰ To summarize, multiple experiments have been conducted over the last decades regarding the chemical modification of methanol ices upon exposure to ionizing radiation simulating astrophysical conditions. Within these studies, a consensus on the formation of small molecules e.g., carbon monoxide (CO), carbon dioxide (CO₂), formaldehyde (H₂CO), methane (CH₄) and for the most part ethanol (C₂H₅OH), glycolaldehyde (HOCH₂CHO), ethylene glycol (HOCH₂CH₂OH), methyl formate (HCOOCH₃), and acetic acid (CH₃COOH) have been ascertained via *in situ* infrared spectroscopy. Unfortunately, relying only on this technique can lead often to ambiguous assignments of large organics with similar functional groups due to the overlap of their group frequencies, in particular of the important carbonyl group.

Recently, utilizing single photoionization reflectron time-of-flight (ReTOF-PI) mass spectrometry in addition to solid state FTIR spectroscopy, significant progress has been made toward a detailed understanding of several key classes of complex organic molecules carrying the carbonyl functional group.^{61, 62} Moreover, we have reported on the detection of glycolaldehyde (HOCH₂CHO) in irradiated methanol and methanol-carbon monoxide ices exposed to energetic electrons via ReTOF-PI mass spectrometry.⁶³ The continued success of ReTOF-PI mass spectrometry approach in identifying astrochemically relevant complex organics synthesized in simple ices of methanol and methanol-carbon monoxide is explored here. In this study, we present compelling evidence on the formation of key classes of complex organic molecules synthesized in irradiated ices of methanol (CH₃OH) and methanol (CH₃OH) – carbon monoxide (CO) from infrared spectral data correlated with temperature program desorption (TPD) studies exploiting ReTOF-PI gas phase detection at doses relevant to the lifetime of an interstellar icy grain within a cold molecular cloud prior to the warm up (star formation) phase.

2. Experimental

The experiments were carried out in a novel, contamination-free ultra-high vacuum (UHV) chamber at the W.M. Keck Research Laboratory in Astrochemistry. A detailed description of the instrumentation has been described previously.⁶¹⁻⁶⁴ Briefly, the main chamber is evacuated down to a base pressure of a few 10^{-11} torr by oil-free magnetically suspended turbomolecular pumps backed with dry scroll pumps. A closed-cycle helium refrigerator (Sumitomo Heavy Industries, RDK-415E) cools a polished silver substrate mounted to the cold finger to final temperature of 5.5 ± 0.1 K. The entire cold finger assembly is freely rotatable within the horizontal center plane and translatable in the vertical direction via an UHV compatible bellow (McAllister, BLT106) and a differential pumped rotational feed through (Thermoionics Vacuum Products, RNN-600/FA/MCO). The corresponding gases (methanol vapor and premixed methanol-carbon monoxide gas) were then deposited through a glass capillary array with a background pressure reading in the main chamber of about 5×10^{-8} torr for approximately 3 minutes. This yielded ice samples with thicknesses of 510 ± 10 nm for pristine methanol ices and 495 ± 10 nm for mixed ices of methanol-carbon monoxide. The thickness of the samples was determined *in situ* using laser interferometry^{65, 66} with a helium-neon (HeNe) laser (CVI Melles-Griot, 25-LHP-213) at 632.8 nm at an incident angle of 4° . From this technique, based upon the ratios of peak to peak intensities,⁶⁷ we derived an index of refraction $n_f = 1.34 \pm 0.02$ for pure methanol, in agreement with published data of 1.35,⁶⁸ and $n_f = 1.35 \pm 0.02$ for the binary $\text{CH}_3\text{OH-CO}$ mixture.

In order to determine the ratios of the components in the methanol – carbon monoxide ices, additional calibration experiments were performed. Here, methanol ices with distinct thicknesses were deposited under identical experimental conditions. Subsequently, the ices were annealed at 0.5 K min^{-1} allowing the ices to sublime with gas phase molecules monitored using a quadrupole mass spectrometer (QMS; Extrel, Model 5221) operated as a residual gas analyzer exploiting electron impact ionization with 100 eV electrons at a current of 1 mA. The resultant total QMS signal at $m/z = 32$ amu (CH_3OH^+) was then integrated and correlated as a function of the deposited molecules determined from the ice thicknesses and known density of the pure methanol samples. As such, we can determine the total number of methanol molecules in the mixed ices of methanol-carbon monoxide by comparing the QMS ion signal at $m/z = 32$ amu with the calibration curve. Here, a total of $(4.6 \pm 0.5) \times 10^{17}$ methanol molecules were

determined; this results in a thickness of 240 ± 20 nm. In the limit of volume additivity,⁶⁹ we can calculate a thickness of (255 ± 30) nm for carbon monoxide by subtracting the methanol thickness (240 ± 20 nm) from total thickness resulting in an estimated value of $(6.3 \pm 0.6) \times 10^{17}$ carbon monoxide molecules. Consequently, the mixed methanol-carbon monoxide ice was found to be in the ratio of $(4.0 \pm 0.2) : (5.0 \pm 0.2)$. Here, the densities of methanol and carbon monoxide ices were used as 1.020 g cm^{-3} , 1.029 g cm^{-3} , respectively.⁵⁴ In addition, isotopically labeled CD_3OD , $^{13}\text{CH}_3\text{OH}$, and $\text{CH}_3^{18}\text{OH}$ ices (Sigma-Aldrich) for pure methanol irradiation experiments and $\text{CD}_3\text{OD-CO}$, $^{13}\text{CH}_3\text{OH-CO}$, $\text{CH}_3^{18}\text{OH-CO}$, $\text{CD}_3\text{OD-}^{13}\text{CO}$, $\text{CH}_3^{18}\text{OH-C}^{18}\text{O}$, and $\text{CH}_3\text{OH-C}^{18}\text{O}$ (labelled CO was supplied by Cambridge Isotope Labs) mixed ices for methanol-carbon monoxide irradiation experiments were also conducted to confirm the identified products via isotope shifts of the infrared absorption bands and in the reflectron time-of-flight data.

The ice systems were then irradiated with 5 keV electrons isothermally at 5.5 ± 0.1 K for one hour at 30 nA over an area of $1.0 \pm 0.1 \text{ cm}^2$ and an angle of incidence of 70° relative to the surface normal of the ice. The total dose deposited into the ice sample was determined from Monte Carlo simulations (CASINO)^{70, 71} taking into consideration the back scattering coefficient, the energy deposited from the back scattered electrons, and the average penetration depth (SI Table S2). The total energy deposited into the ice was 6.5 ± 0.8 eV per CH_3OH molecule, and 5.2 ± 0.8 eV per molecule on average for the irradiation experiments of the binary $\text{CH}_3\text{OH-CO}$ (4:5) ice mixture. It should be noted here, that in determining the applied dose of the isotopic analogs, that both the index of refraction and density were assumed to be that their respective normal counterparts as most of these data are not empirically available. Furthermore, the density of the $\text{CH}_3\text{OH-CO}$ ice mixture was calculated as 1.026 g cm^{-3} based on the weighted fraction of their respective pure densities.⁶⁹

For the *on line* and *in situ* identification of new molecular band carriers of the ices during irradiation, a Fourier transform infrared spectrometer (Nicolet 6700) monitored the samples throughout the duration of the experiment with an IR spectrum collected every two minutes in the range of $6000 - 400 \text{ cm}^{-1}$ at a resolution of 4 cm^{-1} . Each FTIR spectrum was recorded in absorption–reflection–absorption mode (reflection angle of 45°) for two minutes resulting in a set of 30 infrared spectra during the radiation exposure (one hour) for each system. After the irradiation, the sample was kept at 5.5 K for one hour; then, temperature programmed desorption

(TPD) studies were conducted by heating the irradiated ices at a rate of 0.5 K min^{-1} to 300 K. Throughout the thermal sublimation process, the ice samples were monitored via infrared spectroscopy and single photon ionization reflectron time-of-flight mass spectrometry^{61, 62} separately. The products were ionized upon sublimation via *single photon ionization* exploiting pulsed (30 Hz) coherent vacuum ultraviolet (VUV) light at 118.2 nm (10.49 eV). Here, the third harmonic (354.6 nm) of a high-power pulsed Nd:YAG laser (Spectra Physics, PRO – 250; 30 mJ per pulse) was frequency tripled to produce VUV photons utilizing xenon (Xe) gas as the nonlinear medium.⁷² A pulsed valve directed the xenon gas (99.999 %; Specialty Gases of America) at a backing pressure of 1266 Torr into a T-shaped stainless steel adapter with 1 mm diameter hole and 25 mm in length in line with the propagating laser beam. The generated VUV light was then separated and directed to about 1 mm above the ice surface utilizing an off-axis, differentially pumped lithium fluoride (LiF) lens,⁷³ where the sublimating molecules are then photoionized. The molecular ions were detected utilizing a multichannel plate with a dual chevron configuration following a fast preamplifier (Ortec 9306) and shaped with a 100 MHz discriminator (Advanced Research Instruments, F-100TD). The ReTOF spectra were then recorded with a personal-computer-based multichannel scaler (FAST ComTec, P7888-1 E) using a bin width of 4 ns, triggered at 30 Hz with 3600 sweeps per mass spectrum reflecting a 1 K change in temperature. Additionally, the sublimating molecules were also probed via a quadrupole mass spectrometer (Extrel, Model 5221) operating in a residual-gas analyzer mode in the mass range of 1 – 500 amu with electron impact ionization of 100 eV and an emission current of 1 mA.

To assist in the identification of a specific molecules sublimating in the temperature program desorption spectra utilizing ReTOF-PI mass spectrometry, calibration experiments were performed under identical experimental conditions and annealing rates. Here, the vapor of a specific molecule was premixed in pure methanol and/or methanol-carbon monoxide and subsequently deposited onto the substrate kept at 5.5 K. Then, TPD was conducted by heating the premixed ices at the same rate of 0.5 K min^{-1} up to 300 K and subsequently detected using ReTOF-PI mass spectrometry. In summary, a total of 12 calibration experiments was performed with 17 different molecules in both methanol and methanol-carbon monoxide ices. The details of the calibration samples and the relative percent amount in the premixed ices are listed in SI Table S3.

3. Results

3.1. Infrared Spectroscopy

The infrared spectra of the isotopologue ice systems of methanol (CH_3OH , CD_3OD , $^{13}\text{CH}_3\text{OH}$ and $\text{CH}_3^{18}\text{OH}$) and mixed ice systems of methanol-carbon monoxide ($\text{CH}_3\text{OH-CO}$, $\text{CD}_3\text{OD-CO}$, $\text{CH}_3^{18}\text{OH-C}^{18}\text{O}$, $^{13}\text{CH}_3\text{OH-CO}$, $\text{CD}_3\text{OD-}^{13}\text{CO}$, $\text{CH}_3^{18}\text{OH-CO}$ and $\text{CH}_3\text{OH-C}^{18}\text{O}$) recorded before and after the irradiation are shown in Figures 1A and 1B as well as in SI Figure S1, respectively. The newly formed products are also shown in the 2200 - 1600 cm^{-1} and 1400 - 800 cm^{-1} regions of interest along with assignments. Infrared absorption features of the pristine ices and new absorption features that emerged following irradiation are summarized in Table 1 and Table 2, respectively. Upon exposure to ionizing radiation several products were observed *in situ* within the bulk ice. Here, in both the methanol and the mixed methanol-carbon monoxide ices the hydroxymethyl radical (CH_2OH) was identified via the ν_4 fundamental at 1192 cm^{-1} and 1193 cm^{-1} , respectively; the formyl radical (HCO) was gauged from the ν_3 fundamental at 1842 cm^{-1} in both irradiated ices; methane (CH_4) was detected via the ν_4 fundamental at 1304 cm^{-1} and 1303 cm^{-1} . Formation of formaldehyde (H_2CO) was confirmed from the ν_2 , ν_3 , and ν_4 fundamentals at 1246 cm^{-1} , 1499 cm^{-1} and 1726 cm^{-1} in irradiated CH_3OH ices and at 1249 cm^{-1} , 1497 cm^{-1} , and 1726 cm^{-1} in the irradiated $\text{CH}_3\text{OH-CO}$ ices. These absorption frequencies are in agreement with previous studies.^{53-55, 60, 74} Formation of carbon monoxide (CO) was confirmed via the ν_1 fundamental at 2135 cm^{-1} in the irradiated CH_3OH ice systems. Carbon dioxide (CO_2) was as well observed in both the irradiated CH_3OH and mixed $\text{CH}_3\text{OH-CO}$ ices as confirmed by the ν_3 band at 2339 cm^{-1} and 2342 cm^{-1} , respectively. Ethylene glycol ($\text{HOCH}_2\text{CH}_2\text{OH}$) was identified in both the irradiated ices via the ν_9 fundamental at 1094 cm^{-1} based on the assignment of this molecule in previous studies of irradiated methanol ices^{53, 74} at 1090 cm^{-1} and 1088 cm^{-1} . Note that all other relatively stronger infrared absorption bands of ethylene glycol coincidentally overlap with the methanol absorptions^{53, 54} and therefore are masked. The assignments of these absorptions were also confirmed via their isotopic shifts in irradiated ices consisting of CD_3OD , $^{13}\text{CH}_3\text{OH}$, $\text{CH}_3^{18}\text{OH}$ and irradiated binary mixed ices consisting of $\text{CD}_3\text{OD-CO}$, $\text{CH}_3^{18}\text{OH-C}^{18}\text{O}$, $^{13}\text{CH}_3\text{OH-CO}$, $\text{CD}_3\text{OD-}^{13}\text{CO}$, $\text{CH}_3^{18}\text{OH-CO}$ and $\text{CH}_3\text{OH-C}^{18}\text{O}$ as compiled in Table 2. We have also identified ketene (H_2CCO) in $^{13}\text{CH}_3\text{OH}$ and $\text{CH}_3^{18}\text{OH}$ ices via the observation of ν_2 fundamental at 2067 cm^{-1} ($\text{H}_2^{13}\text{C}^{13}\text{CO}$) and 2107 cm^{-1} ($\text{H}_2\text{CC}^{18}\text{O}$), respectively, as shown in Figure 1A. The assignment of ketene agrees with previously reported observations of the ν_2

fundamental at 2071 cm^{-1} for $\text{H}_2^{13}\text{C}^{13}\text{CO}$ and 2107 cm^{-1} for $\text{H}_2\text{CC}^{18}\text{O}$, respectively.^{64, 75} In the case of methanol-carbon monoxide ices, ν_2 absorption features of ketene were also identified at 2107 cm^{-1} ($\text{H}_2\text{CC}^{18}\text{O}$) in $\text{CH}_3^{18}\text{OH-C}^{18}\text{O}$ ice and at 2106 cm^{-1} ($\text{H}_2\text{CC}^{18}\text{O}$) in $\text{CH}_3\text{OH-C}^{18}\text{O}$ ice in agreement with the literature values.^{64, 75} Note that only isotopologues of ketene are observed as the absorption features of the natural H_2CCO isotopomer and the ν_1 absorption band of carbon monoxide directly overlap at $\sim 2135\text{ cm}^{-1}$.

3.1.1. Infrared Absorption Spectra of the Carbonyl Functional Group

The new absorption features connected to the carbonyl functional group in the $1800\text{--}1600\text{ cm}^{-1}$ region deserve special attention. These bands are very broad (Figure 1C and 1D) and subsequent assignment to only one molecular carrier is erroneous. Further evidence suggesting more than one molecular carrier to this functional group is gained from the additional infrared absorption features of the carbonyl band regions in the irradiated mixed isotopic ice systems of methanol-carbon monoxide ($^{13}\text{CH}_3\text{OH-CO}$, $\text{CD}_3\text{OD-}^{13}\text{CO}$, $\text{CH}_3^{18}\text{OH-CO}$ and $\text{CH}_3\text{OH-C}^{18}\text{O}$) as shown in Figure 1D. Therefore, a deconvolution to the absorption features in $1800\text{--}1600\text{ cm}^{-1}$ region was performed with the peak positions and their associated assignments shown in Figure 1 part C and D, and listed in Tables 2 and 3. In both the irradiated ices of methanol (CH_3OH) and methanol-carbon monoxide ($\text{CH}_3\text{OH-CO}$), the deconvolution identified four distinct bands centered at 1743 cm^{-1} , 1726 cm^{-1} , 1714 cm^{-1} , and 1697 cm^{-1} . The band at 1743 cm^{-1} has been assigned to the ν_{14} band of glycolaldehyde (HOCH_2CHO) based on previous identification of this molecule within irradiated methanol ices at 1747 cm^{-1} ,⁵³ irradiated methanol-carbon monoxide ices at 1757 cm^{-1} ,⁵⁴ and matrix isolation studies of glycolaldehyde at 1747 cm^{-1} .^{76, 77} The band at 1714 cm^{-1} was assigned to the ν_{14} fundamental of methyl formate (HCOOCH_3); in agreement to previous electron irradiation experiments of methanol and methanol-carbon monoxide ices,^{53, 54} UV photolysis of methanol ices,⁵⁵ and with pure frozen methyl formate at 16 K .^{58, 59} The absorption at 1726 cm^{-1} has been assigned to the ν_4 fundamental of formaldehyde (H_2CO) again, based on previous literature values.^{53-55, 58, 59} Finally, the band observed at 1697 cm^{-1} can be attributed to the Fermi resonance splitting of the ν_{14} fundamental and the $2\nu_6$ overtone band of glycolaldehyde.^{54, 60, 77} Further support for the above assignments is gained through observation of the frequency shifts in the infrared absorption features of the isotopically labeled ices of

CD_3OD , $^{13}\text{CH}_3\text{OH}$, and $\text{CH}_3^{18}\text{OH}$ and in the binary ices of $\text{CD}_3\text{OD-CO}$, $\text{CH}_3^{18}\text{OH-C}^{18}\text{O}$, $^{13}\text{CH}_3\text{OH-CO}$, $\text{CD}_3\text{OD-}^{13}\text{CO}$, $\text{CH}_3^{18}\text{OH-CO}$ and $\text{CH}_3\text{OH-C}^{18}\text{O}$ as compiled in Table 3.

Recently, we have reported on the formation of a series of saturated and unsaturated aldehyde/ ketones identified in methane-carbon monoxide ices exposed to ionizing radiation.⁶¹ As both irradiated ices in the present study reveal broad complex structure associated with the carbonyl stretching mode, we present a comparison of the deconvoluted band positions in: (i) the pertinent regions observed in the present experiments and (ii) the carbonyl stretching vibrations of the methane-carbon monoxide ices in Table 3. The infrared absorption due to the ν_4 fundamental (CO stretching) of formaldehyde (H_2CO) in both CH_3OH and $\text{CH}_3\text{OH-CO}$ ices were observed at 1726 cm^{-1} . Acetaldehyde (CH_3CHO) was attributed to the band (ν_4) at 1727 cm^{-1} in irradiated $\text{CH}_4\text{-CO}$ ices;⁶¹ as such, acetaldehyde may contribute to the observed band at 1726 cm^{-1} here as well. Further support for the assignment of acetaldehyde stems from the identification of the ν_4 fundamental of the isotopically labeled acetaldehyde in both the irradiated isotopologue methanol and mixed methanol-carbon monoxide ices. Here, deuterated acetaldehyde (CD_3CDO) was previously observed at 1715 cm^{-1} ⁶¹ and therefore contributes to the infrared absorption bands witnessed here at 1711 cm^{-1} in irradiated CD_3OD and at 1714 cm^{-1} in irradiated $\text{CD}_3\text{OD-CO}$ ices. In addition, acetaldehyde isotopomer ($\text{CH}_3\text{CH}^{18}\text{O}$) was previously assigned at 1694 cm^{-1} ⁶¹ and consequently was attributed to the observed bands at 1693 cm^{-1} , 1693 cm^{-1} , 1692 cm^{-1} and 1695 cm^{-1} in the processed $\text{CH}_3^{18}\text{OH}$, $\text{CH}_3^{18}\text{OH-C}^{18}\text{O}$, $\text{CH}_3^{18}\text{OH-CO}$ and $\text{CH}_3\text{OH-C}^{18}\text{O}$ ices respectively, as well. Further, following irradiation of the ^{18}O isotopically mixed ices, $\text{CH}_3^{18}\text{OH-CO}$ and $\text{CH}_3\text{OH-C}^{18}\text{O}$, evidence suggesting the formation of two acetaldehyde isotopomers (CH_3CHO and $\text{CH}_3\text{CH}^{18}\text{O}$) is found in the observed bands at 1724 cm^{-1} and 1694 cm^{-1} , respectively. Further evidence on the formation of acetaldehyde is also confirmed using ReTOF mass spectrometry following TPD studies as discussed below (Section 3.2.).

Glycolaldehyde (HOCH_2CHO) is observed at 1743 cm^{-1} (ν_{14}) in both irradiated CH_3OH and mixed $\text{CH}_3\text{OH-CO}$ ices. However, the infrared absorption band at 1743 cm^{-1} may also have contribution from saturated aldehydes such as propanal ($\text{CH}_3\text{CH}_2\text{CHO}$) and butanal ($\text{C}_3\text{H}_7\text{CHO}$), as the carbonyl stretching mode of these molecules has been attributed previously at 1746 cm^{-1} as well.⁶¹ Further evidence in support of saturated aldehydes contributing to this carbonyl band again stems from the isotopically labeled irradiated ices and the assignments of the deconvoluted

bands of the corresponding carbonyl stretching region (Table 3). Here, the ^{18}O isotope labeled saturated aldehydes (RCH^{18}O) were observed at 1717 cm^{-1} in the irradiated methane-carbon monoxide ices as previously reported,⁶¹ and therefore may contribute here to the ν_{14} of glycolaldehyde ($\text{HOCH}_2\text{CH}^{18}\text{O}$) observed at 1713 cm^{-1} in $\text{CH}_3^{18}\text{OH}$, 1715 cm^{-1} in $\text{CH}_3^{18}\text{OH-C}^{18}\text{O}$, 1708 cm^{-1} in $\text{CH}_3^{18}\text{OH-CO}$ and 1707 cm^{-1} in $\text{CH}_3\text{OH-C}^{18}\text{O}$ ices. Similarly, the ν_{14} fundamental of methyl formate (HCOOCH_3) observed at 1714 cm^{-1} in both the irradiated CH_3OH and $\text{CH}_3\text{OH-CO}$ ices can also have contribution from saturated ketones (1717 cm^{-1}) e.g. acetone (CH_3COCH_3) and butanone ($\text{C}_2\text{H}_5\text{COCH}_3$). Here, the carbonyl absorption band of ^{18}O labeled saturated ketones (1683 cm^{-1}) was also identified in the isotopically labeled irradiated ices of $\text{CH}_3^{18}\text{OH}$ (1682 cm^{-1}), $\text{CH}_3^{18}\text{OH-C}^{18}\text{O}$ (1680 cm^{-1}), $\text{CH}_3^{18}\text{OH-CO}$ (1680 cm^{-1}) and $\text{CH}_3\text{OH-C}^{18}\text{O}$ (1684 cm^{-1}), (Table 3). In summary, we wish to stress that FTIR spectroscopy can only elucidate particular vibrational modes of complex organics synthesized *in situ* of bulk ices from exposure to ionizing radiation and very rarely, actual molecular isomers. Consequently, we then turn our attention to a more sensitive technique allowing for the identification of *individual molecules* via their molecular formula, temperature program desorption coupled with single photoionization reflectron time-of-flight mass spectrometry.

3.2. Reflectron Time-of-Flight Mass Spectra

Following the *in situ* identification of small molecules and vibrational modes of more complex organics as described above, we employed the use of temperature programmed desorption (TPD) to monitor the products sublimating via ReTOF-PI mass spectrometry. The full product spectrum of processed methanol and methanol-carbon monoxide isotopologue ices are displayed in Figure 2A and Figure 2B, respectively, as a function of temperature during the post-irradiation warm-up stage. In the case of methanol ice, molecules with a mass-to-charge ratio (m/z) up to 90 amu are observed (Figure 2A). However, in the case of methanol-carbon monoxide ices, large molecules up to 150 amu are observed (Figure 2B). This observation alone implies the presence of rich and complex chemistry in the mixed methanol-carbon monoxide ices compared pure methanol ices despite the similar doses deposited into both systems.

Products identified utilizing ReTOF mass spectrometry following photoionization at $E_{\text{hv}} = 10.49\text{ eV}$ are described below for the irradiated methanol and mixed methanol-carbon monoxide ices, respectively. Here, the detected products in the methanol ice are also observed in the irradiated

methanol-carbon monoxide system. The corresponding mass-to-charge ratios (m/z) of the identified products and their isotopomers are listed in Tables 4A and 4B. Note that in the methanol (CH_3OH , CD_3OD , $^{13}\text{CH}_3\text{OH}$ and $\text{CH}_3^{18}\text{OH}$) ices, only one isotope of each element is present and thus only one isotopic mass for each product are observed as expected. As an example, $\text{C}_2\text{H}_4\text{O}$ isotopomers were detected at $m/z = 44$ amu ($\text{C}_2\text{H}_4\text{O}$), 48 amu ($\text{C}_2\text{D}_4\text{O}$), 46 amu ($^{13}\text{C}_2\text{H}_4\text{O}$) and 46 amu ($\text{C}_2\text{H}_4^{18}\text{O}$) in the exposed CH_3OH , CD_3OD , $^{13}\text{CH}_3\text{OH}$ and $\text{CH}_3^{18}\text{OH}$ systems, respectively. Similarly, in the mixed isotopically pure methanol-carbon monoxide ices, e.g. $\text{CH}_3\text{OH-CO}$, $\text{CD}_3\text{OD-CO}$, and $\text{CH}_3^{18}\text{OH-C}^{18}\text{O}$ only one isotopomer of each product is detected. However, in the case isotopically mixed ices such as $^{13}\text{CH}_3\text{OH-CO}$, $\text{CD}_3\text{OD-}^{13}\text{CO}$, $\text{CH}_3^{18}\text{OH-CO}$ and $\text{CH}_3\text{OH-C}^{18}\text{O}$, several isotopomers corresponding to one molecular formula are observed (Table 4B). Again for the sake of clarity, consider the three distinct $\text{C}_2\text{H}_4\text{O}$ isomers that were observed in $^{13}\text{CH}_3\text{OH-CO}$ processed ice; here at, $m/z = 44$ amu ($\text{C}_2\text{H}_4\text{O}$), 45 amu ($^{13}\text{CCH}_4\text{O}$), and 46 amu ($^{13}\text{C}_2\text{H}_4\text{O}$).

Furthermore, we should mention here that several mass peaks were observed simultaneously at about 124 K, 145 K and 203 K as can be seen in Figures 2A and 2B in both irradiated methanol and methanol-carbon monoxide isotopologue ices. Note for the simplicity that the uncertainty associated with peak sublimation temperatures is ± 2 K, unless otherwise noted. For example, the sublimation of mass-to-charge ratios corresponding to $\text{C}_2\text{H}_2\text{O}$, $\text{C}_2\text{H}_4\text{O}$, $\text{C}_2\text{H}_6\text{O}$, $\text{C}_3\text{H}_6\text{O}$, $\text{C}_3\text{H}_8\text{O}$ are all observed at 124 K in both irradiated methanol and methanol-carbon monoxide ices. The above observations are indication of either co-sublimation of several different products at a specific temperature and/or fragmentation of a high mass organic from photoionization. During the warm-up phase, the amorphous ices of methanol experiences a phase change within temperature range 100-125 K as reported earlier^{53, 63, 78, 79} and may trigger the sublimation of the products formed via a ‘molecular volcano’ process as reported before with frozen amorphous water⁸⁰ resulting in the observation of several products with identical sublimation temperatures of 124 K. Further, peak methanol sublimation occurs at 145 K in both irradiated methanol and methanol-carbon monoxide ice systems. As such, the observed sublimation of $\text{C}_2\text{H}_4\text{O}$, $\text{C}_3\text{H}_6\text{O}$, $\text{C}_4\text{H}_8\text{O}$, $\text{C}_2\text{H}_6\text{O}$, $\text{C}_3\text{H}_8\text{O}$ and $\text{C}_2\text{H}_2\text{O}_2$ at 145 K can be correlated to the co-sublimation with methanol molecules. Similarly, the sublimation of a group of products peaking at 203 K is correlated with co-sublimation of ethylene glycol (formed in the radiolysis process). A detailed discussion of these products is discussed in the following sections.

3.2.1. Molecules with Definitive Assignments

3.2.1.1. Single Oxygen Bearing Molecules

Evidence from the ReTOF mass spectrometry data combined with isotopic labeling led to the identification of molecules which can be formally classified as a carbonyl, alcohol, and/or ether. The corresponding sublimation profiles along with their respective shifted isotopologue masses are shown in Figures 3A and SI Figures S2, S3. In the case of methanol-carbon monoxide ices we have also identified two additional high mass organics C_3H_4O and $C_4H_{10}O$ as shown in Figure 3B and SI Figures S4, S5. A detailed analysis on the identification of these products is discussed in the following section, please note that the stated energy in electron volts (eV) is the adiabatic ionization energy (I.E.) of the molecule for sake of clarity.

Ketene (H_2CCO)

Temperature program desorption spectra at $m/z = 42$ amu in the irradiated ice samples is attributed to molecular formula C_2H_2O and has been assigned to ketene (H_2CCO ; 9.6 eV^{81}). The sublimation profile at $m/z = 42$ amu in irradiated methanol ice is observed with a single peak centered at 121 K as shown in Figures 3A along with the mass shifted isotopomers at $m/z = 44$ amu for D_2CCO in CD_3OD ice, $H_2CC^{18}O$ in $CH_3^{18}OH$ ice and $H_2^{13}C^{13}CO$ in $^{13}CH_3OH$ ice. All are in excellent agreement with each other as shown, confirming the assignment of this molecular formula. With regards to the irradiated methanol-carbon monoxide ice systems, the sublimation profile at $m/z = 42$ amu (H_2CCO) in CH_3OH-CO ice (Figure 3B) also depicts a single peak centered at 123 K. Similarly, ketene isotopomers were observed in the irradiated labeled ices as shown in Figure 3B. Recall that, we have also identified ν_2 fundamental of ketene isotopomers $H_2CC^{18}O$ in irradiated $CH_3^{18}OH$ ices and $H_2^{13}C^{13}CO$ in irradiated $^{13}CH_3OH$ using infrared spectroscopy (Figure 1A, Table 2), along with the observation of ν_2 fundamental of ketene isotopomers $H_2CC^{18}O$ in both $CH_3^{18}OH-C^{18}O$ and $CH_3OH-C^{18}O$ ices at 2107 cm^{-1} and 2106 cm^{-1} , respectively as shown in Figure 1B, Table 2 as discussed previously. Note that all masses corresponding to the *in situ* identified isotopomers of ketene via FTIR spectroscopy were observed following warm up.

Acetaldehyde (CH₃CHO)

Sublimation profiles for masses corresponding C₂H₄O isomers formed in both irradiated methanol and methanol-carbon monoxide isotopologue ices are shown in Figure 3A and 3B, respectively. In both irradiated ice systems the agreement between the sublimation profiles of C₂H₄O isotopomers confirm identification of radiolytic product with molecular formula C₂H₄O. Here we should mention that, among the three possible isomers with molecular formula C₂H₄O [ethylene oxide (c-C₂H₄O, I.E. = 10.56 eV), acetaldehyde (CH₃CHO, I.E.=10.23 eV) and vinyl alcohol (CH₂CHOH), I.E. = 9.33 eV] that only the latter two can contribute to signal at the corresponding masses observed. Sublimation profiles of C₂H₄O isotopomers from the irradiated methanol ices reveal five distinct peaks centered at 122 K, 147 K, 170 K, 203 K and 238 K. The multiple sublimation peak temperatures imply the possibility of (i) sublimation of different isomers with different functional groups and overall polarity, (ii) co-sublimation of a specific isomer at different temperatures due to intermolecular interactions with neighboring molecules and/or (iii) photo-fragmentation of a higher mass product producing a fragment ion related to C₂H₄O⁺. As mentioned above, only two isomers, acetaldehyde (CH₃CHO) and vinyl alcohol (CH₂CHOH) can be ionized at 10.49 eV. Here, the sublimation of acetaldehyde is expected at a lower temperature than vinyl alcohol (if formed) due to the less polar (CO) compared to the OH functional group in vinyl alcohol. In order to verify the identification of acetaldehyde (CH₃CHO) the irradiated methanol ices, calibration experiments were conducted by simply depositing a sample containing 1.0 ± 0.2 % of acetaldehyde (CH₃CHO) in CH₃OH (Sample 1; SI Table S3). The subsequent sublimation profile of m/z = 44 amu (Figure 3C) does indeed display two peaks centered although slightly lower temperatures at 109 K and 134 K. Coincidentally, methanol begins a phase transition from amorphous to crystalline at 100 – 125 K⁷⁹ forcing the acetaldehyde to escape via a molecular volcano type mechanism.⁸⁰ Here, the first peak at 109 K is due to sublimation of acetaldehyde induced from the phase change of methanol. However, some acetaldehyde is trapped within the methanol matrix; hence the appearance of the second peak at 134 K as it co-sublimates with methanol. Here, the sublimation of acetaldehyde is observed until about 150 K, which clearly suggests that the trapped acetaldehyde molecules are subliming together with the methanol matrix. A comparison of sublimation profiles from both the calibration sample and the irradiated CH₃OH ices (Figure 3C) suggests that the first two peaks at 122 K and 147 K in irradiated methanol ices are due to the sublimation of acetaldehyde.

Although, the peak temperatures do not match perfectly, the overall trend does in that acetaldehyde sublimates as methanol changes from amorphous to crystalline, followed by co-sublimation with methanol. To further enhance the latter point, the sublimation profile of photoionization fragment CH_3O^+ (appearance energy = 10.4 eV)^{81, 82} of methanol at $m/z = 31$ amu are shown in Figure 3C which displays a sublimation peak at 147 K. Note that the difference in peak temperatures between the irradiated methanol ice and the acetaldehyde methanol doped calibration sample are 13 K warmer for both peaks; the shift towards a higher temperature (higher binding energy) may be attributed to intermolecular interactions resulting from the additional large complex organics that were synthesized in the irradiated ice than that of the simple simulation sample. The peak sublimation temperatures at 170 and 203 K are discussed below along with their tentative assignments. Recall that evidence of acetaldehyde was confirmed via infrared absorption at 1724 cm^{-1} (ν_4) together with the isotopically labeled counterparts as discussed in section 3.1.1. Finally, the sublimation peak at 238 K can be assigned to fragmentation of $\text{C}_3\text{H}_8\text{O}_3$ (glycerol) which shows a prominent fragmentation pattern at 10.49 eV.⁸³ Note that due to the astrobiological importance pertaining to the prebiotic formation of glycerol, we chose to focus on this specific molecule in a separate publication.

In the case of methanol-carbon monoxide systems, the sublimation profiles of $\text{C}_2\text{H}_4\text{O}$ isotopomers are shown in Figure 3B and display four distinct sublimation peaks centered at 125 K, 147 K, 183 K, and 240 K. Similar calibration experiments were conducted with a sample containing $0.5 \pm 0.1\%$ of acetaldehyde in a mixed $\text{CH}_3\text{OH-CO}$ (4:5) ice system (Sample 2). Here, the sublimation profile at $m/z = 44$ amu recorded during the calibration experiment (Figure 3C) depicts a sharp peak at 114 K with two shoulders at 105 K and 136 K. The shoulder at 105 K can be correlated to sublimation of acetaldehyde induced via the phase change similar to that observed in methanol/acetaldehyde simulation that peaked at 109 K; however, this observation is the only similarity. A highly porous methanol ice results from carbon monoxide having already sublimated at these temperatures allowing for more binding sites of the acetaldehyde within the pores of the methanol matrix. The lack of two distinct peaks as observed in the methanol calibration sample is most likely a reflection of the initial porosity of the methanol matrix. Here, most of the acetaldehyde was allowed to sublime in the mixed methanol-carbon monoxide from a combination of the high initial porosity followed with the phase transition, whereas the pure methanol ice simulation sample trapped more of the acetaldehyde during the phase

transition resulting in significant co-sublimation. However, some of the acetaldehyde did remain trapped, thereby explaining the small shoulder at 136 K. Note that the difference of sublimation temperatures between the observed peaks of the irradiated binary mixture and calibration sample are 11 K warmer. Again, this shift towards higher temperatures and thus higher binding energies is attributed to the intermolecular interactions with other complex organics left in the refractory material. The drastic difference in sublimation profiles of the calibration and irradiated sample may simply be due to the inherent effect that these large organics acting as 'impurities' have on the phase change behavior of the ice sample.

C₂H₆O Isomers: Identification of Ethanol (C₂H₅OH) and Dimethyl ether (CH₃OCH₃)

Integrated ion counts at mass-to-charge ratios corresponding to isotopomers of C₂H₆O products were observed in both irradiated methanol and methanol-carbon monoxide isotopologue ices and are shown in Figures 3A and 3B, respectively. In irradiated methanol ices, sublimation of C₂H₆O depicts two distinct sublimation peaks centered at 122 K and 144 K as shown in Figure 3A. The sublimation profile of the product C₂H₆O from irradiated methanol-carbon monoxide ices, depicts a pronounced peak at 124 K with a shoulder at 143 K (Figure 3B). Note that both C₂H₆O isomers, ethanol (C₂H₅OH; 10.48 eV) and dimethyl ether (CH₃OCH₃; 10.0 eV), can be ionized with the 10.49 eV VUV photons. In order to ensure the assignment of these isomers, calibration experiments are performed with ethanol and dimethyl ether in both methanol (Samples 3 and 5) and methanol-carbon monoxide (Samples 4 and 6) ices are compared with sublimation profiles of the C₂H₆O irradiation product obtained from both irradiated methanol and methanol-carbon monoxide ices shown in Figure 3D.

In the calibration experiments with methanol ices, the sublimation of dimethyl ether started at 102 K and the sublimation profile shows two peaks positioned at 112 K and 128 K with a shoulder at 142 K. The lower sublimation temperature of dimethyl ether is reasonable due to its lower polarity compared to methanol. Here, the peak at 112 K can be correlated to the sublimation of dimethyl ether (CH₃OCH₃) from methanol ices whereas the peak at 128 K follows the same pattern as observed with the acetaldehyde (HCOCH₃), i.e. methanol phase change from amorphous to crystalline resulting in a molecular volcano. Finally, the shoulder at 145 K is the result of co-sublimation of trapped dimethyl ether (CH₃OCH₃) within the methanol matrix. Note that the temperature difference between the irradiated methanol ice sample and the dimethyl

ether calibration sample is similar to that observed for the acetaldehyde sample (about 12 K); again this shift in temperature is attributed to intermolecular forces of the large refractory organics formed in the process of irradiation. In case of methanol-carbon monoxide ices, the calibration experiment with dimethyl ether displays two peaks at 108 K and 119 K with a small shoulder at 145 K. In a similar way, the first peak can be assigned to the sublimation of dimethyl ether (CH_3OCH_3) molecules followed with sublimation of trapped dimethyl ether (CH_3OCH_3) molecules during the phase change, and finally co-sublimation with methanol at 145 K; as discussed above, the residual methanol matrix at these temperatures is most likely of higher porosity compared to the pure methanol samples due to the prior sublimation of carbon monoxide. As such, allowing most of the dimethyl ether to leave. We are again attributing the differences in sublimations profiles of the irradiated and calibration sample to the intrinsic effects of what could be considered contamination from the remaining organics on the phase change behavior of methanol.

The calibration experiments (Figure 3D) also depict that the sublimation of ethanol ($\text{C}_2\text{H}_5\text{OH}$) with both peaks positioned at 145 K in the methanol and methanol-carbon monoxide ices, matching well the observed profile of the irradiated samples. This observation is not unexpected as ethanol is completely miscible with methanol. In addition, QMS traces of $\text{C}_2\text{H}_6^{18}\text{O}^+$ ($m/z = 48$ amu) and $\text{C}_2\text{H}_5^{18}\text{O}^+$ ($m/z = 47$ amu) ions show two peaks at temperatures of 122 K and 144 K in irradiated $\text{CH}_3^{18}\text{OH}$ ice and at 124 K and 146 K in irradiated $\text{CH}_3^{18}\text{OH-C}^{18}\text{O}$ ice (SI Figure S6). Note that, both ethanol ($\text{CH}_3\text{CH}_2^{18}\text{OH}$) and dimethyl ether ($\text{CH}_3^{18}\text{OCH}_3$) show prominent fragmentation at $\text{C}_2\text{H}_5^{18}\text{O}^+$ during the electron impact ionization.⁸¹ Giving further evidence supporting our assignment of dimethyl ether and ethanol formed in irradiated methanol and methanol-carbon monoxide ices.

3.2.1.2. Complex Organic Molecules with Two Oxygen Atoms

By comparing the sublimation profiles of the integrated ion counts observed from the isotopically labeled ices of both methanol and methanol-carbon monoxide ices, products with molecular formula $\text{C}_2\text{H}_2\text{O}_2$, $\text{C}_2\text{H}_4\text{O}_2$, and $\text{C}_2\text{H}_6\text{O}_2$ are identified. It is worth mentioning that the sublimation profiles of the products in the irradiated methanol ices are relatively narrow with sharp peaks compared to the sublimation profiles observed in irradiated methanol-carbon monoxide ices as can be seen in Figures 4-8 and SI Figures S7, S8. The broad sublimation

features observed in the latter mixed ices are most likely due to the intermolecular interactions with the residual high mass organics (up to 150 amu) formed within the processed mixed ices (Figure 2B). In comparison, the radiation induced chemical processing of methanol isotopologue ices resulted identification of fewer products with mass-to-charge ratios only up to 90 amu (Figure 2A); as such, diminished dipole-dipole interactions of the subliming molecules with the residual organic matrix resulting in the relatively narrow sublimation profiles observed in the case of methanol systems.

Identification of Glyoxal (C₂H₂O₂)

A product with molecular formula C₂H₂O₂ and the respective mass shifted isotopomers were observed only in the irradiated mixed methanol-carbon monoxide isotopologue ices with a sublimation peak at 145 K as shown in Figure 4. We are assigning this sublimation of the molecule to glyoxal (HCOCHO) for two reasons as follows. First, note that 2-oxiranone [Cyc(CH₂OC)O] (an isomer of glyoxal) is 38 kJ mol⁻¹ less stable than the former and holds an ionization energy of 10.96 eV (calculated),⁸⁴ and therefore not should attribute to any ion signal collected at this particular photon energy whereas glyoxal can with its ionization energy at 10.2 eV. Second, the third most stable isomer (63 kJ mol⁻¹ less stable than glyoxal) ethyne-1,2-diol (HOCCOH) has an ionization energy 9.3 eV⁸⁴ and can be ionized; however, this diol isomer is expected to sublime at temperatures greater than the sublimation of ethylene glycol (HOCH₂CH₂OH) which displays a sublimation peak about 200 K (see below) due to their trends in boiling points (ethylene glycol = 471 K, ethyne-1,2-diol = 530 K), yet no detectable signal was collected temperatures greater than 200 K. Therefore, we can conclude that in irradiated methanol-carbon monoxide ices that ethyne-1,2-diol did not form or was below the detection limit. Finally, please note the similar trend in sublimation peaks as discussed above; here, the weak sublimation peak observed at 125 K is related to the phase change of methanol followed with co-sublimation at 145 K.

C₂H₄O₂ Isomers: Identification of Glycolaldehyde and Ethene-1,2-diol

Among the four stable isomers of C₂H₄O₂, glycolaldehyde (HOCH₂CHO; 10.2 eV), ethene-1,2-diol (HOCHCHOH; 9.62 eV), acetic acid (CH₃COOH; 10.65 eV) and methyl formate (HCOOCH₃; 10.84 eV), only glycolaldehyde and ethene-1,2-diol can be ionized with 10.49 eV

VUV photons used in the present study. A significantly more detailed discussion related to assignment of glycolaldehyde and ethene-1,2-diol can be found in a previous publication.⁶³ Very briefly though, five sublimation peaks at 123 K, 166 K, 200 K, 210 K and 234 K in each isotopically labeled methanol ice (Figure 5) were observed for the sublimation of C₂H₄O₂ isomers in the irradiated methanol ices. The first peak at 123 K is most likely the induced sublimation of isomers C₂H₄O₂ resulting from the amorphous to crystalline phase change inducing a molecular cryo-volcano. Following is the sublimation peak at 166 K which is assigned to the sublimation of glycolaldehyde based on the coincidentally decreasing ν_{14} band from *in situ* FTIR observations. Next, the observed peak at 200 K is from co-sublimation with ethylene glycol followed with the direct sublimation of ethene-1,2-diol at 210 K.⁶³ Finally, the distinct peak around 234 K is assigned to the fragmentation from glycerol (C₃H₈O₃) based on a recent study on the photoionization of glycerol (C₃H₈O₃) in which a prominent photo ion fragment (C₂H₄O₂) was identified with an appearance energy of 9.9 eV.⁸³ In the case of irradiated methanol-carbon monoxide isotopologue ices, the C₂H₄O₂ product is confirmed sublimating at 125 K, 195 K and 218 K (Figure 5) with the latter two peaks assigned to glycolaldehyde and ethene-1,2-diol, respectively and the first peak related to the sublimation of phase change of methanol at 125 K.

Identification of Ethylene Glycol (HOCH₂CH₂OH)

The sublimation profiles of C₂H₆O₂ in both irradiated methanol and methanol-carbon monoxide ices show a prominent peak at 198 K along with a weak sublimation peak at 125 K as shown in Figure 6. In the case of irradiated methanol systems, the sublimation profiles also display a slight peak at 236 K. Here, the intense peak at 198 K suggests the sublimation of a single isomer of with molecular formula C₂H₆O₂. In order to ensure the assignment of ethylene glycol (HOCH₂CH₂OH; I.E. = 10.16 eV)⁸¹ in both methanol and methanol-carbon monoxide ices, calibration experiments are performed with ethylene glycol in CH₃OH and CH₃OH-CO displayed in Figure 7. The sublimation profiles of the ion counts at $m/z = 62$ amu recorded from the calibration experiments are compared with the sublimation profiles of C₂H₆O₂ observed in both irradiated CH₃OH and CH₃OH-CO ices. The sublimation of ethylene glycol (Figure 7) shows a single peak at 193 K in CH₃OH ice (Sample 11; SI Table S3) and at 194 K in CH₃OH-CO (Sample 12) ices, respectively. As expected and observed, ethylene glycol holds two hydroxyl groups and will sublime at warmer temperatures higher than methanol. The sublimation

profile of $C_2H_6O_2$ product obtained in both irradiated ices of methanol and methanol-carbon monoxide ices are in reasonable agreement with the desorption profile of ethylene glycol obtained from the calibration experiments. In addition, QMS traces corresponding to $C_2H_6O^+$ are also observed at about 198 K in both irradiated methanol and methanol-carbon monoxide ices. Also observed were ion fragments of typical of ethylene glycol due to electron impact ionization at $C_2H_3O^+$, $C_2H_4O^+$, $C_2H_5O^+$, $C_2H_5O_2^+$, as shown in SI Figure S6. Therefore, the sublimation peak at 198 K recorded using ReTOF mass spectrometry in irradiated methanol and methanol-carbon monoxide ices is assigned to the ethylene glycol ($HOCH_2CH_2OH$). Also recall that, we have identified ethylene glycol via the observation of ν_9 band of ethylene glycol at 1094 cm^{-1} using *in situ* infrared spectroscopy.

As mentioned, a weak peak is also observed at about 125 K (Figure 6) in both irradiated methanol and methanol-carbon monoxide ices. As this temperature is well below the sublimation of methanol ($\sim 145\text{ K}$) and is correlated with the amorphous to crystalline phase change, the peak observed at this temperature could either indicate a ‘cyro-volcano’ of ethylene glycol or possibly the sublimation of a less polar $C_2H_6O_2$ isomer. Among the isomers are: ethylene glycol (470 K), ethylhydroperoxide (368 K), methoxymethanol (356 K), and dimethyl peroxide (239 K) with the boiling points given in parentheses. Of these isomers, dimethyl peroxide is expected to sublime at temperatures below the sublimation of methanol (338 K). Consequently, the weak sublimation peak at 125 K may be related to dimethyl peroxide (CH_3OOCH_3 ; 9.1 eV). Finally, the sublimation peak at 236 K (Figure 7) in the irradiated methanol isotopologue ices is once again attributed to glycerol ($C_3H_8O_3$) in which a prominent photo fragment at $m/z = 62$ amu ($C_2H_6O_2$) has been identified with an appearance energy of 9.9 eV.⁸³

Identification of methoxymethanol (CH_3OCH_2OH)

Methoxymethanol is a rather interesting radiation byproduct as it has been previously identified only in the low energy electron radiolysis of methanol ices.^{57, 85} Based on the functional groups present in methoxymethanol (CH_3OCH_2OH) and a comparison of the boiling point trends, methoxymethanol (356 K) is expected to sublime at a temperature higher than methanol (338 K) but at a lower temperature compared to ethylene glycol (470 K). However, there are no significant ion counts of $C_2H_6O_2$ (Figure 8) at temperatures between the sublimation of methanol and ethylene glycol (140 – 170 K) that would normally indicate the sublimation of a different

molecular isomer. Previously, methoxymethanol was assigned as a low energy electron radiolysis product of methanol ice from the combination of a unique sublimation profile and fragmentation pattern. The justification was based heavily on a previous mass spectroscopic analysis of synthesized methoxymethanol which identified a prominent ion fragment at $m/z = 61$ amu corresponding to $C_2H_5O_2^+$; whereas the expected parent molecular ion peak at $m/z = 62$ amu ($C_2H_6O_2^+$) was not observed or determined to be within the noise level.⁸⁶ Following a similar approach here, we concur with the previous identification of methoxymethanol in energetically processed methanol ices and present the novel identification of this product in irradiated binary ice mixture of methanol and carbon monoxide. Evidence supporting the identification methoxymethanol is twofold as presented here. First, upon examination of the QMS data, isotopomers connected with $C_2H_5O_2^+$ were observed subliming with peak ion counts at 170 K, with no detectable signal contributing from the parent ($C_2H_6O_2$) at these temperatures, in agreement to the previous studies.^{57, 85} Second, $C_2H_5O_2^+$ isotopomers that were detected utilizing single photoionization ReTOF mass spectrometry and have *identical sublimation profiles* to that derived from the QMS data. Sublimation profiles observed at these mass-to-charge ratios are shown in Figure 8 for irradiated methanol and methanol-carbon monoxide ices. Note that possibility of radicals sublimating is discounted as the applied thermal energy would allow for any trapped radicals to diffuse and easily react at these temperatures. Also, previous attempts at dosing the irradiated methanol ice with oxygen atoms did not decrease the overall TPD signal of $C_2H_5O_2^+$ further implying that $C_2H_5O_2$ radicals are not directly sublimating.⁵⁷ From our observations, i.e. the direct correlation between two different gas phase detection methods; methoxymethanol is suggested to be either an extremely thermally liable compound or photoionization at 10.49 eV leads to fragmentation thereby explaining the lack of parent ion signal in the TPD analysis. In both irradiated methanol and methanol-carbon monoxide ices, the sublimation of $C_2H_5O_2^+$ started at 143 K with a prominent peak positioned at 170 K and 184 K, respectively. Additional sublimation peaks observed at this m/z linked to $C_2H_5O_2^+$ in irradiated CH_3OH ices (Figure 8) at 202 K and 238 K are attributed to the co-sublimation of methoxymethanol (CH_3OCH_2OH) with ethylene glycol ($HOCH_2CH_2OH$) and photofragmentation of glycerol ($C_3H_8O_3$),⁸³ respectively. The sublimation peak at 202 K is excluded as a fragmentation of ethylene glycol ($HOCH_2CH_2OH$) as the calibration experiments with ethylene glycol did not exhibit any fragmentation at $m/z = 61$ amu ($C_2H_5O_2$).

3.2.2. Molecules with tentative assignments

Vinyl Alcohol (CH₂CHOH): Vinyl alcohol (CH₂CHOH; 9.3 eV) is tentatively assigned to account for the ion signal ($m/z = 44$ amu) observed at the sublimation temperature (peak) of 170 ± 2 K in the irradiated methanol ice systems and at 185 ± 2 K in the processed methanol-carbon monoxide systems (Figures 3A and 3B). Here, the sublimation of vinyl alcohol at temperatures higher than acetaldehyde is reasonable since the molecule is overall more polar, and thus will have a higher energy of desorption. The sublimation peak at 203 ± 2 K observed in the TPD spectra of the processed methanol ices coincides with the sublimation of ethylene glycol and thus may possibly be attributed to co-sublimation of vinyl alcohol with ethylene glycol due to the similar polarity. Photo-fragmentation from ethylene glycol is excluded since photoionization of the ethylene glycol calibration sample did not show any fragmentation. Unfortunately, similar calibration experiments with vinyl alcohol could not be conducted due to the inherent instability of the molecule (and commercially unavailability) as it will tautomerize to acetaldehyde.

C₃H₄O Isomers: A radiolysis by product with molecular formula C₃H₄O was identified only in the irradiated methanol-carbon monoxide ices. In Figure 3A, the sublimation profile of C₃H₄O isotopomers shows two distinct peaks centered at 127 K and 144 K which again is attributed to the phase change induced molecular volcano followed with co-sublimation of methanol. However, a broad sublimation profile that extends up to 300 K is observed and again is most likely a combination of different isomers sublimating and photofragmentation of high mass organics. Molecular isomers that may contribute to the ion counts at the derived molecular formula are: propenal (CH₂CHCHO; 10.1 eV), cyclopropanone (CH₂(CO)CH₂; 9.1 eV), methyl ketene (CH₃CHCO; 8.95 eV). Of these, only propenal (CH₂CHCHO) is readily available and was used as a calibration with $1.5 \pm 0.5\%$ in methanol-carbon monoxide ice in order to help with the possible identification. The sublimation profile at $m/z = 56$ amu of propenal recorded from calibration sample together with the sublimation profile of C₃H₄O isomers observed in irradiated CH₃OH-CO ices are shown in SI Figure 9. The sublimation profile at $m/z = 56$ amu shows two peaks at 128 K and 138 K and these temperatures can be correlated to the sublimation of propenal during the phase change and sublimation of methanol matrix as discussed above. The correlation of the TPD spectra would suggest that sublimation of propenal; however, we again cannot eliminated the possibility of cyclopropanone (CH₂(CO)CH₂) and methyl ketene (CH₃CHCO) isomers and therefore can only present a tentative assignment here.

C₃H₆O Isomers: Products with the molecular formula C₃H₆O were identified in both irradiated methanol and methanol-carbon monoxide ices. The sublimation profiles at m/z corresponding to isotopologues of C₃H₆O isomers are shown in Figures 3A and 3B. Of the molecular isomers, acetone (CH₃COCH₃; 9.7 eV), propanal (C₂H₅CHO; 10.0 eV), and allyl alcohol (CH₂CHCH₂OH; 9.7 eV) can account for the observed ion signal as these have ionization energies below the 10.49 eV threshold. The TPD spectra of C₃H₆O molecular product depicts four distinct peaks centered at 125 K, 145 K, 172 K, and 203 K in irradiated methanol ices. While in the irradiated mixed methanol-carbon monoxide ices, displayed two sharp peaks at 126 K and 146 K together with a broad peak centered at about 187 K. Similar to that previously discussed, the first sublimation peaks at about 125 K and 145 K are associated with the phase transition of amorphous to crystalline (125 K) inducing a molecular volcano followed with co-sublimation of methanol near 145 K. To help identify which isomers were sublimating, calibration experiments (SI Table S3) were performed with acetone (CH₃COCH₃; Samples 1 and 2), propanal (CH₃CH₂CHO; Samples 3 and 4) and allyl alcohol (CH₂CHCH₂OH; Samples 5 and 6) in both methanol and methanol-carbon monoxide ices. The sublimation profiles of ion counts at m/z = 58 amu (C₃H₆O⁺) recorded from the calibration experiments are shown in SI Figure S10 with comparison of the sublimation profile at m/z = 58 amu recorded from both irradiated CH₃OH and CH₃OH-CO ices. The sublimation temperatures of these molecules are lower than the sublimation temperature of methanol as expected based on their polarity and subsequent boiling point trends, whereas allyl alcohol (CH₂CHCH₂OH) is expected to sublime at a higher temperature than methanol. Here, acetone and propanal both exhibited peak sublimation temperatures of 137 K from methanol ice and 128 K and 126 K, respectively in the mixed methanol carbon monoxide ice and the sublimation profiles of allyl alcohol from both methanol and methanol-carbon monoxide ices depict single sublimation peak at 154 K and 152 K, respectively. Unfortunately, the TPD profiles of the calibration samples are not adequately unique to disentangle for a definitive assignment. Moreover, *in situ* IR spectroscopy did not yield strong evidence on the formation of these molecules to allow for certainty in the assignment either in agreement with previous examinations on the energetic processing of methanol rich ices.^{53, 74, 79} However, ion counts were observed corresponding to molecular formula C₃H₆O and thus we can only suggest that the possibility that acetone, propanal, and/or allyl alcohol were/was formed. In addition possible contributions from photofragmentation of the higher mass products

(such as $C_4H_8O_2$) may contribute to the ion counts observed at higher temperatures, namely the broad sublimation profile extending from 170 – 250 K in the irradiated methanol carbon monoxide ice along with the peaks at 172 K and 203 K in the TPD spectra of irradiated methanol ices. For example, the appearance energies of $C_3H_6O^+$ from $C_4H_8O_2$ isomers, 3-methoxypropanal and methoxymethyloxirane, are 8.5 eV and 10.2 eV, respectively. The sublimation of product with the derived molecular formula $C_4H_8O_2$ (discussed below) resulted in three peaks at 179 K, 208 K and 254 K in irradiated methanol ices and a broad sublimation feature within 175-275 K temperature range in irradiated methanol-carbon monoxide ices. Future experiments using tunable vacuum ultraviolet light for selective photoionization will allow for us to make specific assignments based upon their ionization energies.

C_3H_8O Isomers: Products were identified in the TPD spectra of the irradiated ice systems with molecular formula C_3H_8O as shown in Figures 3A and 3B. The molecular isomers of this group are either alcohols such as 1-propanol ($CH_3CH_2CH_2OH$; 10.2 eV), 2-propanol ($CH_3CH(OH)CH_3$; 10.2 eV) or an ether molecule such as methoxyethane ($CH_3OCH_2CH_3$; 9.7 eV). In irradiated methanol ices, the sublimation of C_3H_8O is identified via a distinct sublimation peak at 124 K. In the case of methanol-carbon monoxide ices, C_3H_8O isomers are observed sublimating at 125 K and 142 K. In order to assist in the determination of which C_3H_8O isomers were detected, calibration experiments were performed with only 1-propanol and 2-propanol in both methanol and methanol-carbon monoxide ices as methoxyethane is not commercially available. The TPD profiles of 1-propanol and 2-propanol peak 155 K and 153 K, respectively in CH_3OH ices and 152 K and 149 K, respectively, in CH_3OH-CO ices, as shown in SI Figure S11. The above information clearly suggests that 1-propanol and 2-propanol isomers sublime at higher temperatures than the methanol. Furthermore, the sublimation profiles of C_3H_8O radiolytic byproduct isomers ($m/z = 60$ amu) do not agree with the alcohol calibration samples. As such we can only postulate the possible formation of methoxy ethane with the observed peaks attributed to the molecular volcano induced from the amorphous to crystalline phase change at 125 K and co-sublimation of C_3H_8O isomers with methanol at 145 K.

C_4H_8O Isomers: Ion counts associated with the molecular formula C_4H_8O are observed in both the TPD spectra of irradiated methanol and methanol-carbon monoxide ices (Figures 3A and 3B). Molecules such as butanal (C_3H_7CHO ; 9.8 eV), *iso*-butanal ($CH_3CH(CH_3)CHO$; 9.7 eV), butanone ($C_2H_5COCH_3$; 9.1 eV), and 2-buten-1-ol ($HOCH_2CHCHCH_3$; 9.1 eV) can contribute

to the observed signal here. As mentioned previously, both irradiated ices exhibited peaks at the sublimation temperature of methanol, and thus ion counts for these masses correspond again to co-sublimation with methanol. However, the broad peak positioned at about 208 K is most likely photofragmentation of higher mass organics, such as $C_3H_4O_2$ ($m/z = 72$ amu) isomers discussed below. Similarly in the irradiated methanol-carbon monoxide ices (Figure 3B), the sublimation profiles at C_4D_8O displays a broad sublimation feature centered at ~ 200 K which may be attributed again to the photofragmentation of higher mass organics. Calibration experiments were once again conducted in an effort to remove some of the ambiguity observed in the TPD spectra of the potential carriers for the observed C_4H_8O isomers. Here, samples containing butanal (Sample 3 and 4), *iso*-butanal (Sample 7 and 8) and butanone (Sample 5 and 6) in both CH_3OH and CH_3OH-CO (4:5) ices. The sublimation profiles of the ion counts of C_4H_8O isomers at $m/z = 72$ amu are shown in SI Figure 12 and are compared with the sublimation profiles observed at $m/z = 72$ amu (C_4H_8O) in irradiated CH_3OH ices and $m/z = 80$ amu (C_4D_8O) in irradiated CD_3OD-CO ices. As shown in SI Figure 12, all TPD spectra are again not sufficiently unique to make a definitive assignment and typically sublimate with methanol. Based on the above information alone, we can only suggest that at least one of these molecules is formed within irradiated methanol ices.

$C_4H_{10}O$ Isomers: We have also identified $C_4H_{10}O$ molecular isomers; however, only in irradiated methanol-carbon monoxide ices. Here, the sublimation profiles of integrated ion counts corresponding to $C_4H_{10}O$ isotopomers are shown in Figure 3B and are observed with peaks at 128 K and 143 K. Alcohols and ethers are possible isomers and include: 1-butanol ($CH_3CH_2CH_2CH_2OH$; 10.0 eV), 2-butanol ($CH_3CH_2CH(OH)CH_3$; 9.9 eV), *iso*-butanol ($(CH_3)_2CHCH_2OH$; 10.0 eV), *tert*-butanol ($(CH_3)_3COH$; 9.9 eV), methoxypropane ($CH_3OC_3H_7$; 9.41 eV) and ethoxyethane ($C_2H_5OC_2H_5$; 9.51 eV). In order to quantify which isomers were detected in the irradiated samples calibration experiments were performed with 1-butanol, 2-butanol, *iso*-butanol and *tert*-butanol in CH_3OH-CO ices. The sublimation profile of these $C_4H_{10}O$ isomers at $m/z = 74$ amu are compared with the sublimation profile of the irradiation product $C_4H_{10}O$ ($m/z = 74$ amu) and shown in SI Figure S13. The TPD profile of 1-butanol, 2-butanol, *iso*-butanol and *tert*-butanol peak at 159 K, 154 K, 159 K and 155 K, respectively, and are not in agreement to the observed profile nor peak positions recorded in irradiated CH_3OH-CO ice (128 K and 143 K). Consequently, we once more can only suggest the possible

identification of less polar ether molecules methoxypropane ($\text{CH}_3\text{OC}_3\text{H}_7$) and ethoxyethane ($\text{C}_2\text{H}_5\text{OC}_2\text{H}_5$) isomers; while again attributing the compaction of the methanol phase change at ~ 125 K inducing a cryo-volcano along co-sublimation with methanol at ~ 145 K of $\text{C}_4\text{H}_{10}\text{O}$ alcohols and ethers.

$\text{C}_3\text{H}_4\text{O}_2$ Isomers: Ions counts attributed to $\text{C}_3\text{H}_4\text{O}_2$ molecular formula have been detected in both irradiated methanol and methanol-carbon monoxide ices. The TPD spectra of irradiated methanol ices show $\text{C}_3\text{H}_4\text{O}_2$ isomers sublimating with peaks at 208 K and 236 K in irradiated methanol ices (SI Figure S7) and 183 K and 236 K in the irradiated methanol-carbon monoxide ices (SI Figure S14). These observations suggest the formation isomers with at least two different functional groups resulting in different polarities and subsequently different desorption energies. Molecules such as methyl glyoxal (CH_3COCHO ; 9.6 eV), 1,3-propanedial (HCOCH_2CHO) can account for the $\text{C}_3\text{H}_4\text{O}_2$ isomers. In addition, more polar en-ol isomers, such as 2-hydroxyacrylaldehyde (HCOC(OH)CH_2) and 3-hydroxyacrylaldehyde (HOCHCHCHO) can also be correlated to this product as well. Here, the sublimation peaks at 203 K in irradiated methanol ice and 183 K in irradiated methanol-carbon monoxide ices, can be correlated to the less polar isomers (possibly methyl glyoxal and 1,3-propanedial) and the sublimation peaks centered at 236 K in both methanol and methanol-carbon monoxide ices can be assigned to the sublimation of glycerol, at photoionization of this molecule at 10.49 eV results in an ion fragmentation.⁸³

$\text{C}_3\text{H}_6\text{O}_2$ Isomers: The sublimation profiles recorded connected to $\text{C}_3\text{H}_6\text{O}_2$ isotopomers in methanol ices (SI Figure S7) depict three prominent peaks at 173 K, 210 K and 236 K. The peak at 236 K are most has been assigned to photofragmentation of glycerol ($\text{C}_3\text{H}_8\text{O}_3$).⁸³ In irradiated methanol-carbon monoxide ices, $\text{C}_3\text{H}_6\text{O}_2$ were identified via a broad sublimation profile (150 - 300 K) with two peaks at 192 K and 244 K (SI Figure S14). Methyl sugar molecules such as hydroxyacetone ($\text{CH}_3\text{COCH}_2\text{OH}$; 10.0 eV), 2-hydroxypropanal ($\text{CH}_3\text{CH(OH)CHO}$) and 3-hydroxypropanal ($\text{HOCH}_2\text{CH}_2\text{CHO}$) can be linked to the product $\text{C}_3\text{H}_6\text{O}_2$ with one hydroxyl and one carbonyl functional groups. In addition, isomers bearing acid and ester functional groups such as propionic acid ($\text{C}_2\text{H}_5\text{COOH}$; 10.44 eV) and methyl acetate ($\text{CH}_3\text{COOCH}_3$; 10.25 eV) can also be linked to $\text{C}_3\text{H}_6\text{O}_2$ isomers.

$\text{C}_3\text{H}_8\text{O}_2$ Isomers: Isomers with molecular formula $\text{C}_3\text{H}_8\text{O}_2$ have been identified in both irradiated methanol and methanol-carbon monoxide ices as shown in SI Figures S7 and S14,

respectively. In irradiated methanol ices, the sublimation profile shows two prominent peaks at 171 K and 203 K. Molecules such as methoxyethanol ($\text{CH}_3\text{OCH}_2\text{CH}_2\text{OH}$) and ethoxymethanol ($\text{CH}_3\text{CH}_2\text{OCH}_2\text{OH}$) may be responsible for the observed ion counts at 171 K as these molecules are expected to sublime at temperatures similar to methoxymethanol. Similarly, the sublimation of di-ol isomers are expected to be at temperatures close to ethylene glycol. Hence, 1,2-propanediol and/or 1,3-propanediol isomers may be responsible for the signal at 203 K. In the case of irradiated methanol-carbon monoxide ices, the sublimation of $\text{C}_3\text{H}_8\text{O}_2$ (SI Figure S14) shows a broad profile extends from 150 K to at least 270 K. The broad sublimation profile is most likely due to possible intermolecular interactions with higher mass organics, as we have mentioned before. Here, the peak at ~ 185 K may possibly be attributed to the sublimation of methoxyethanol ($\text{CH}_3\text{OCH}_2\text{CH}_2\text{OH}$) or ethoxymethanol ($\text{CH}_3\text{CH}_2\text{OCH}_2\text{OH}$) isomers as the peak position is close to the observed temperature for methoxymethanol (184 K). Whereas more polar di-ol isomers such as 1,2-propanediol and/or 1,3-propanediol may account for the extended sublimation tail due to their higher desorption energies.

$\text{C}_4\text{H}_6\text{O}_2$ Isomers: Product with formula $\text{C}_4\text{H}_6\text{O}_2$ were only detected in the TPD spectra of irradiated methanol-carbon monoxide ices and is shown SI Figure S14 which shows a broad sublimation profile with two subtle peaks at 192 K and 236 K which again suggest that isomers of $\text{C}_4\text{H}_6\text{O}_2$ with different polarity are sublimating. The weak features observed ~ 145 K can be linked to the co-sublimation of $\text{C}_4\text{H}_6\text{O}_2$ isomers with methanol matrix. Isomers of $\text{C}_4\text{H}_6\text{O}_2$ can be associated to dicarbonyl molecules such as butane-2,3-dione ($\text{CH}_3\text{COCOCH}_3$; 9.3 eV), 2-oxobutanal ($\text{HCOCOCH}_2\text{CH}_3$), and molecules bearing single carbonyl (CO) and single hydroxyl (OH) groups such as 2-hydroxybut-3-enal ($\text{HCOCH}(\text{OH})\text{CHCH}_2$) and 4-hydroxybut-2-enal ($\text{HCOCHCHCH}_2\text{OH}$). The dicarbonyl isomers are expected to sublime at lower temperatures (~ 192 K) due to their less polar functional group compared to hydroxy-bearing groups isomers. Fragmentation of glycerol at 10.49 eV⁸³ is once again attributed to the peak at 236 K.

$\text{C}_4\text{H}_8\text{O}_2$ Isomers: The sublimation profiles of due to $\text{C}_4\text{H}_8\text{O}_2$ isomers are depicted in SI Figures S15 and S16. In irradiated methanol ices, the sublimation of $\text{C}_4\text{H}_8\text{O}_2$ displays three peaks at 179 K, 207 K and 254 K; however, in irradiated methanol-carbon monoxide ices, the sublimation profile of $\text{C}_4\text{H}_8\text{O}_2$ shows a broad profile with a slight peak positioned at 236 K. These observations again suggest the possible formation of multiple isomers of $\text{C}_4\text{H}_8\text{O}_2$ with different

polarities. Hydroxyl-carbonyl isomers of hydroxybutanal and hydroxybutanone, ester molecules such as methyl propionate ($\text{CH}_3\text{CH}_2\text{COOCH}_3$; 10.2 eV), ethyl acetate ($\text{CH}_3\text{COOCH}_2\text{CH}_3$; 10.0 eV) and di-ol molecules such as but-2-ene-1,4-diol ($\text{HOCH}_2\text{CHCHCH}_2\text{OH}$) can be considered as the possible isomers of the product $\text{C}_4\text{H}_8\text{O}_2$.

Complex Organic Molecules bearing Three, Four and Five Oxygen Atoms.

$\text{C}_3\text{H}_6\text{O}_3$: Isomers corresponding to molecular formula $\text{C}_3\text{H}_6\text{O}_3$ were observed in the TPD spectra of the irradiated methanol and mixed methanol-carbon monoxide isotopologue ice systems as shown in SI Figure S15 and SI Figure S16, respectively. The sublimation profiles of $\text{C}_3\text{H}_6\text{O}_3$ molecular isomers in both irradiated ice systems are broad and show at two slight sublimation peaks at ~ 210 K and ~ 240 K and imply different isomers with various polarities. Molecular isomers with $\text{C}_3\text{H}_6\text{O}_3$ formula consist of astrobiologically important C3-sugar molecules: glyceraldehyde ($\text{HOCH}_2\text{CH}(\text{OH})\text{CHO}$) and 1,3-dihydroxyacetone ($\text{HOCH}_2\text{COCH}_2\text{OH}$). In addition, molecules with ester functional such as methyl-2-hydroxyacetate ($\text{CH}_3\text{OCOCH}_2\text{OH}$; 10.42 eV), methoxymethylformate ($\text{CH}_3\text{OCH}_2\text{OCHO}$) can also be associated to the product $\text{C}_3\text{H}_6\text{O}_3$. Additional complex organics bearing three oxygen atoms ($\text{C}_3\text{H}_4\text{O}_3$) were identified only in irradiated methanol-carbon monoxide isotopologue ices (SI Figure S16).

$\text{C}_4\text{H}_8\text{O}_3$: In the case of methanol-carbon monoxide systems, product with a molecular formula $\text{C}_4\text{H}_8\text{O}_3$ was also observed with the TPD profile of $\text{C}_4\text{H}_8\text{O}_3$ shown in SI Figure S17. The sublimation of $\text{C}_4\text{H}_8\text{O}_3$ in irradiated methanol-carbon monoxide ices depicts a profile similar to $\text{C}_3\text{H}_6\text{O}_3$ (SI Figure 16) however, extends up to 300 K. Among the $\text{C}_4\text{H}_8\text{O}_3$ isomers include sugar molecules with a methyl group such as 2,3-dihydroxybutanal ($\text{HCOCH}(\text{OH})\text{CH}(\text{OH})\text{CH}_3$), 1,3-dihydroxy-2-butanone ($\text{HOCH}_2\text{COCH}(\text{OH})\text{CH}_3$). In addition, molecules with ester functional such as 1-hydroxyethylacetate ($\text{CH}_3\text{COOCH}(\text{OH})\text{CH}_3$), methyl-2-hydroxypropanoate ($\text{CH}_3\text{OCOCH}(\text{OH})\text{CH}_3$), 2-hydroxyethylacetate ($\text{CH}_3\text{COOCH}_2\text{CH}_2\text{OH}$) are also possible $\text{C}_4\text{H}_8\text{O}_3$ isomers; the chemical structures of these isomers are shown in SI Figure 19. Additional complex organics bearing ($\text{C}_4\text{H}_6\text{O}_3$) were only identified in irradiated methanol-carbon monoxide isotopologue ices (SI Figure S16). The TPD spectra of these products are broad implying the formation of an abundant mixture of isomers with various desorption energies.

$C_nH_mO_{4,5}$: Molecules bearing four and five oxygen atoms are only detected in the TPD spectra of irradiated methanol-carbon monoxide ice systems. The ReTOF mass spectroscopic analysis resulted identification of five products bearing four oxygen atoms which include isomers of molecules formula: $C_4H_4O_4$, $C_4H_6O_4$, $C_4H_8O_4$, $C_5H_6O_4$, $C_5H_8O_4$, $C_5H_6O_5$ and $C_5H_8O_5$ with their respective sublimation profiles shown in SI Figures S17 and S18. Astrobiologically relevant sugar related molecules shown in SI Figure S19 could possibly make up a subset of sublimating molecules. However, a numerous molecules can be associated with these products; therefore no specific assignment can be made as the result would be ambiguous. A summary of molecular formula observed in this study and their corresponding chemical structures, with identified molecules marked in bold, is presented in SI Figure 20.

4. Discussion

4.1. Formation Pathways based on ReTOF Mass Spectrometry.

Within the irradiated mixed isotopologue binary ice systems of methanol and carbon monoxide ($^{13}CH_3OH-CO$, $CD_3OD-^{13}CO$, $CH_3^{18}OH-CO$ and $CH_3OH-C^{18}O$), products with mixed isotopes of the same molecular formula were observed, see Table 4. However, in the irradiated methanol isotopologue ices (CH_3OH , CD_3OD , $^{13}CH_3OH$ and $CH_3^{18}OH$) and the mixed isotopically pure methanol-carbon monoxide ices (CH_3OH-CO , CD_3OD-CO , and $CH_3^{18}OH-C^{18}O$) only products containing one isotope were identified, as expected. From these observations, we can comment on the reaction pathways as discussed below. The most intense isotopomers are marked in Table 4. A detailed discussion on the most likely formation pathways are discussed in the following sections.

4.1.1. Ketene (H_2CCO)

Evidence on the synthesis of ketene via three competing formation pathways in irradiated methanol-carbon monoxide ices was observed in this study. For sake of clarity, these pathways are labelled as (i) "2 CH_3OH " (ii) "1 CH_3OH + 1 CO " and (iii) "2 CO ". The resultant isotopomers of ketene via each pathway are listed in Table 5. It should be noted that several of the ketene isotopomers observed have an identical mass at 44 amu in the $^{13}CH_3OH-CO$ system ($H_2^{13}C^{13}CO$), the $CH_3^{18}OH-CO$ system ($H_2CC^{18}O$) and the $CH_3OH-C^{18}O$ system ($H_2CC^{18}O$) and overlap in mass with over possible C_2H_4O molecular isotopomers. However, in the irradiated

CD₃OD-¹³C ice system, isotopomers of ketene were observed at distinctive mass-to-charge ratios [$m/z = 44$ amu (D₂CCO), 45 amu (D₂C¹³CO) and 46 amu (D₂¹³C¹³CO)] allowing for a quantitative contribution of each formulation pathway. Specifically, the isotopically labeled carbon atom in this system can act as a tracer thereby elucidating reaction pathways. Here for example, D₂CCO, can only be produced stemming from a "2 CH₃OH" pathway whereas D₂C¹³CO and D₂¹³C¹³CO isotopomers are the products formed via "1 CH₃OH + 1 CO" and "2 CO" reaction mechanism respectively. Ion counts at $m/z = 44$ amu (D₂CCO), 45 amu (D₂C¹³CO) and 46 amu (D₂¹³C¹³CO) in irradiated CD₃OD-¹³C ice are indeed observed and shown in Figure 9. The most intense ion counts occur $m/z = 45$ (D₂C¹³CO) as shown in Figure 9 and imply the most prominent pathway is the "1 CH₃OH + 1 CO" reaction pathway. Surprisingly, the ion signal at $m/z = 46$ amu (D₂¹³C¹³CO) is about 70 ± 5 % of the total ion counts observed at $m/z = 45$ amu implying the overall significance of the "2 CO" formulation pathway. Whereas, the isotopomer D₂CCO ($m/z = 44$ amu) formed via the "2 CH₃OH" formulation pathway was observed at only 6 ± 2 % of the total ion counts at $m/z = 45$ amu in the methanol-carbon monoxide ices.

4.1.2. Acetaldehyde (CH₃CHO)

Following compelling evidence to the formation of acetaldehyde in both irradiated pure methanol ice and binary ices of methanol-carbon monoxide together with their isotopologue ices, we can discuss formulation pathways. Here, building blocks for the formation of acetaldehyde in pure methanol ices (CH₄ and CO) can only originate from radiolysis of CH₃OH and that both have been identified as products in the irradiated methanol systems as shown in Figure 1 and Table 2. In the case mixed methanol-carbon monoxide systems, the introduction of the carbon monoxide can further enhance the formation of acetaldehyde in a similar manner to ketene described above. Here, evidence of acetaldehyde formation via the three identified formulation pathways "2 CH₃OH", "1 CH₃OH + 1 CO" and "2 CO" are observed as well. Again in the isotopically pure ices (CH₃OH-CO, CD₃OD-CO and CH₃¹⁸OH-C¹⁸O) acetaldehyde was only detected at a single mass-to-charge ratio such as $m/z = 44$ amu (CH₃CHO), 48 amu (CD₃CDO), 46 amu (CH₃CH¹⁸O), respectively. However, in the mixed isotopic ices, especially in the case of CD₃OD-¹³C ice, acetaldehyde isotopomers formed via these three established formulation pathways are observed at $m/z = 48$ amu (CD₃CDO), 49 amu (CD₃¹³CDO), and 48 amu

($^{13}\text{CD}_3^{13}\text{CDO}$) as highlighted in the Table 5 and shown in Figure 9. The ion signals shown in Figure 9 are quite intense at $m/z = 49$ ($\text{CD}_3^{13}\text{CDO}$), further implying a predominant "1 $\text{CH}_3\text{OH} + 1 \text{CO}$ " reaction pathway. Unlike ketene formation however, acetaldehyde shows a stronger ion peak corresponding to the "2 CH_3OH " formulation pathway (CD_3CDO) with a weak "2 CO " formulation product ($^{13}\text{CD}_3^{13}\text{CDO}$).

4.1.3. $\text{C}_2\text{H}_6\text{O}$ isomers

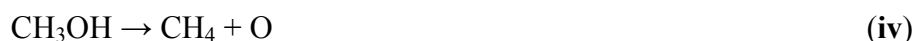
The detection of ethanol ($\text{C}_2\text{H}_5\text{OH}$) and dimethyl ether (CH_3OCH_3) in the irradiated ices of methanol and methanol-carbon monoxide ices are discussed in section 3.2.1.2. Following a similar discussion as above for ketene and acetaldehyde, we can comment on the formation pathways of these isomers based on the integrated ion counts of $\text{C}_2\text{H}_6\text{O}$ isotopomers observed in the mixed isotopic ices. The isotopomers of $\text{C}_2\text{H}_6\text{O}$ formed via "2 CH_3OH ", "1 $\text{CH}_3\text{OH} + 1 \text{CO}$ " and "2 CO " formulation pathways are listed in Table 5. It should be noted from Table 5 that, the mass-to-charge ratios of $\text{C}_2\text{H}_6\text{O}$ isotopomers are again unique only in the processed $\text{CD}_3\text{OD-}^{13}\text{CO}$ ice system. Here, $\text{C}_2\text{H}_6\text{O}$ isotopomers are expected at $m/z = 52$ amu ($\text{C}_2\text{D}_6\text{O}$), 53 amu ($^{13}\text{CCD}_6\text{O}$) and 54 amu ($^{13}\text{C}_2\text{D}_6\text{O}$) with their sublimation profiles shown in Figure 9. Here, the strong integrated ion counts at $m/z = 52$ amu ($\text{C}_2\text{D}_6\text{O}$) indicated a predominant "2 CH_3OH " formulation pathways as the integrated ion counts at $m/z = 53$ amu ($^{13}\text{CCD}_6\text{O}$) and 54 amu ($^{13}\text{C}_2\text{D}_6\text{O}$) are only $7 \pm 3\%$ and $2 \pm 1\%$ compared to the dominant ion counts at $m/z = 52$ amu. In this particular scenario, the "2 CH_3OH " formation pathway to the formation of $\text{C}_2\text{H}_6\text{O}$ product isomers is the most prevalent.

4.2. Reaction Pathways

Here, we would like to discuss the underlying reaction mechanism to the formation of ketene (H_2CCO), acetaldehyde (CH_3CHO), methyl formate (HCOOCH_3), glycolaldehyde (HOCH_2CHO) and ethylene glycol ($\text{HOCH}_2\text{CH}_2\text{OH}$) identified in irradiated methanol and methanol-carbon monoxide ices.^{53, 54, 63} Figure 10 compiles the reaction pathways which have previously been identified mostly in irradiated CH_3OH and $\text{CH}_3\text{OH-CO}$ ices based on the temporal evolution of the products recorded using infrared spectroscopy.^{53, 54} In addition, the formation mechanism of both ketene (H_2CCO) and acetaldehyde (CH_3CHO) is also included in Figure 10. Formation pathways of ketene and acetaldehyde are not verified based on their

temporal evolution in both irradiated methanol and methanol-carbon monoxide ices. However, these molecules were identified in the irradiated CH₄-CO ices.^{61, 64} Since, both CH₄ and CO are present within irradiated CH₃OH and CH₃OH-CO ices (Figure 1 and Table 2), we tried to discuss the validity of the reported formation pathways of both ketene (H₂CCO) and acetaldehyde (CH₃CHO) in the present experiments.

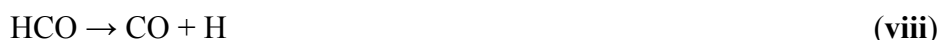
Previous experiments on the radiation induced decomposition of methanol have identified four reaction pathways as follows^{53, 54}: (i) unimolecular decomposition to hydroxymethyl (CH₂OH) radical and a suprathreshold hydrogen atom, (ii) unimolecular decomposition to methoxy (CH₃O) radical and a suprathreshold hydrogen atom, (iii) decomposition to formaldehyde (H₂CO) and molecular hydrogen and/or two hydrogen atoms and (iv) decomposition to form methane (CH₄) and atomic oxygen (term symbols have been omitted for clarity).



Further, both hydroxymethyl radical and methoxy radical were found to undergo subsequent unimolecular decomposition to produce formaldehyde (H₂CO) and atomic hydrogen via reactions v and vi, respectively.^{53, 54}



Formaldehyde may further undergo successive unimolecular decompositions via atomic hydrogen elimination to form the formyl (HCO) radical (reaction vii) and carbon monoxide (CO) (reaction viii).



In summary, the radiolysis of frozen methanol results in the formation of formyl radical (HCO), carbon monoxide (CO), methane (CH₄), formaldehyde (H₂CO), methoxy radical (CH₃O) and the hydroxymethyl radical (CH₂OH). Save for the methoxy radical (CH₃O), all of the radiolysis products have been identified via *in situ* infrared spectroscopy in the irradiated methanol isotopologue ices as presented in this study and in previous examinations.

Previous experiments demonstrated that, the newly formed products within irradiated methanol ices predominantly follow radical-radical reaction pathways.^{53, 54} Here, the radicals formed through the reactions **i** - **viii** undergo a barrierless reaction resulting in the formation of larger and more complex organics. Consider for example the reaction of formyl (HCO) radical with the hydroxymethyl (CH₂OH) radical resulting in the formation glycolaldehyde (HOCH₂CHO) as shown in reaction **ix**.



A radical-radical recombination of formyl radical (HCO) with a methoxy (CH₃O) radical (reaction **x**) can lead to the formation of methyl formate (HCOOCH₃).



Similarly, ethylene glycol (HOCH₂CH₂OH) can be formed via the dimerization of hydroxymethyl (CH₂OH) radical as shown below (reaction **xi**).



The above observations suggest that these molecules are most likely formed within the same matrix cage and a subsequent radical-radical reaction pathway is most plausible at 5.5 K where diffusion of these radicals is severely inhibited.^{53, 54}

In the case of methanol-carbon monoxide ices, the decomposition of methanol follows reaction pathways **i** - **viii**, as discussed above. In addition, hydrogenation of carbon monoxide (CO) is also possible since the suprathreshold atomic hydrogen produced during the decomposition of

methanol (reactions **i** - **viii**) can add stepwise to carbon monoxide leading to the formation of formyl radical via reaction **xii** with successive hydrogenation (reaction **xiii** and **xiv**) of formyl radical ultimately producing formaldehyde and the CH₂OH radical as well.



Recall that, in mixed isotopic ices of methanol-carbon monoxide, ¹³CH₃OH-CO, CH₃¹⁸OH-CO, CD₃OD-¹³CO and CH₃OH-C¹⁸O, two isotopomers of formaldehyde were identified (Table 2) in each system via *in situ* IR spectroscopy. As an example, in CH₃¹⁸OH-CO ices, formaldehyde was identified at 1692 cm⁻¹ and 1724 cm⁻¹ and these band positions agree within experimental uncertainty to the formaldehyde bands observed in irradiated CH₃¹⁸OH ices (H₂C¹⁸O; 1693 cm⁻¹) and CH₃OH ices (H₂CO; 1726 cm⁻¹). Therefore, we can confidently state that H₂C¹⁸O is formed following two distinct reaction pathways; first via decomposition of methanol (CH₃¹⁸OH) following reactions **iii** and **v** and secondly via the hydrogenation reaction of carbon monoxide (CO) following reactions **xii** and **xiii**. Similarly, glycolaldehyde (HOCH₂CHO) and methyl formate (HCOOCH₃) are formed via reaction via reactions **ix** and **x** which show the radical-radical recombination of a CH₂OH unit with HCO unit. As such, inclusion of two different isotopically labeled HCO unit in both glycolaldehyde (HOCH₂CHO) and methyl formate (HCOOCH₃) is expected in the processed mixed isotope systems (¹³CH₃OH-CO, CH₃¹⁸OH-CO, CD₃OD-¹³CO and CH₃OH-C¹⁸O). Indeed, the deconvolution of infrared spectra in the carbonyl absorption stretching region did reveal vibrational frequencies associated with isotopomers of glycolaldehyde and methyl formate; thereby supporting the proposed "1 CH₃OH + 1 CO" mechanism identified above.

Next is a discussion on the identified formation mechanism of acetaldehyde (CH₃CHO) and ketene (H₂CCO). Since both of these products were identified in irradiated CH₄-CO ices⁶¹ similar reaction pathways are expected as both CH₄ and CO have been identified in all of the processed ice systems. Here, the decomposition of methane produces the methyl radical (CH₃) and the methylene radical (CH₂) following reactions **xv** - **xvii**.





In the irradiated methanol ices, acetaldehyde can then be formed via the radical-radical recombination of CH_3 radical and HCO radical.



In the case of isotopologue ices of $\text{CH}_3\text{OH-CO}$, HCO can be produced via either decomposition of methanol (reactions **iii** and **vii**) or hydrogenation of carbon monoxide via reaction **xii**. Consequently, two different carbonyl stretching frequencies for acetaldehyde isotopomers are expected with evidence of this confirmed through *in situ* IR spectroscopy shown in Table 3. As an example, the formyl unit (HCO) of CH_3CHO (1726 cm^{-1}) and $\text{CH}_3\text{CH}^{18}\text{O}$ (1695 cm^{-1}) must have originated from CH_3OH and C^{18}O , respectively, in the irradiated $\text{CH}_3\text{OH-C}^{18}\text{O}$ ice. Further, evidence of this is also supported from ReTOF mass spectrometry as discussed above. Here, acetaldehyde synthesis via the "1 CH_3OH + 1 CO " formulation was found to be the dominant reaction pathway. In addition, we have also identified acetaldehyde formation following the "2 CH_3OH " reaction pathway using ReTOF mass spectrometry implying the formation of HCO radical via decomposition of a methanol molecule as shown in reactions **iii** and **vii**.

In the irradiated methanol ices, ketene (H_2CCO) can be formed via the reaction of the CH_2 radical (reactions **xvi** and **xvii**) with CO formed via the decomposition of CH_3OH molecule (reactions **i** and **v-viii**).



In addition, ketene can also be formed via reaction **xx** - **xxii** in carbon monoxide rich ices, as identified previously.⁶⁴



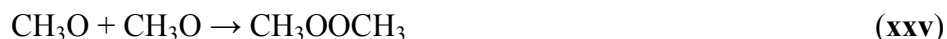
The validity of the reaction **xx** is verified via the detection of CO_2 in the present experiment (Figure 1 and Table 2). In addition, CCO has been previously observed following 5 keV electron irradiation of pure carbon monoxide ices⁸⁷ at 1988 cm^{-1} and post broadband UV photolysis of carbon monoxide ice at 1990 cm^{-1} .⁸⁸ Further evidence in support of the proposed reaction pathway to ketene is also enhanced from ReTOF mass spectroscopic analysis. The ReTOF mass

spectroscopic analysis resulted identification of ion counts at three different mass-to-charge ratios, $m/z = 44$ amu (D_2CCO), 45 amu ($D_2C^{13}CO$) and 46 amu ($D_2^{13}C^{13}CO$) as shown in Figure 9. Here, in the processed CD_3OD - ^{13}CO ice system two ketene isotopomers, D_2CCO ($m/z = 44$ amu) and $D_2C^{13}CO$ (45 amu) are expected to form via reaction **xix** and the reactions **xx-case** is expected to produce $D_2^{13}C^{13}CO$ ($m/z = 46$ amu) since both the carbon atoms are originated from ^{13}CO molecules.

Finally, we would like to comment on the general reaction pathways ultimately producing larger molecules identified above. Here, radical-radical recombination of a methyl radical (CH_3) with methoxy radical (CH_3O) (reaction **xxiii**) and hydroxymethyl radical (CH_2OH) (reaction **xxiv**) can lead to the formation of C_2H_6O isomers, dimethyl ether (CH_3OCH_3) and ethanol (CH_3CH_2OH), respectively.



Similarly, dimerization of the CH_3O radical (reaction **xxv**) and reaction with CH_2OH (reaction **xxvi**) can result the formation of dimethyl peroxide (CH_3OOCH_3) and methoxymethanol (CH_3OCH_2OH), respectively.



In addition, dimerization of HCO radical can also form the product glyoxal ($HCOCHO$) via reaction **xxvii**.



A summary schematic of the overall formation routes of the products identified using ReTOF mass spectroscopic analysis and *in situ* IR spectroscopy is presented in Figure 11. Among them, the possible formation pathways mostly via radical-radical recombination pathways are discussed above for ketene (C_2H_2O), acetaldehyde (C_2H_4O), glycolaldehyde ($C_2H_4O_2$) and ethylene glycol ($C_2H_6O_2$). Also, a possible formation route to methoxymethane (C_2H_6O), ethanol (C_2H_6O), dimethyl peroxide ($C_2H_6O_2$), methoxymethanol ($C_2H_6O_2$) and glyoxal ($C_2H_2O_2$) are discussed.

5. Summary

The present experiments demonstrated that complex organics are formed in methanol and mixed methanol-carbon monoxide ices exposed to ionizing radiation at 5.5 K. Frozen methanol and carbon monoxide have long been identified as key constituents within molecular clouds of the interstellar medium in addition to ubiquitous water along with minor amounts of methane, ammonia and carbon dioxide.³⁵⁻⁴¹ The molecular abundances of methanol within the icy mantles vary from 5% to 30% relative to water in several low mass star-forming regions or dark molecular clouds.^{36, 89, 90} In addition, carbon monoxide is often present with methanol in numerous sources with abundances in icy mantles typically around 20% with respect to water.³⁵⁻⁴¹ These icy mantles are constantly being bombarded with high energy galactic cosmic rays and/or from the interstellar UV field. Consequently, an understanding of the radiation induced chemical modifications of methanol and mixed methanol-carbon monoxide ices remains extremely important in understanding the chemical evolution of molecular clouds. In the current study presented here, a combined *in situ* infrared spectroscopic (solid state) and mass spectroscopic (gas phase) detection scheme was employed to identify the endogenous products formed within methanol and methanol-carbon monoxide ices exposed to energetic electrons simulating the equivalent exposure of chemical processing via galactic cosmic rays⁹¹⁻⁹³. Experiments with isotopically labeled methanol (CH_3OH , CD_3OD , $^{13}\text{CH}_3\text{OH}$, and $\text{CH}_3^{18}\text{OH}$) and methanol-carbon monoxide ices ($\text{CH}_3\text{OH-CO}$, $\text{CD}_3\text{OD-CO}$, $^{13}\text{CH}_3\text{OH-CO}$, $\text{CH}_3^{18}\text{OH-CO}$, $\text{CD}_3\text{OD-}^{13}\text{CO}$, $\text{CH}_3^{18}\text{OH-C}^{18}\text{O}$, and $\text{CH}_3\text{OH-C}^{18}\text{O}$) were conducted to help identify products and reaction pathways via the observed frequency shifts of functional groups and mass shifts in gas phase detection of TPD spectra. *The infrared spectroscopic analysis resulted in the identification of the following radiolysis products: hydroxymethyl radical (CH_2OH), formyl radical (HCO), methane (CH_4), formaldehyde (H_2CO), carbon dioxide (CO_2), ethylene glycol ($\text{HOCH}_2\text{CH}_2\text{OH}$), glycolaldehyde (HOCH_2CHO), methyl formate (HCOOCH_3), and ketene (H_2CCO).* Also of note is the suggested formation of large and complex carbonyl bearing organics such as acetaldehyde, saturated/unsaturated high mass aldehydes (e.g. propanal and propenal) and ketones (e.g. acetone) through deconvolution of the carbonyl absorption bands, observed in both methanol and methanol-carbon monoxide isotopologue ices. However, the infrared spectroscopic analysis is limited as similar functional groups overlap together resulting in an ambiguous assignment. Subsequently, we conducted temperature programmed desorption (TPD) complimented with single photon ionization ReTOF mass spectrometry at 10.49 eV to monitor the endogenous

products sublimating. Using ReTOF mass spectrometry of the sublimating species, we have definitively identified ketene (H_2CCO), acetaldehyde (CH_3COH), ethanol (C_2H_5OH), dimethyl ether (CH_3OCH_3), glyoxal ($HCOCOH$), glycolaldehyde ($HOCH_2CHO$), ethene-1,2-diol ($HOCHCHOH$), ethylene glycol ($HOCH_2CH_2OH$), methoxy methanol (CH_3OCH_2OH) and glycerol ($CH_2OHCHOHCH_2OH$) in the irradiated ice systems. Moreover, we were able to identify molecules containing up to five oxygen atoms sublimating from the processed ices; however, no specific assignments of these large organics could be made at this time.

Here it is worth comparing the identified products in the present experiments with the C/H/O bearing molecules detected in the interstellar medium which are displayed in Figure 12. All of the alcohols that have been observed in the ISM have been identified in this study, save for that of vinyl alcohol (CH_2CHOH) which has at this time been labelled as tentatively identified. Among the aldehydes detected in the ISM, formaldehyde (H_2CO) and acetaldehyde (CH_3CHO) were confirmed as an endogenous synthesized products following exposure to ionizing radiation. Higher mass aldehydes such as propanal (CH_3CH_2CHO) and propenal (CH_2CHCHO) have been tentatively identified as possible isomers of C_3H_6O and C_3H_4O identified via ReTOF spectrometry. Within the group ester type molecules, methyl formate ($HCOOCH_3$) was confirmed from only infrared spectroscopy as the ionization energy (10.84 eV) is greater than available ionization energy (10.49 eV) used in the present study while methyl acetate (CH_3COOCH_3) and ethyl formate ($HCOOC_2H_5$) were only tentatively assigned as possible $C_3H_6O_2$ isomers. The only sugar molecule observed thus far in the ISM is glycolaldehyde ($HOCH_2CHO$) and has been confirmed via both infrared spectroscopy and ReTOF mass spectrometry in all ice systems upon exposure to ionizing radiation presented here. Both of the ether type molecules that have been detected in the interstellar medium, dimethyl ether (CH_3OCH_3) and methoxyethane ($CH_3OCH_2CH_3$), are identified as well in both the irradiated methanol and methanol-carbon monoxide ices using ReTOF mass spectrometry. Finally, ketene (H_2CCO) has been identified as a radiolytic byproduct in all ice systems, via both FTIR spectroscopy and ReTOF mass spectrometry. Unfortunately, in the present study we could not elucidate the majority of the higher mass organics containing anywhere from three to five oxygen atoms as the calibration experiments were not unique enough to disentangle the contribution from each possible isomer. However, future experimental investigations with

tunable vacuum ultraviolet light for selective ionization will allow the specific assignment of isomers based on the unique ionization energy, complimented with their m/z ratios and unique temperature or energy of desorption.

Several novel reaction pathways have been identified in this study as well. These reaction pathways have been classified for the sake of simplicity as (i) "2 CH₃OH" (ii) "1 CH₃OH + 1 CO" and (iii) "2 CO" and are summarized in Figures 10 and 11. By conducting experiments with mixed isotopes of a specific atom, we were able to trace the isotope in the observed m/z shift in the TPD spectra and frequency shift via *in situ* IR spectroscopy. As anticipated in the processed mixed ices the "1 CH₃OH + 1 CO" is the most prominent reaction pathway producing the expected isotopologues as is correlated with the most intense ion peaks. However, the "2 CH₃OH" and "2 CO" reaction pathways as described in section 4.2, did result in enough products with high enough column densities to be observed via IR spectroscopy and ionized in the gas phase during TPD ReTOF analysis; as such are not inconsequential in the formation of complex organics. Future experiments will explore the possibility of isotopic fractionation resulting from these identified pathways.

Finally, we would like to comment on the astrobiological relevance of the present reaction products. We have identified several products associated with the sugar related molecules formed within methanol and methanol-carbon monoxide ices systems exposed to ionizing radiation. As mentioned, the simplest form of sugar, glycolaldehyde (HOCH₂CHO) has been identified. In addition, the sugar alcohol (ethylene glycol; HOCH₂CH₂OH) and the dehydrogenated form of glycolaldehyde (glyoxal; HCOCHO) were also identified in irradiated methanol ice (only ethylene glycol) and methanol carbon monoxide ice (both ethylene glycol and glyoxal). We have also found evidence on the possible formation of higher mass sugar molecules as shown in Figure 13. Here, we observed products sublimating with molecular formula C₃H₆O₃ in both all of the processed ice systems. Unfortunately we can only suggest that within these group of isomers that C₃ sugar molecules (glyceraldehyde and 1,3-dihydroxyacetone) are formed. Previous searches for these C₃-sugar molecules, glyceraldehyde (HOCH₂CH(OH)CHO)²¹ and 1,3-dihydroxyacetone ((HOCH₂)₂CO)²²⁻²⁴ in the ISM have been remained inconclusive until now. However, these molecules were found on the recovered

carbonaceous meteorites on Earth,⁹ implying the presence of an extraterrestrial origin and the possibility of an *ex situ* delivery to a prebiotic earth. In addition, the survivability of glycolaldehyde has recently been demonstrated in simulated meteoric impacts.⁹⁴ Finally, we have also identified C₄H₈O₄ and C₅H₈O₅ in irradiated methanol-carbon monoxide ices. These products can be linked to the C₄-sugar molecules erythrose (CH₂OH(CHOH)₂CHO) and tetulose (CH₂OHCHOHC(O)HCH₂OH) and dehydrated forms of Ribose and Ribulose (C₅-sugars) as shown in Figure 13. These molecules are key components of RNA, DNA and cell membranes, as well as important energy sources. Consequently, the prebiotic origin of large sugar molecules is essential for aiding in the overall understanding of the origin of life.

The results presented here demonstrate that significantly large complex organics are synthesized as a result from exposure to ionizing radiation at relatively low doses, i.e. a few eV per molecule as typical for an icy covered grain within a cold molecular cloud. Furthermore, our results imply that state-of-the-art experimental techniques are necessary to fully elucidate the rich and complex chemistry that is induced within these simulated astrophysical environments. As described above, many of the molecules were masked within the *in situ* FTIR spectroscopy due to the similar functional groups and subsequent overlapping frequencies. Utilizing temperature program desorption coupled with single photoionization reflectron time-of-flight mass spectrometry, a plethora of large complex organics were detected. Unfortunately, many of the molecules could not specifically be identified based on their TPD profile alone. Next generation experiments are currently being designed to reveal the exact molecular structure of the tentatively assigned molecules based upon their unique ionization energies correlated with their distinct temperature of desorption. Exploiting each molecule's exclusive ionization energy will be accomplished from the use of *tunable* vacuum ultraviolet light photons generated via four wave mixing. This technique has recently been successfully implemented with promising results to be disseminated in the near future and will be used more extensively with upcoming experimental studies.

Acknowledgements

The authors would like to thank the NASA Exobiology Program MNX13AH62G, W. M. Keck Foundation and the University of Hawaii at Manoa for their financial support.

Supplementary Information

The supplementary information section contains additional information the reader may find useful but not particularly necessary for understanding the results presented here. For example, tables explaining the composition of the calibration samples along with figures displaying numerous TPD profiles relevant for the molecules that were only tentatively assigned have been placed in this section.

References

1. Cologne, The Cologne Database for Molecular Spectroscopy: <http://www.astro.uni-koeln.de/cdms>, 2013, DOI: The Cologne Database for Molecular Spectroscopy.
2. E. Herbst, *Physical Chemistry Chemical Physics*, 2014, 16, 3344-3359.
3. E. Herbst and E. F. van Dishoeck, *Annual Review of Astronomy and Astrophysics*, 2009, 47, 427-480.
4. A. I. Vasyunin and E. Herbst, *The Astronomical Journal*, 2013, 769, 34.
5. Å. Hjalmarson, Bergman, P., Nummelin, A., Noordwijk, ESA, 2001.
6. D. T. Halfen, V. Ilyushin and L. M. Ziurys, *The Astronomical Journal*, 2011, 743, 60.
7. A. F. Jalbout, *Orig. Life Evol. Biosph.*, 2008, 38, 489-497.
8. J. E. Elsila, J. P. Dworkin, M. P. Bernstein, M. P. Martin and S. A. Sandford, *Astrophys. J.*, 2007, 660, 911.
9. G. Cooper, N. Kimmich, W. Belisle, J. Sarinana, K. Brabham and L. Garrel, *Nature*, 2001, 414, 879-883.
10. M. H. Engel and S. A. Macko, *Precambrian Res.*, 2001, 106, 35-45.
11. M. H. Engel and S. A. Macko, *Nature*, 1997, 389, 265-268.
12. H. Busemann, A. F. Young, C. M. D. Alexander, P. Hoppe, S. Mukhopadhyay and L. R. Nittler, *Science*, 2006, 312, 727-730.
13. O. Botta, D. Glavin, G. Kminek and J. Bada, *Origins of life and evolution of the biosphere*, 2002, 32, 143-163.
14. J. M. Hollis, F. J. Lovas and P. R. Jewell, *The Astrophysical Journal Letters*, 2000, 540, L107-L110.
15. J. M. Hollis, S. N. Vogel, L. E. Snyder, P. R. Jewell and F. J. Lovas, *The Astrophysical Journal Letters*, 2001, 554, L81-L85.
16. D. T. Halfen, A. J. Apponi, N. Woolf, R. Polt and L. M. Ziurys, *Astrophys. J.*, 2006, 639, 237-245.
17. M. A. Requena-Torres, J. Martín-Pintado, S. Martín and M. R. Morris, *Astrophys. J.*, 2008, 672, 352.
18. J. K. Jørgensen, C. Favre, S. E. Bisschop, T. L. Bourke, E. F. van Dishoeck and M. Schmalzl, *The Astrophysical Journal Letters*, 2012, 757, L4.
19. J. M. Hollis, F. J. Lovas, P. R. Jewell and L. H. Coudert, *The Astrophysical Journal Letters*, 2002, 571, L59-L62.
20. J. Crovisier, D. Bockelee-Morvan, N. Biver, P. Colom, D. Despois and D. C. Lis, *Astronomy and Astrophysics*, 2004, 418, L35-L38.
21. J. M. Hollis, P. R. Jewell, F. J. Lovas, A. Remijan and H. Mollendal, *The Astrophysical Journal Letters*, 2004, 610, L21.
22. W. S. L. Weaver and G. A. Blake, *Astrophys. J.*, 2005, 624, L33-L36.
23. S. L. Widicus, R. Braakman, D. R. Kent Iv and G. A. Blake, *J. Mol. Spectrosc.*, 2004, 224, 101-106.
24. A. J. Apponi, D. T. Halfen, L. M. Ziurys, J. M. Hollis, A. J. Remijan and F. J. Lovas, *The Astrophysical Journal Letters*, 2006, 643, L29-L32.
25. M. A. Requena-Torres, J. Martín-Pintado, A. Rodríguez-Franco, S. Martín, N. J. Rodríguez-Fernández and P. De Vicente, *Astronomy and Astrophysics*, 2006, 455, 971-985.

26. A. Bacmann, V. Taquet, A. Faure, C. Kahane and C. Ceccarelli, *Astronomy and Astrophysics*, 2012, 541, L12.
27. A. G. G. M. Tielens and W. Hagen, *Astronomy and Astrophysics*, 1982, 114, 245-260.
28. D. P. Ruffle and E. Herbst, *MNRAS*, 2001, 322, 770.
29. R. T. Garrod and E. Herbst, *A&A*, 2006, 457, 927-936.
30. R. T. Garrod, S. L. W. Weaver and E. Herbst, *Astrophys. J.*, 2008, 682, 283.
31. A. Belloche, R. T. Garrod, H. S. P. Muller, K. M. Menten, C. Comito and P. Schilke, *Astronomy and Astrophysics*, 2009, 499, 215-232.
32. R. T. Garrod and S. L. Widicus Weaver, *Chem. Rev. (Washington, DC, U. S.)*, 2013, 113, 8939-8960.
33. T. G. Robin, *Astrophys. J.*, 2013, 765, 60.
34. H. G. Arce, J. Santiago-Garcia, J. K. Jorgensen, M. Tafalla and R. Bachiller, *The Astrophysical Journal Letters*, 2008, 681, L21-L24.
35. E. L. Gibb, D. C. B. Whittet, W. A. Schutte, A. C. A. Boogert, J. E. Chiar, P. Ehrenfreund, P. A. Gerakines, J. V. Keane, A. G. G. M. Tielens, E. F. v. Dishoeck and O. Kerkhof, *Astrophys. J.*, 2000, 536, 347.
36. E. L. Gibb, D. C. B. Whittet, A. C. A. Boogert and A. G. G. M. Tielens, *The Astrophysical Journal Supplement Series*, 2004, 151, 35-73.
37. A. C. A. Boogert, K. M. Pontoppidan, C. Knez, F. Lahuis, J. Kessler-Silacci, E. F. Van Dishoeck, G. A. Blake, J. C. Augereau, S. E. Bisschop and S. Bottinelli, *Astrophys. J.*, 2008, 678, 985.
38. K. I. Öberg, A. C. A. Boogert, K. M. Pontoppidan, G. A. Blake, N. J. Evans, F. Lahuis and E. F. v. Dishoeck, *Astrophys. J.*, 2008, 678, 1032.
39. K. M. Pontoppidan, A. C. A. Boogert, H. J. Fraser, E. F. van Dishoeck, G. A. Blake, F. Lahuis, K. I. Öberg, N. J. Evans and C. Salyk, *Astrophys. J.*, 2008, 678, 1005.
40. K. I. Öberg, A. C. A. Boogert, K. M. Pontoppidan, B. Saskia van den, E. F. v. Dishoeck, B. Sandrine, A. B. Geoffrey and I. Neal J. Evans, *Astrophys. J.*, 2011, 740, 109.
41. W. T. Reach, M. S. Kelley and J. Vaubaillon, in *ArXiv e-prints*, 2013, vol. 1306, p. 2381.
42. R. I. Kaiser, G. Eich, A. Gabrysch and K. Roessler, *Astrophys. J.*, 1997, 484, 487-498.
43. R. I. Kaiser and K. Roessler, *Astrophys. J.*, 1998, 503, 959.
44. M. Garozzo, D. Fulvio, Z. Kanuchova, M. E. Palumbo and G. Strazzulla, *Astronomy and Astrophysics*, 2010, 509, A67.
45. S. E. Bisschop, G. W. Fuchs, E. F. van-Dishoeck and H. Linnartz, *Astron. Astrophys.*, 2007, 474, 1061-1071.
46. W. D. Geppert, M. Hamberg and R. D. Thomas, et al. , *Faraday Discuss.*, 2006, 133, 177.
47. N. J. Mason, A. Dawes, P. D. Holtom, R. J. Mukerji, M. P. Davis, B. Sivaraman, R. I. Kaiser, S. V. Hoffmann and D. A. Shaw, *Faraday Discuss.*, 2006, 133, 311-329.
48. C. J. Bennett, C. S. Jamieson, Y. Osamura and R. I. Kaiser, *Astrophys. J.*, 2005, 624, 1097-1115.
49. C. J. Bennett, Y. Osamura, M. D. Lebar and R. I. Kaiser, *The Astronomical Journal*, 2005, 634, 698-711
50. L. Zhou, R. I. Kaiser, L. G. Gao, A. H. H. Chang, M. C. Liang and Y. Y. Yung, *ApJ*, 2008, 686, 1493-1502.
51. C. J. Bennett, T. Hama, Y. S. Kim, M. Kawasaki and R. I. Kaiser, *ApJ*, 2011, 727, 27-37.
52. C. J. Bennett and R. I. Kaiser, *Astrophys. J.*, 2007, 660, 1289-1295.

53. C. J. Bennett, S.-H. Chen, B.-J. Sun, A. H. H. Chang and R. I. Kaiser, *Astrophys. J.*, 2007, 660, 1588.
54. C. J. Bennett and R. I. Kaiser, *Astrophys. J.*, 2007, 661, 899-909.
55. P. A. Gerakines, W. A. Schutte and P. Ehrenfreund, *Astronomy and Astrophysics*, 1996, 312, 289-305.
56. K. I. Öberg, R. T. Garrod, E. F. van Dishoeck and H. Linnartz, *Astronomy and Astrophysics*, 2009, 504, 891-913.
57. T. D. Harris, D. H. Lee, M. Q. Blumberg and C. R. Arumainayagam, *The Journal of Physical Chemistry*, 1995, 99, 9530-9535.
58. P. Modica and M. E. Palumbo, *Astronomy and Astrophysics*, 2010, 519, 22.
59. P. Modica, M. E. Palumbo and G. Strazzulla, *Planetary and Space Science*, 2012, 73, 425-429.
60. Y. J. Chen, A. Ciaravella, G. M. M. Caro, C. Cecchi-Pestellini, A. Jimenez-Escobar, K. J. Juang and T. S. Yih, *Astrophys. J.*, 2013, 778, 162.
61. R. I. Kaiser, S. Maity and B. M. Jones, *Physical Chemistry Chemical Physics*, 2014, 16, 3399-3424.
62. B. M. Jones and R. I. Kaiser, *The Journal of Physical Chemistry Letters*, 2013, 4, 1965-1971.
63. S. Maity, R. I. Kaiser and B. M. Jones, *Faraday Discuss.*, 2014, 168, 485-516.
64. S. Maity, R. I. Kaiser and B. M. Jones, *The Astronomical Journal*, 2014, 788, 36.
65. M. S. Westley, G. A. Baratta and R. A. Baragiola, *The Journal of Chemical Physics*, 1998, 108, 3321-3326.
66. R. Brunetto, G. Caniglia, G. A. Baratta and M. E. Palumbo, *Astrophys. J.*, 2008, 686, 1480-1485.
67. A. M. Goodman, *Appl. Opt.*, 1978, 17, 2779-2787.
68. W. R. M. Rocha and S. Pilling, *Spectrochimica Acta Part A: Molecular and Biomolecular Spectroscopy*, 2014, 123, 436-446.
69. R. Luna, M. Á. Satorre, M. Domingo, C. Millán and C. Santonja, *Icarus*, 2012, 221, 186-191.
70. P. Hovington, D. Drouin and R. Gauvin, *Scanning*, 1997, 19, 1-14.
71. D. Drouin, C. A. R., D. Joly, X. Tastet, V. Aimez and R. Gauvin, *Scanning*, 2007, 29, 92-101.
72. R. Hilbig and R. Wallenstein, *Quantum Electronics, IEEE Journal of*, 1981, 17, 1566-1573.
73. W. A. VonDraese, S. Okajima and J. P. Hessler, *Appl. Opt.*, 1988, 27, 4057-4061.
74. R. L. Hudson and M. H. Moore, *Icarus*, 2000, 145, 661-663.
75. R. L. Hudson and M. J. Loeffler, *Astrophys. J.*, 2013, 77, 109.
76. A. Aspiala, J. Murto and P. Sten, *Chem. Phys.*, 1986, 106, 399-412.
77. J. Ceponkus, W. Chin, M. Chevalier, M. Broquier, A. Limongi and C. Crépin, *J. Chem. Physics*, 2010, 133, 094502/094501-094502/094507.
78. R. L. Hudson and M. H. Moore, *Radiat. Phys. Chem.*, 1995, 45, 779-789.
79. G. A. Baratta, A. C. Castorina, G. Leto, M. E. Palumbo, F. Spinella and G. Strazzulla, *Planetary and Space Science*, 1994, 42, 759-766.
80. M. P. Collings, J. W. Dever, H. J. Fraser and M. R. S. McCoustra, *Astrophys. Space Sci.*, 2003, 285, 633-659.

81. H. Y. Afeefy, J. F. Liebman and S. E. Stein, in *Neutral Thermochemical Data*, eds. P. J. Linstrom and W. G. Mallard, National Institute of Standards and Technology, Gaithersburg, MD, 2013, vol. 69.
82. Y. J. Shi, S. Consta, A. K. Das, B. Mallik, D. Lacey and R. H. Lipson, *The Journal of Chemical Physics*, 2002, 116, 6990-6999.
83. F. Bell, Q. N. Ruan, A. Golan, P. R. Horn, M. Ahmed, S. R. Leone and M. Head-Gordon, *J. Am. Chem. Soc.*, 2013, 135, 14229-14239.
84. D. Vijay and G. N. Sastry, *Journal of Molecular Structure: THEOCHEM*, 2005, 714, 199-207.
85. M. D. Boamah, K. K. Sullivan, K. K. Shulenberger, C. M. Soe, L. M. Jacob, F. C. Yhee, K. E. Atkinson, M. C. Boyer, D. R. Haines and C. R. Arumainayagam, *Faraday Discuss.*, 2014, 168, 1-18.
86. R. A. Johnson and A. E. Stanley, *Appl. Spectrosc.*, 1991, 45, 218-222.
87. C. S. Jamieson, A. M. Mebel and R. I. Kaiser, *The Astrophysical Journal Supplement Series*, 2006, 163, 184-206.
88. P. A. Gerakines and M. H. Moore, *Icarus*, 2001, 154, 372.
89. E. Dartois, W. Schutte, T. R. Geballe, K. Demyk, P. Ehrenfreund and L. d'Hendecourt, *Astronomy and Astrophysics*, 1999, 342, L32-L35.
90. K. M. Pontoppidan, E. Dartois, E. F. van Dishoeck, W.-F. Thi and L. d'Hendecourt, *Astronomy and Astrophysics*, 2003, 404, L17-L20.
91. M. H. Moore, R. L. Hudson and P. A. Gerakines, *Spectrochimica Acta*, 2001, 57, 843-858.
92. R. I. Kaiser and K. Roessler, *Astrophys. J.*, 1997, 475, 144-154.
93. G. Strazzulla, A. C. Castorina and M. E. Palumbo, *Planetary and Space Science*, 1995, 43, 1247-1251.
94. V. P. McCaffrey, N. E. B. Zellner, C. M. Waun, E. R. Bennett and E. K. Earl, *Origins of Life and Evolution of Biospheres*, 2014, DOI: 10.1007/s11084-014-9358-5, 1-14.

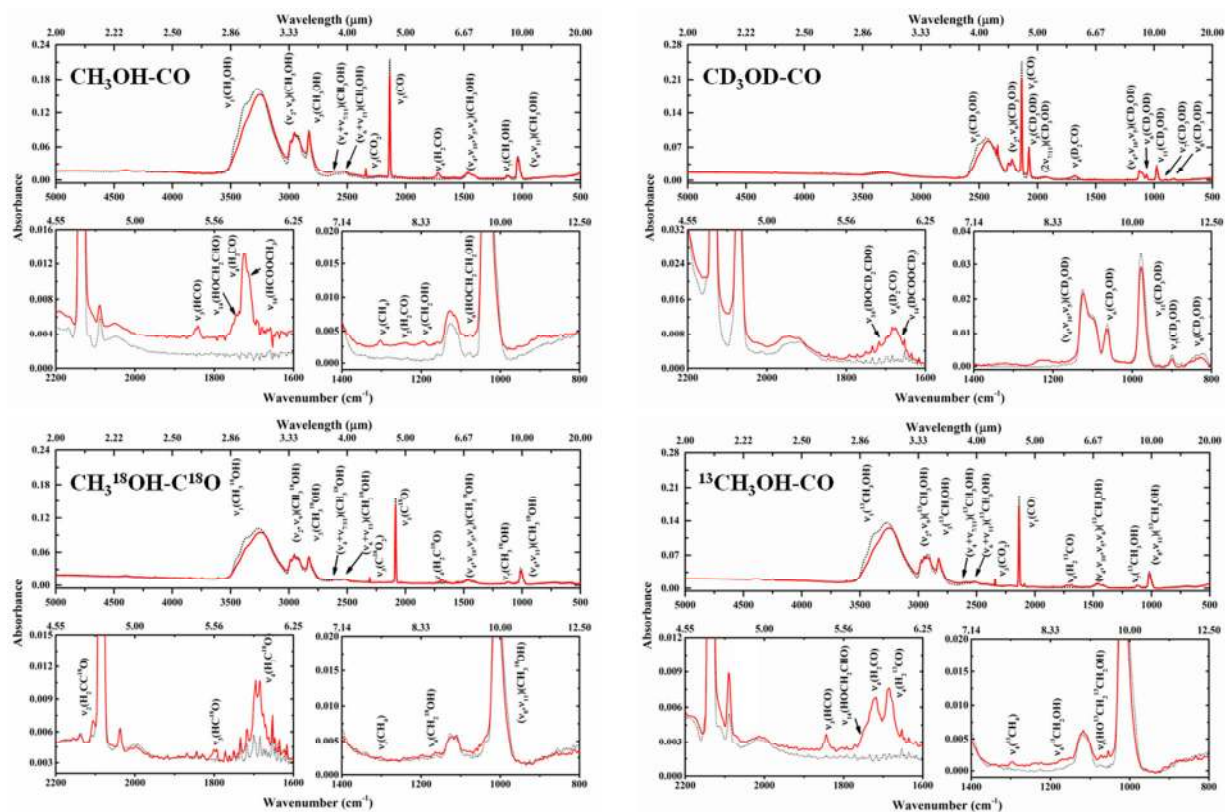


Figure 1B. Infrared absorption spectra of methanol - carbon monoxide mixed ices ($\text{CH}_3\text{OH-CO}$, $\text{CD}_3\text{OD-CO}$, $\text{CH}_3^{18}\text{OH-C}^{18}\text{O}$, $^{13}\text{CH}_3\text{OH-CO}$) before (dotted trace) and after (solid trace) irradiation at 5.5 K. Newly emerged absorption features in each ice are shown in $2200 - 1600 \text{ cm}^{-1}$ and $1400 - 800 \text{ cm}^{-1}$ regions along with the assignments as listed in Table 2.

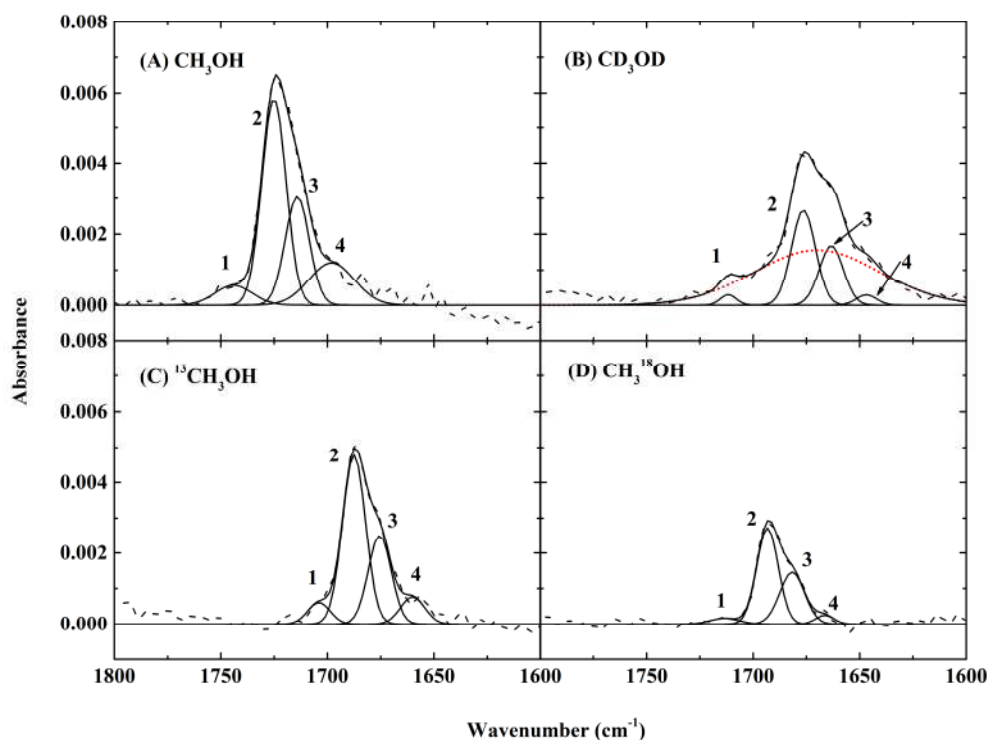


Figure 1C. Deconvoluted infrared absorption features in the region of the carbonyl functional group in (A) CH_3OH , (B) CD_3OD , (C) $^{13}\text{CH}_3\text{OH}$, and (D) $\text{CH}_3^{18}\text{OH}$ ices. The bands marked as (1) and (4) are assigned as the ν_{14} and $2\nu_6$ bands of glycolaldehyde (HOCH_2CHO), respectively. The bands marked as (2) and (3) are assigned to formaldehyde (H_2CO) and methyl formate (HCOOCH_3). The dotted line in (B) corresponds to $2\nu_8$ of CD_3OD as in the pristine ice.

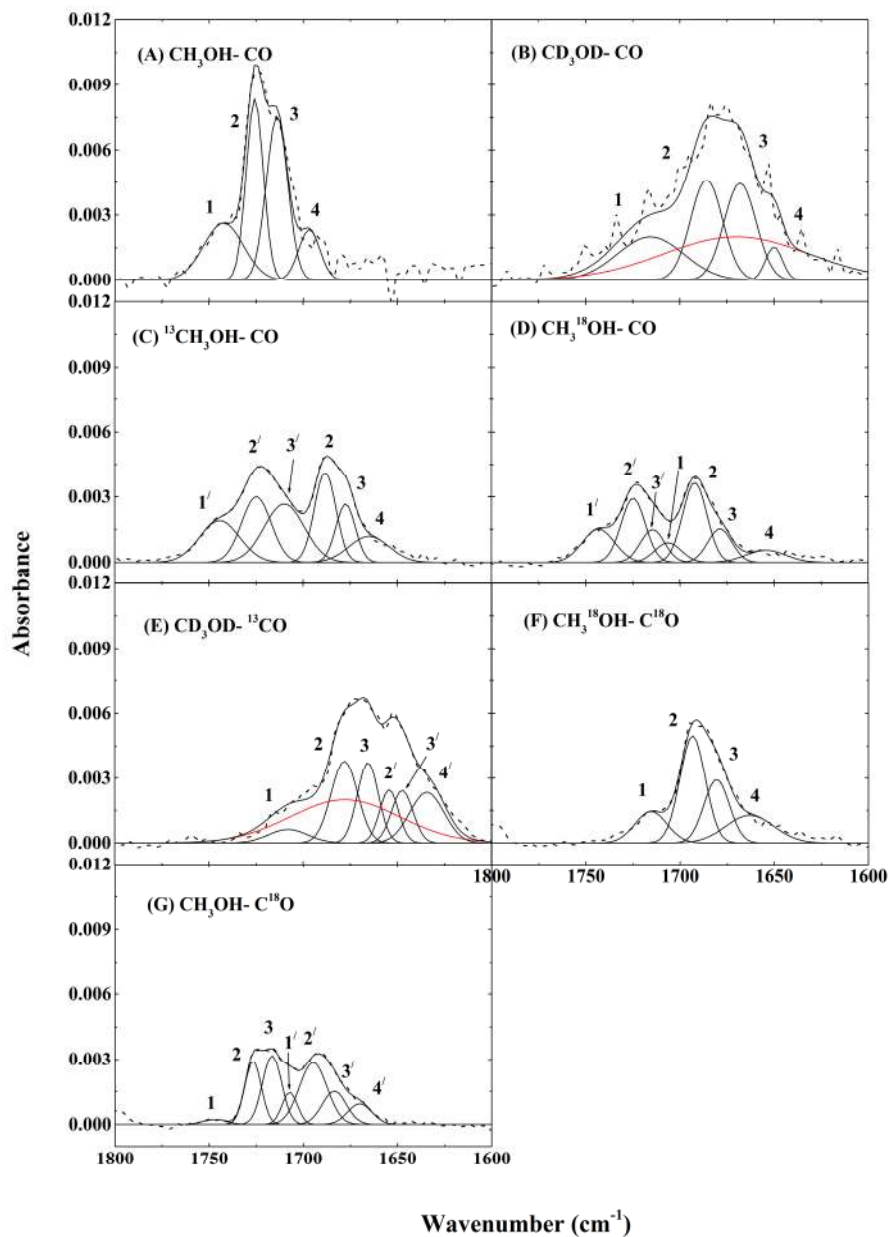


Figure 1D. Deconvoluted infrared absorption features in the region of the carbonyl functional group in (A) $\text{CH}_3\text{OH-CO}$, (B) $\text{CD}_3\text{OD-CO}$, (C) $^{13}\text{CH}_3\text{OH-CO}$, (D) $\text{CH}_3^{18}\text{OH-CO}$, (E) $\text{CD}_3\text{OD-}^{13}\text{CO}$, (F) $\text{CH}_3^{18}\text{OH-C}^{18}\text{O}$, and (G) $\text{CH}_3\text{OH-C}^{18}\text{O}$ ices. The bands marked as (1), (2), (3) and (4) are assigned to ν_{14} of glycolaldehyde, ν_4 of formaldehyde and ν_{14} of methyl formate, and $2\nu_6$ bands of glycolaldehyde and their isotopomers (Table 2), respectively. In C, D, E, and G, bands marked as (1'), (2'), (3') and (4') are assigned to ν_{14} of glycolaldehyde, ν_4 of formaldehyde and ν_{14} of methyl formate, and $2\nu_6$ bands of glycolaldehyde and their isotopomers, respectively. The dotted lines in (B) and (E) correspond to $2\nu_8$ of CD_3OD as in the pristine ice.

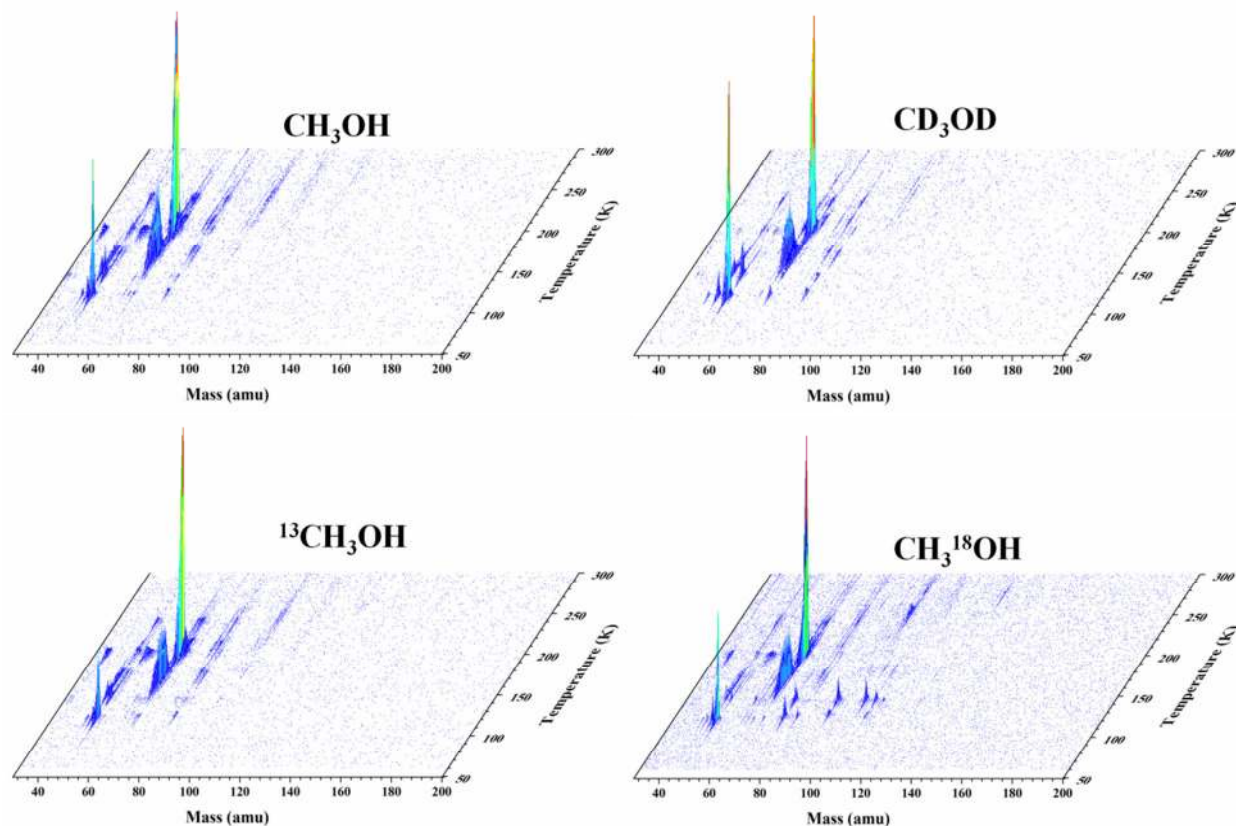


Figure 2A. Reflectron time-of-flight (ReTOF) mass spectra as a function of temperature showing newly formed products subliming into the gas phase from radiation processed methanol isotopologue ices recorded at a photoionization energy of 10.49 eV.

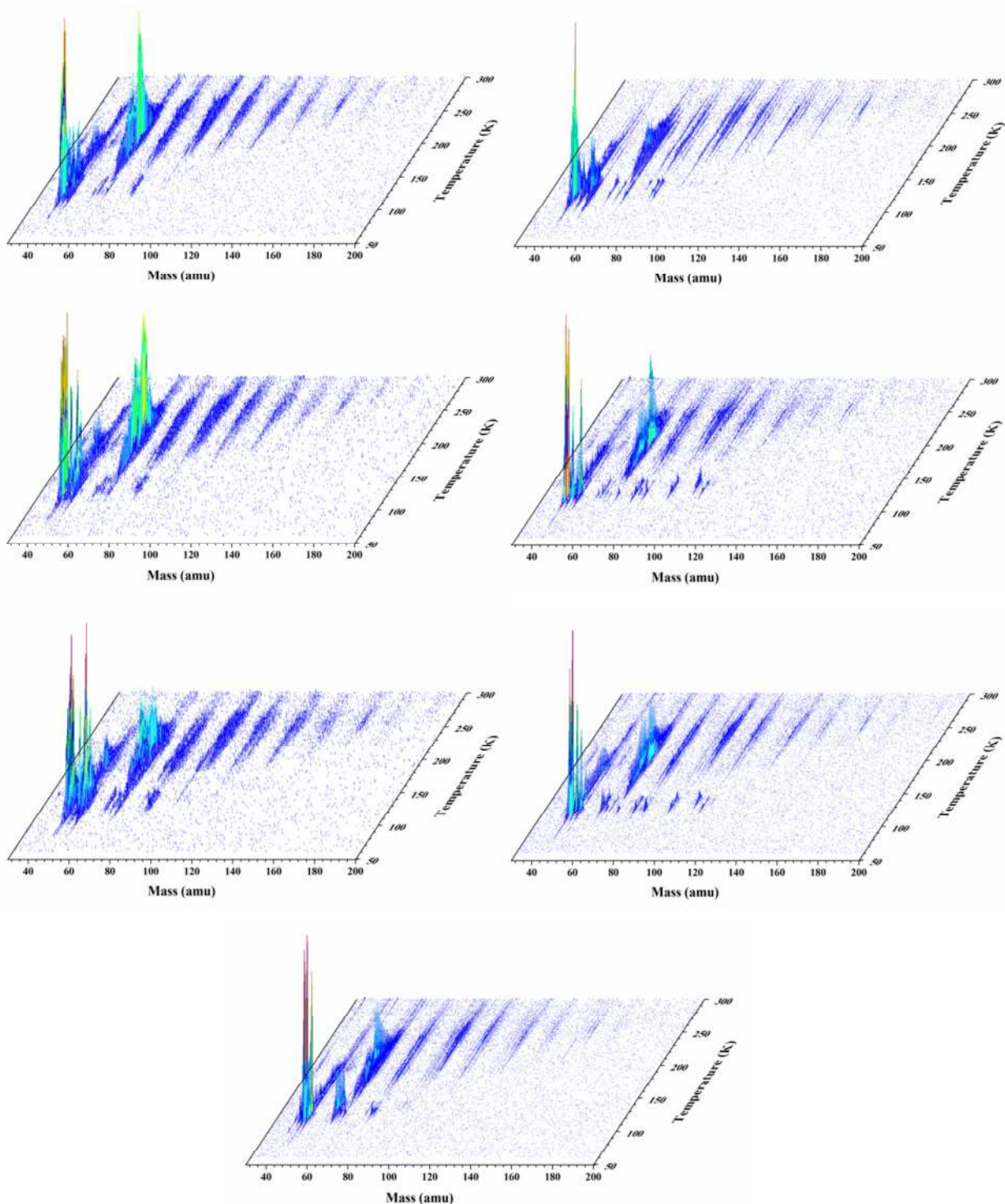


Figure 2B. Reflectron time-of-flight (ReTOF) mass spectra as a function of temperature showing newly formed products subliming in to the gas phase from radiation processed methanol - carbon monoxide isotopologue ices recorded at a photoionization energy of 10.49 eV.

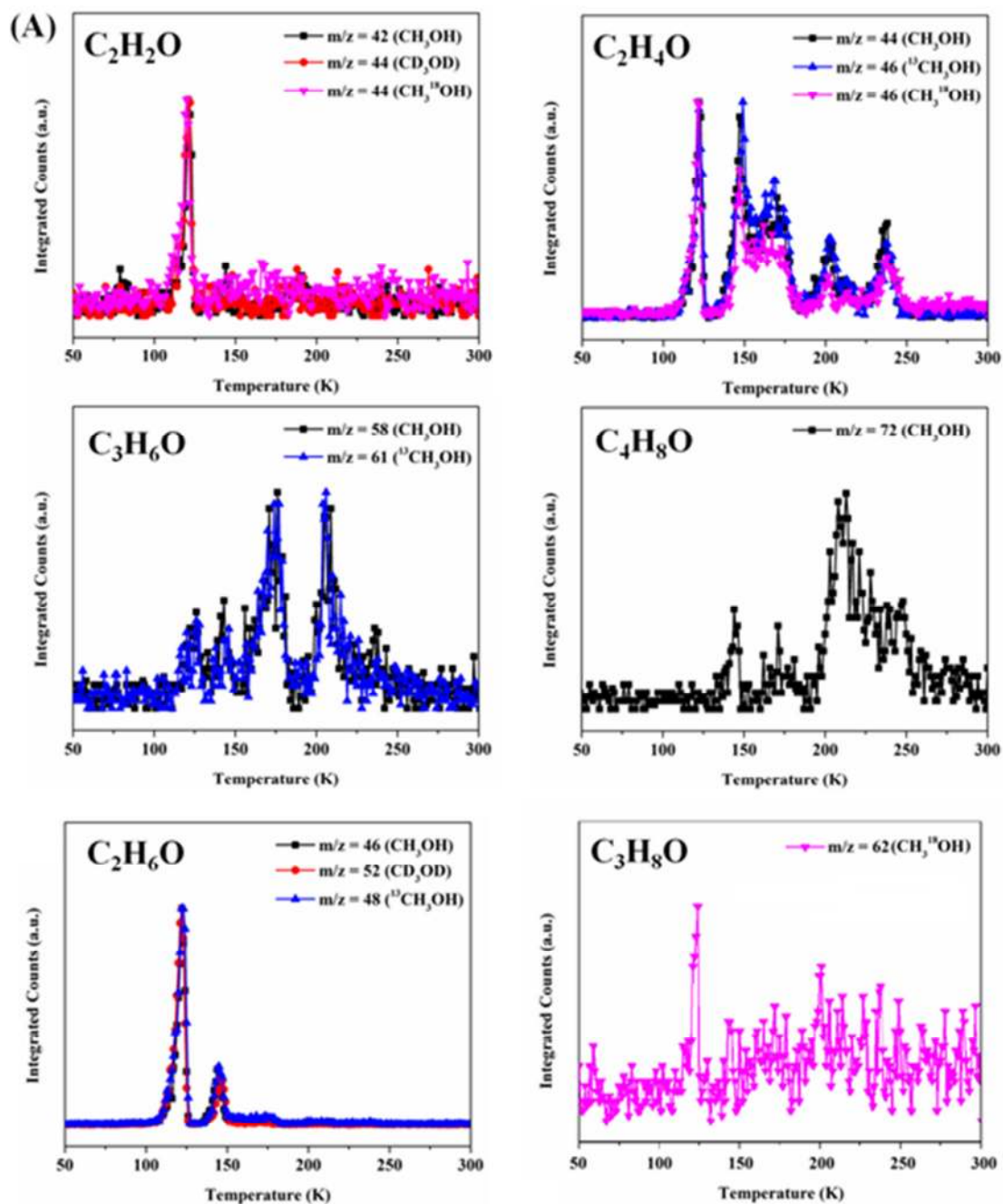


Figure 3A. Sublimation profiles of newly formed products with a single oxygen atom observed in irradiated methanol ices.

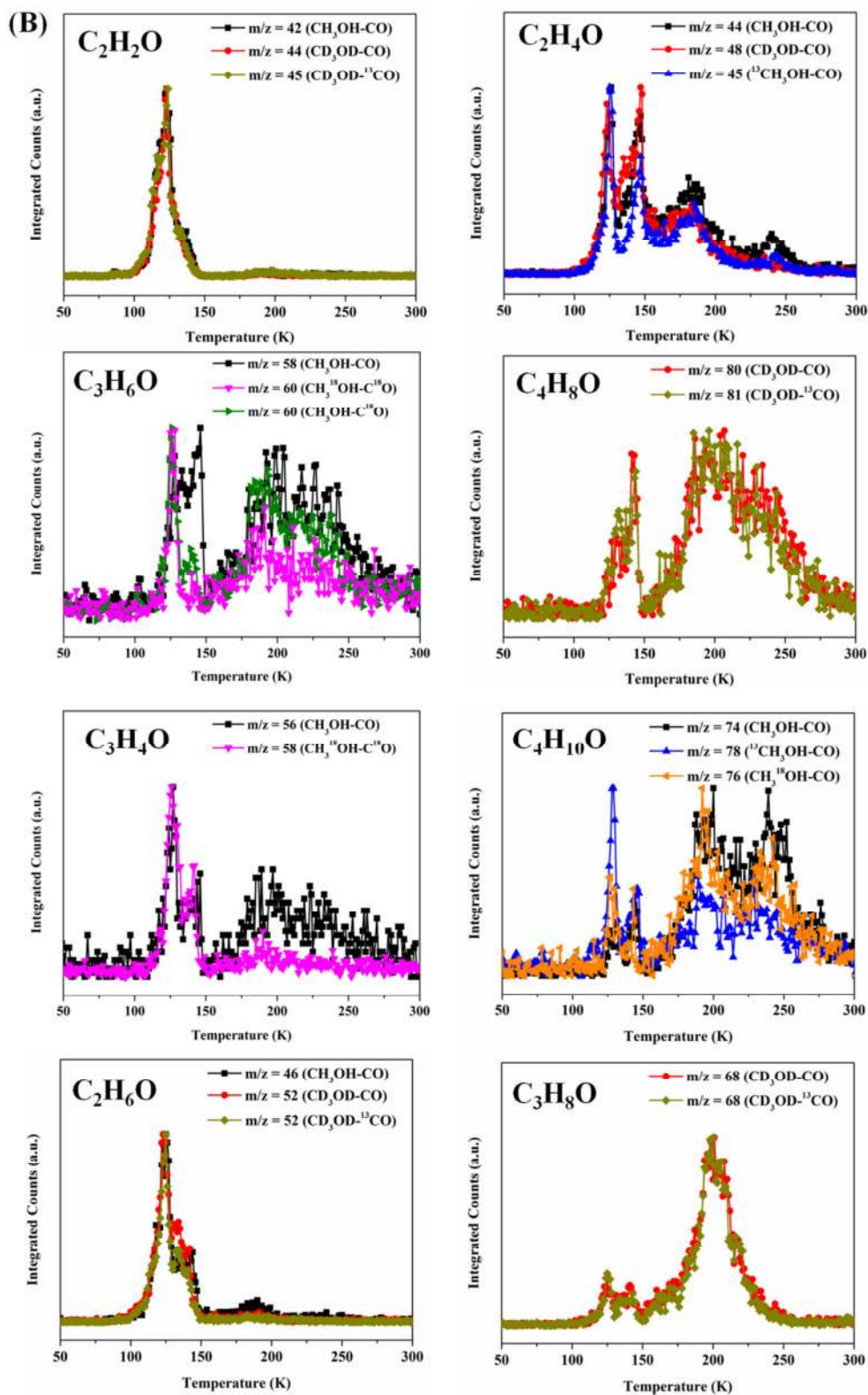


Figure 3B. Sublimation profiles of newly formed products detected with a single oxygen atom observed in irradiated methanol-carbon monoxide (4:5) ice systems.

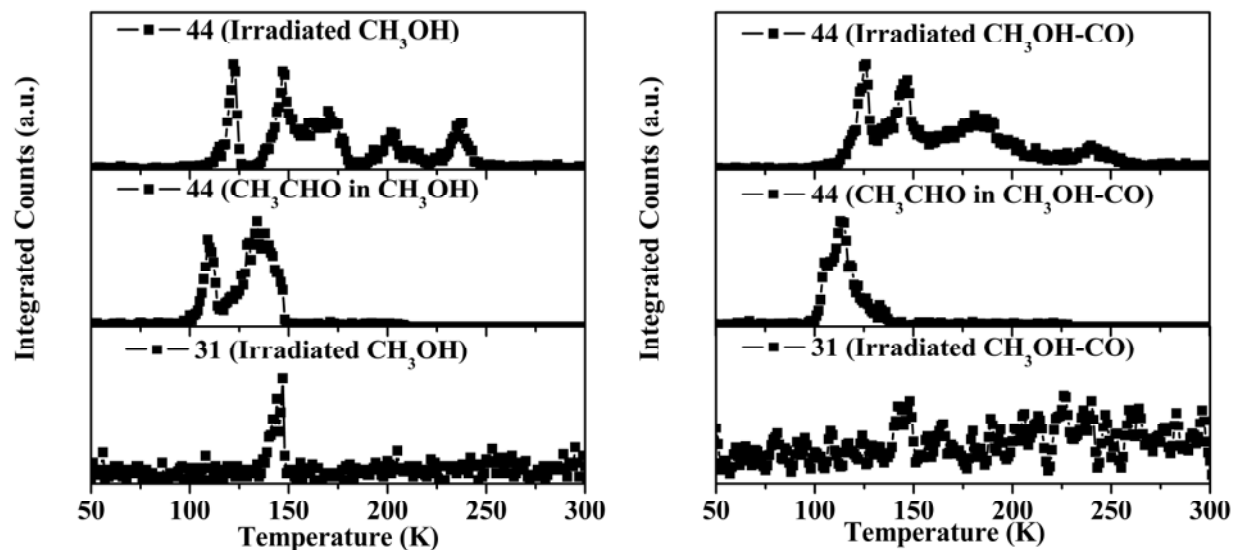


Figure 3C. Sublimation profiles of the calibration samples containing acetaldehyde (CH_3CHO ; $m/z = 44$ amu) in (left) CH_3OH (Sample 1) and (right) $\text{CH}_3\text{OH-CO}$ (4:5) (Sample 2) are compared with the sublimation profiles of $\text{C}_2\text{H}_4\text{O}^+$ ion counts recorded in irradiated CH_3OH and $\text{CH}_3\text{OH-CO}$ (4:5) ices. Sublimation profiles of photoionization fragment CH_3O^+ of methanol at $m/z = 31$ amu are also shown.

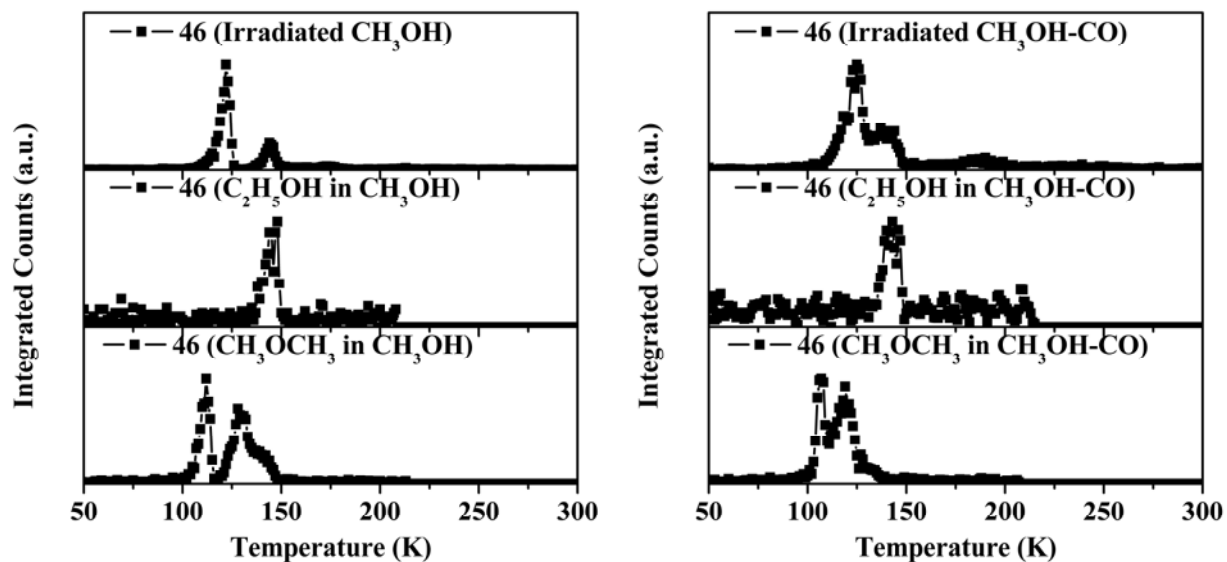


Figure 3D. Sublimation profiles of the calibration samples containing $\text{C}_2\text{H}_6\text{O}$ isomers [Ethanol ($\text{CH}_3\text{CH}_2\text{OH}$) and Methoxymethane (CH_3OCH_3); $m/z = 46$ amu] in (left) CH_3OH (Samples 3 and 5) and (right) $\text{CH}_3\text{OH-CO}$ (4:5) (Samples 4 and 6) ices are compared with the sublimation profiles of $m/z = 46$ amu recorded in irradiated CH_3OH and $\text{CH}_3\text{OH-CO}$ (4:5) ices.

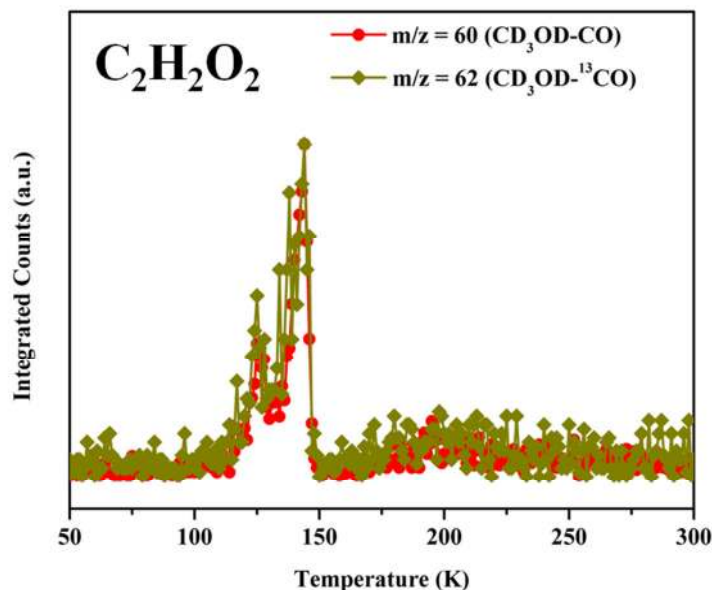


Figure 4: Sublimation profile of $C_2H_2O_2$ isotopomers identified as glyoxal ($HCOCOH$), only in the processed mixed methanol – carbon monoxide (4:5) ice systems.

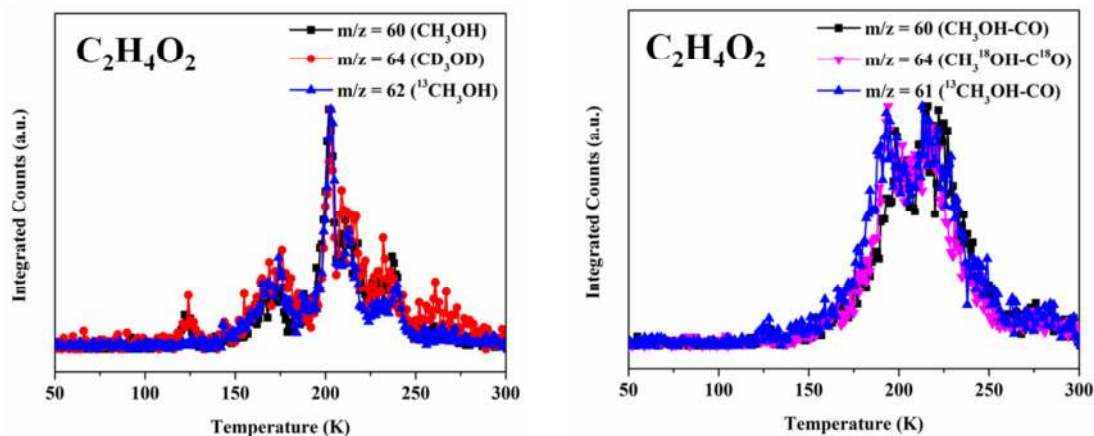


Figure 5. Sublimation profiles of $C_2H_4O_2$ isotopomers of irradiated methanol ice systems (left) and methanol – carbon monoxide systems (right). Molecular isomers, glycolaldehyde and ethane-1,2-diol are assigned to the observed ion signal. For a detailed discussion on the assignment, please see main text.

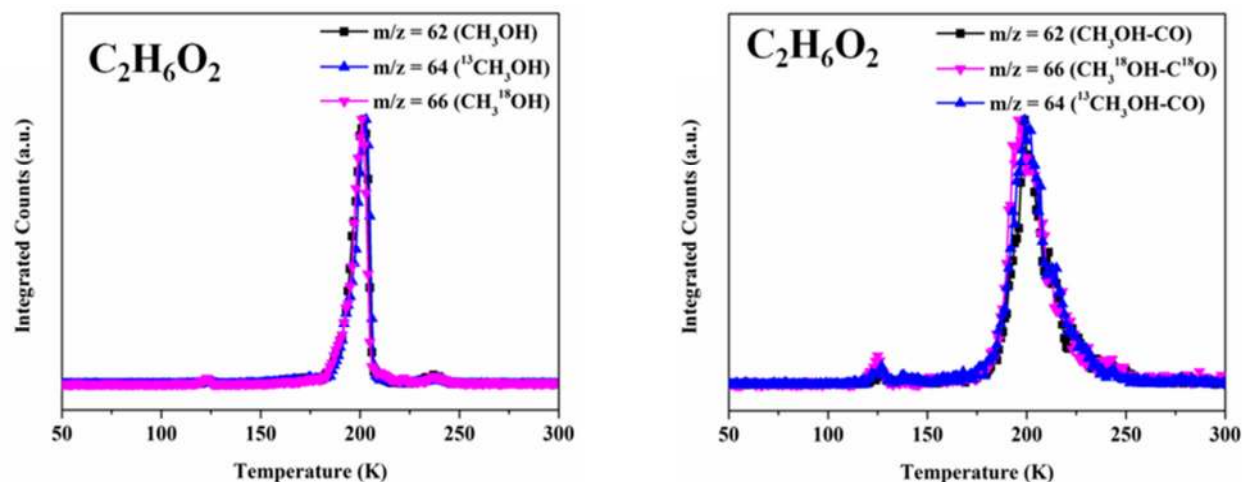


Figure 6. Sublimation profiles of $C_2H_6O_2$ isotopomers of irradiated methanol ice systems (left) and methanol – carbon monoxide systems (right). Ethylene glycol $HOCH_2CH_2OH$ is assigned to the observed ion signal. For a detailed discussion on the assignment, please see main text.

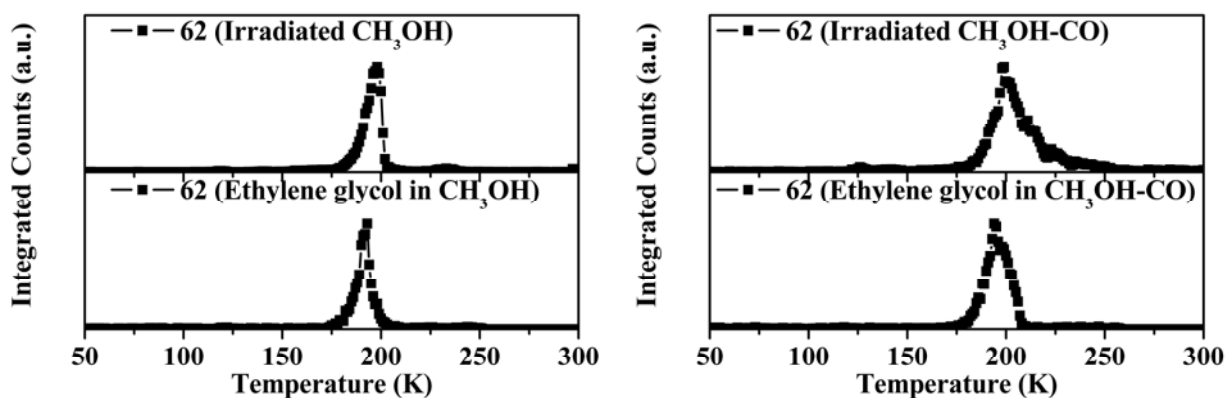


Figure 7. Sublimation profiles of the calibration samples containing ethylene glycol ($HOCH_2CH_2OH$; $m/z = 62$ amu) in (left) CH_3OH (Sample 11) and (right) CH_3OH-CO (4:5) (Sample 12) are compared with the sublimation profiles of $C_2H_6O_2^+$ ion counts recorded in irradiated CH_3OH and CH_3OH-CO (4:5) ices.

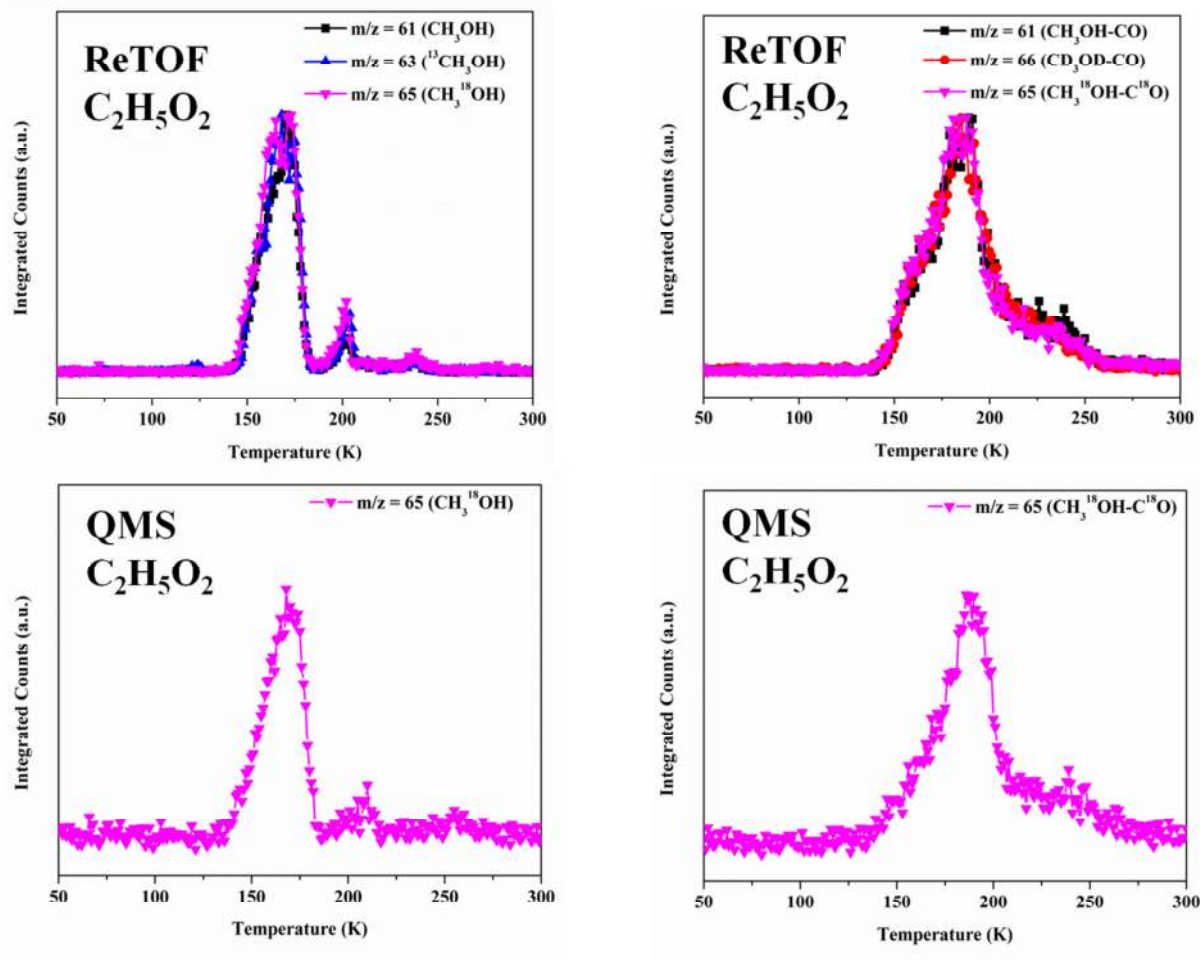


Figure 8. ReTOF Sublimation profiles and QMS traces of $C_2H_5O_2$ isotopomers of irradiated methanol ice systems (left) and methanol – carbon monoxide systems (right). Methoxy methanol (CH_3OCH_2OH) is assigned to the observed ion signal.

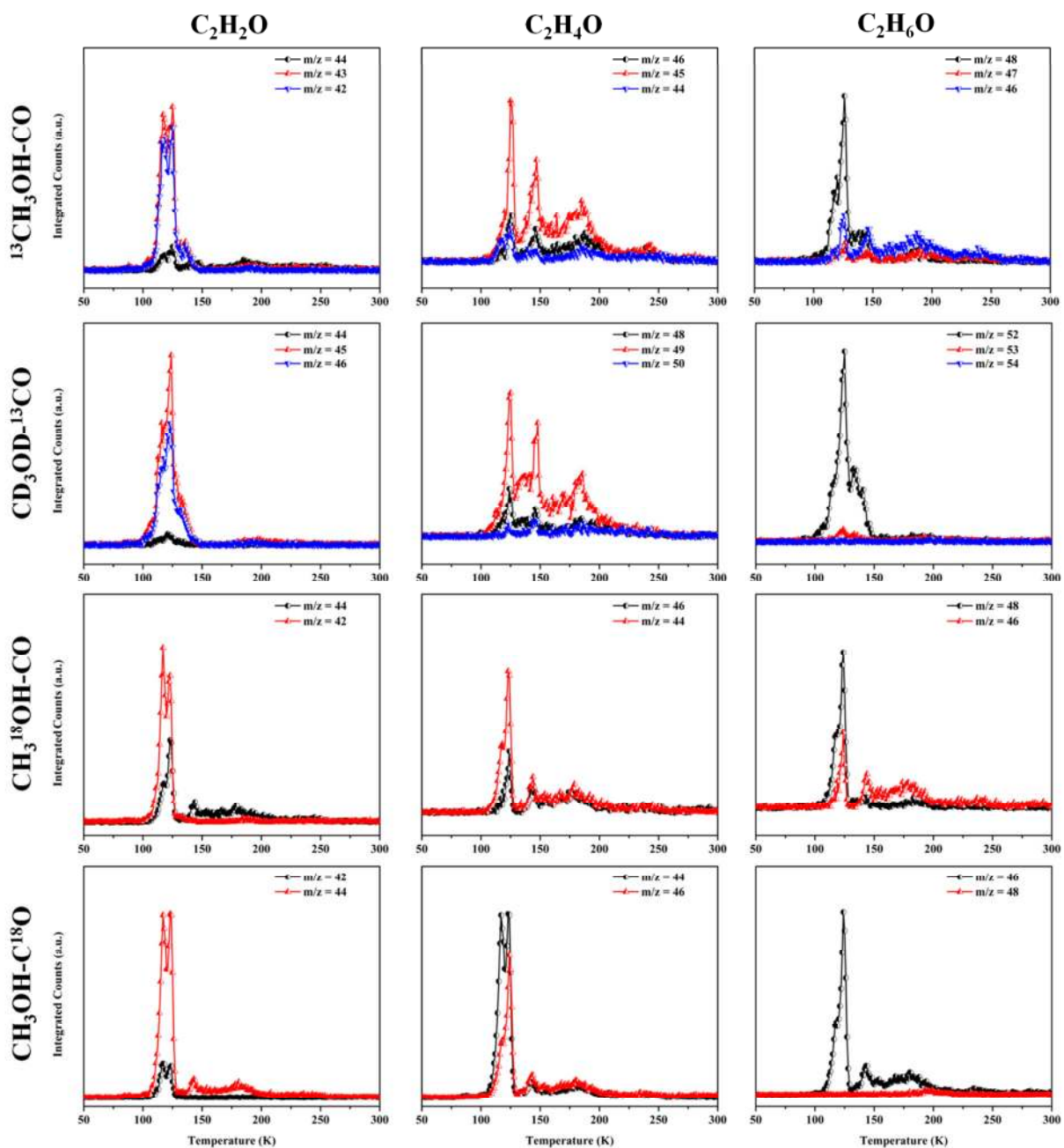


Figure 9. Sublimation profiles of the integrated ion counts of (left) C_2H_2O , (center) C_2H_4O and (right) C_2H_6O isotopomers subliming from irradiated mixed isotopic ices: $^{13}CH_3OH-CO$, $CD_3OD-^{13}CO$, $CH_3^{18}OH-CO$ and $CH_3OH-C^{18}O$.

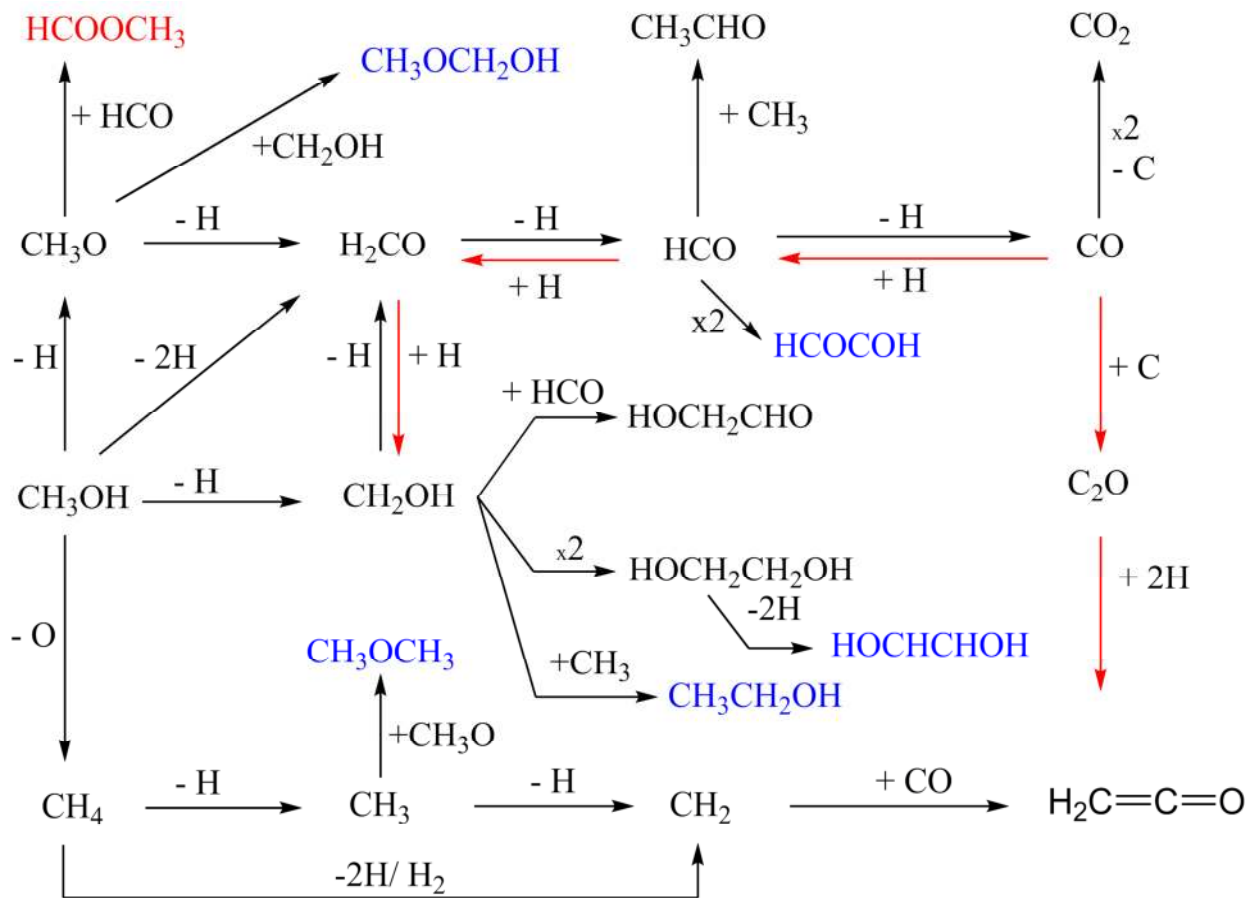


Figure 10. Formation pathways of ketene (H_2CCO), acetaldehyde (CH_3CHO), methyl formate (HCOOCH_3), ethanol ($\text{CH}_3\text{CH}_2\text{OH}$), dimethyl ether (CH_3OCH_3), glyoxal (HCOCOH), ethene-1,2-diol (HOCHCHOH), glycolaldehyde (HOCH_2CHO), ethylene glycol ($\text{HOCH}_2\text{CH}_2\text{OH}$) and methoxy methanol ($\text{CH}_3\text{OCH}_2\text{OH}$) in irradiated methanol and methanol - carbon monoxide ices, determined previously.^{48, 54, 61} The molecules presented in red have been identified based upon IR spectroscopy alone, blue are those molecules based on gas phase detection via single photoionization ReTOF mass spectrometry, and black are those identified with both analytical techniques.

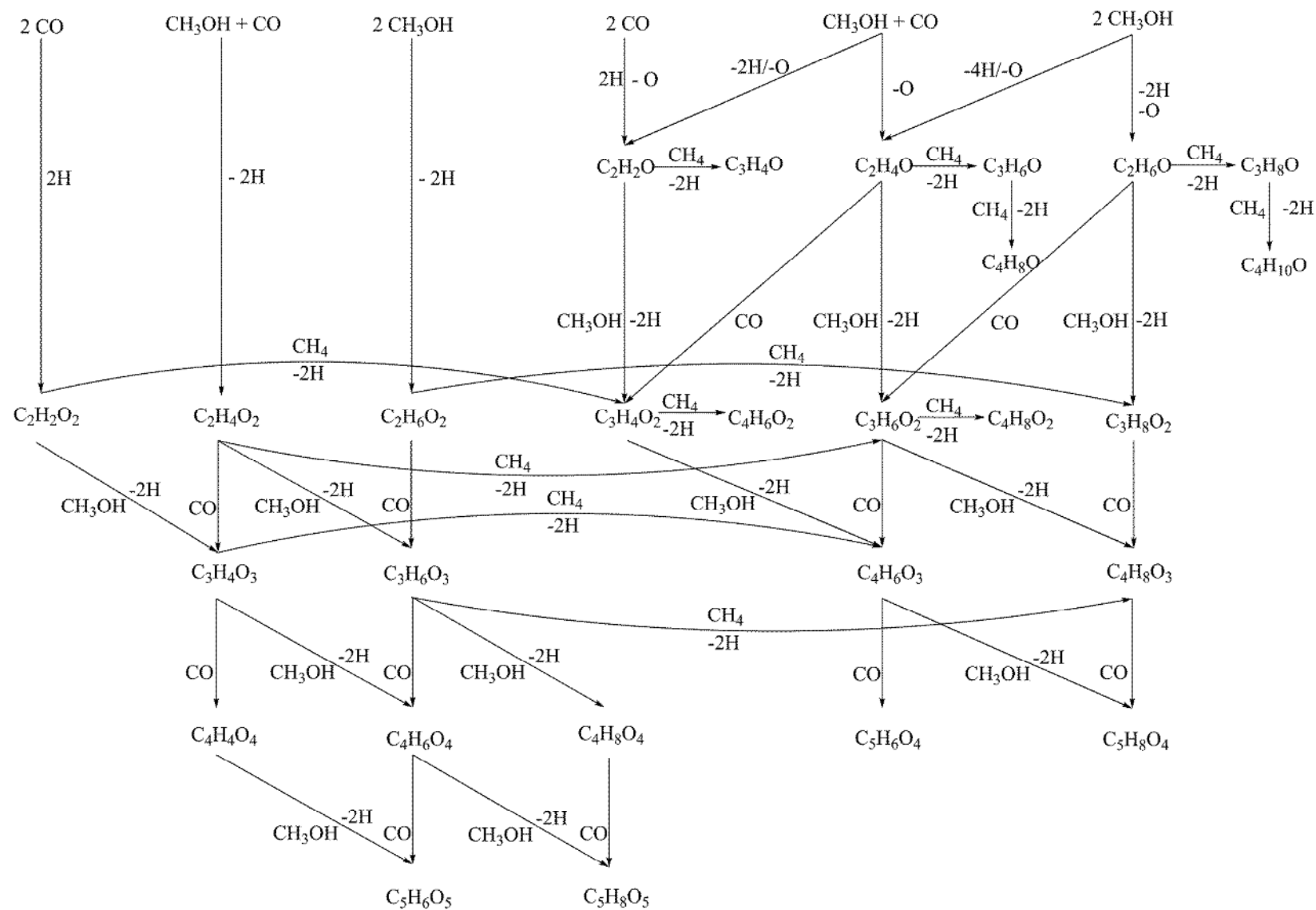


Figure 11. Schematic representation of the formation routes of the newly formed products detected in the irradiated methanol and methanol - carbon monoxide ices.

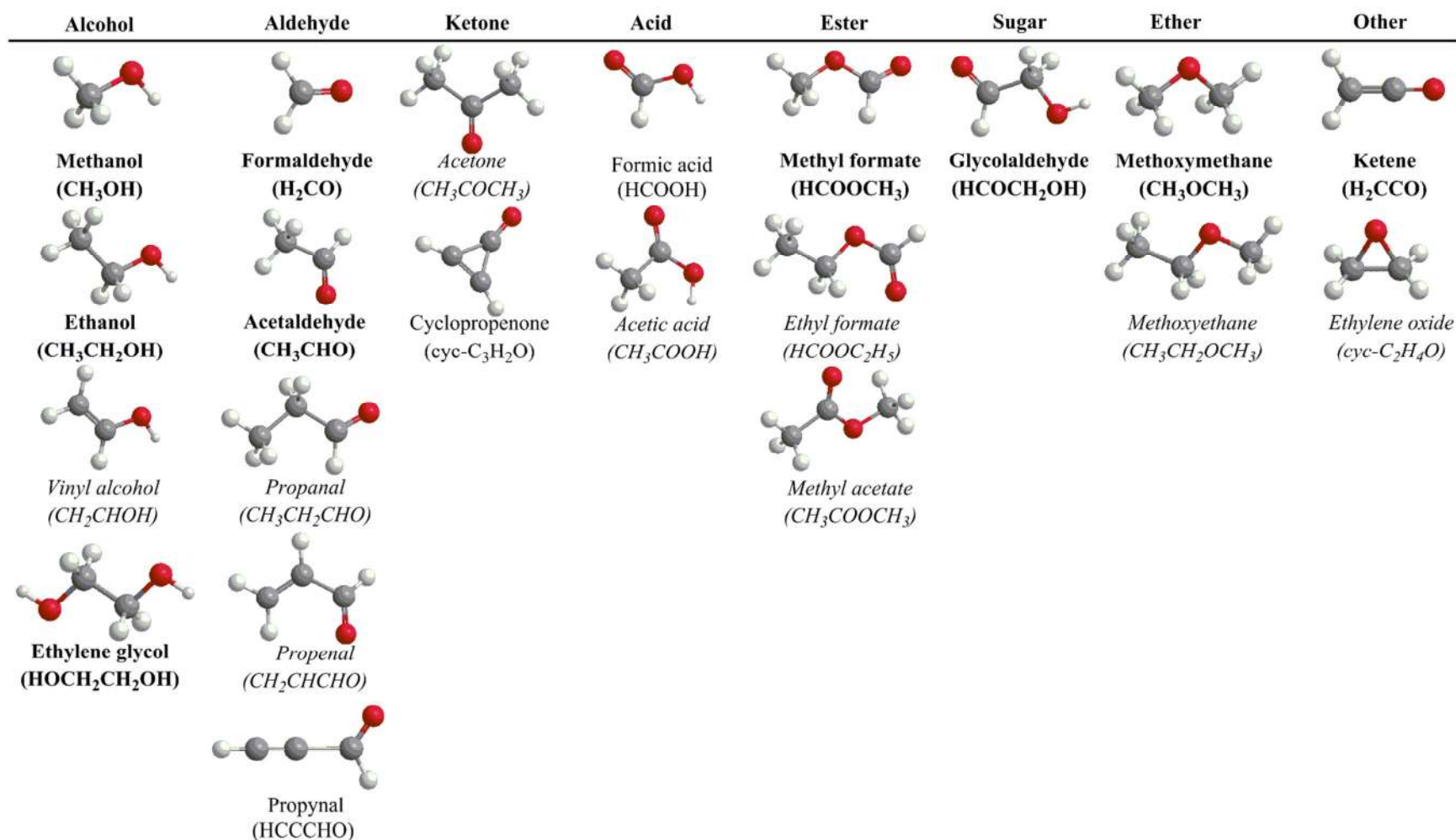


Figure 12. List of C/H/O bearing stable molecules detected in the interstellar medium (ISM). The molecules indicated in bold letters are identified in the present study. The molecules indicated in *italics* are the possible isomers of the products identified in the present study.

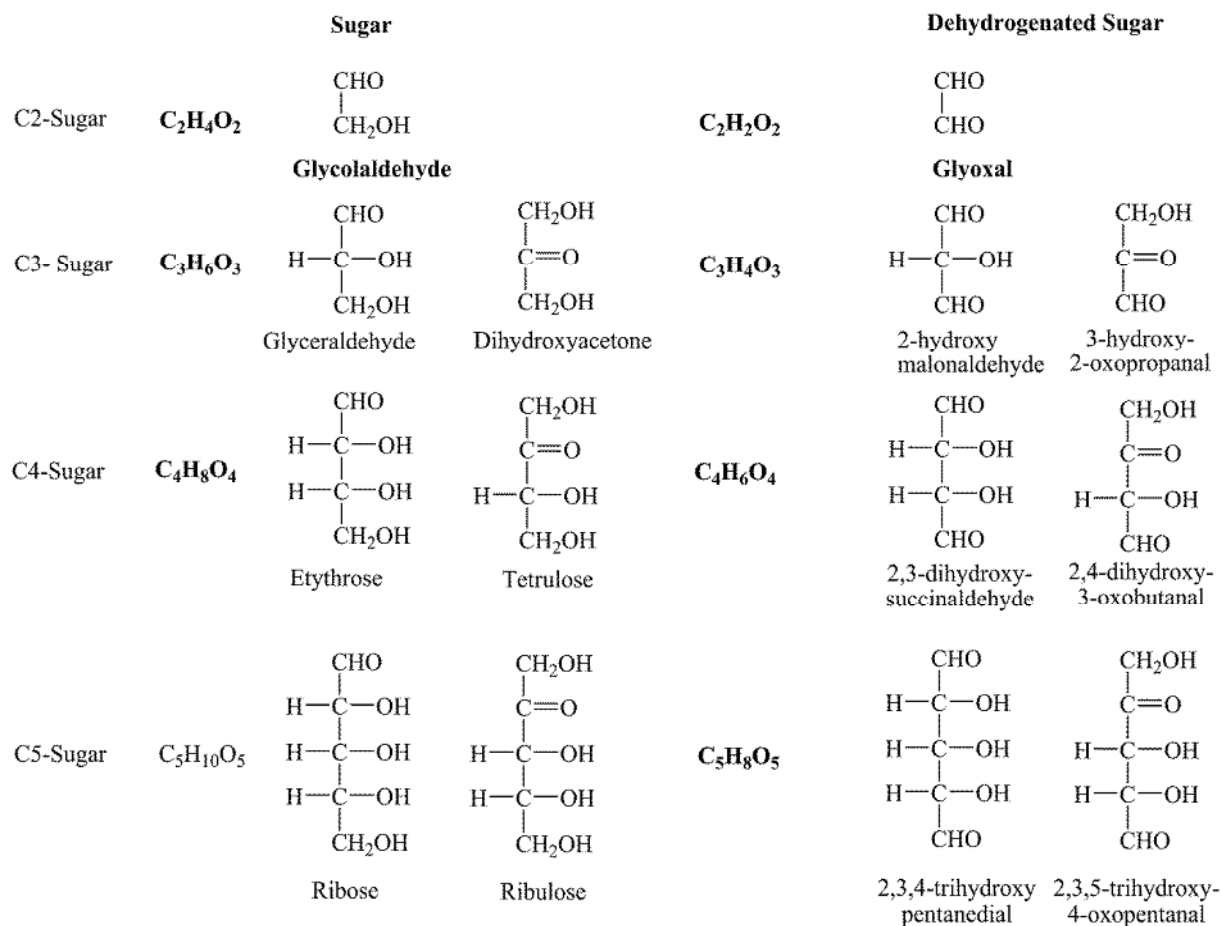


Figure 13. Examples of C2-C5 sugar and dehydrogenated sugar with corresponding molecular formula. Molecules with these potential molecular structures that have been identified in irradiated methanol and methanol-carbon monoxide mixed ices are depicted in bold.

Table 1. Infrared absorption features of the pristine ices of methanol and methanol - carbon monoxide (4:5) at 5.5 K.

Assignments	CH ₃ OH	CD ₃ OD	¹³ CH ₃ OH	CH ₃ ¹⁸ OH	CH ₃ OH- CO	CD ₃ OD- CO	CH ₃ ¹⁸ OH- C ¹⁸ O	¹³ CH ₃ OH- CO	CD ₃ OD- ¹³ CO	CH ₃ ¹⁸ OH- CO	CH ₃ OH- C ¹⁸ O
v ₂ /v ₉ +v ₄ /v ₆ /v ₁₀ (CH ₃ OH)	4399	...	4380	4398	4399	...	4397	4385	...	4395	4403
v ₂ /v ₉ +v ₄ (CH ₃ OH)	4274	...	4270	4273	4274	...	4274	4276	...	4276	4277
2 v ₁ (CO)	4247	4246	4146	4246	4152	4245	4145
v ₂ /v ₉ +v ₈ (CH ₃ OH)	4016	3989	4021	...	3998	3993	...	3994	4023
v ₂ /v ₉ +v ₈ (CH ₃ OH)	3987	...	3963	3960	3987	...	3962	3959	...	3960	3987
v ₁ (CH ₃ OH ... CO)	3623	2674	3608	3621	2674	3609	3620
v ₁ (CH ₃ OH)	3248	2428	3248	3372	3271	2439	3251	3277	2439	3251	3271
v ₂ (CH ₃ OH)	2990	2245	2975	2984	2985	2248	2985	2975	2248	2984	2986
v ₉ (CH ₃ OH)	2958	2216	2945	2956	2956	2217	2952	2949	2218	2956	2956
v ₄ +v ₅ /v ₄ +v ₁₀ /v ₅ +v ₁₀ /2v ₄ / 2v ₁₀ /2v ₅ (CH ₃ OH)	2918	2151	2920	2928	2925	2150	2921	2923, 2906	2150	2928	2925
v ₃ /2v ₆ (CH ₃ OH)	2825	2071	2824	2825	2828	2073	2828	2824	2073	2828	2828
v ₄ + v ₁₁ /v ₇ +v ₄ /v ₆ /v ₁₀ (CH ₃ OH)	2603	2010	2610	2607	2604	2013	2601	2594	2013	2604	2601
v ₆ +v ₁₁ (CH ₃ OH)	2524	...	2511	2526	2524	..	2519	2511	...	2520	2524
v ₆ +v ₈ (CH ₃ OH)	2432	...	2412	2419	2438	..	2419	2419	...	2429	2438
2v ₁₁ /2v ₇ (CH ₃ OH)	2241	1938	2229	2223	2226	1931	2227	2219	1932	2220	2223
v ₁ (CO)	2135	2136	2086	2135	2137	2136	2086
2v ₈ (CH ₃ OH)	2040	1661	2004	1991	2047	1666	2001	2014	1666	1995	2047
v ₄ (CH ₃ OH)	1475	1124	1475	1475	1475	1124	1474	1475	1124	1475	1476
v ₁₀ (CH ₃ OH)	1460	1062	1458	1461	1461	1063	1458	1458	1063	1461	1460
v ₅ (CH ₃ OH)	1445	1099	1440	1445	1445	1099	1449	1444	1101	1445	1445
v ₆ (CH ₃ OH)	1420	1062	1420	1417	1421	1062	1421	1420	1062	1417	1425
v ₇ (CH ₃ OH)	1130	900	1124	1130	1129	900	1125	1124	900	1123	1129
v ₁₁ (CH ₃ OH)	1040	979	1022	1015	1039	977	1010	1019	978	1011	1039
v ₈ (CH ₃ OH)	1028	831	1010	...	1028	833	831

Table 2. Infrared absorption features of the newly formed products observed in the methanol and methanol - carbon monoxide (4:5) ices after the irradiation at 5.5 K.

Assignments	CH ₃ OH	CD ₃ OD	¹³ CH ₃ OH	CH ₃ ¹⁸ OH	CH ₃ OH- CO	CD ₃ OD- CO	CH ₃ ¹⁸ OH- C ¹⁸ O	¹³ CH ₃ OH- CO	CD ₃ OD- ¹³ CO	CH ₃ ¹⁸ OH- CO	CH ₃ OH- C ¹⁸ O
v ₃ (CO ₂)	2339	...	2274	...	2342	2342	2307	2341, 2275	2275	2342, 2324	2342, 2307
v ₂ (H ₂ CCO)	2067	2107	2107	2106
v ₁ (CO)	2135	...	2087	2083	...	2136	2086, 2037	2135, 2089	2137	...	2137
v ₃ (HCO)	1842	1746	1797	1844	1842	...	1799	1844	...	1844	1799
v ₁₄ (HOCH ₂ CHO)	1743(1)	1711(1)	1703(1)	1713(1)	1743(1)	1714(1)	1715(1)	... 1743(1')	1709(1) ...	1708(1) 1743(1')	1747(1) 1707(1')
v ₄ (H ₂ CO)	1726(2)	1676(2)	1687(2)	1693(2)	1726(2)	1686(2)	1693(2)	1692(2) 1724(2')	1678(2) 1655(2')	1692(2) 1724(2')	1726(2) 1695(2')
v ₁₄ (HCOOCH ₃)	1714(3)	1664(3)	1676(3)	1682(3)	1714(3)	1668(3)	1680(3)	1678(3) 1710(3')	1666(3) 1647(3')	1680(3) 1714(3')	1716(3) 1684(3')
2v ₆ (HOCH ₂ CHO)	1697(4)	1647(4)	1659(4)	1666(4)	1697(4)	1651(4)	1662(4)	1664(4)	1633(4')	1654(4)	1670(4')
v ₃ (H ₂ CO)	1499	...	1499	1496	1497	...	1488	1499	...	1496	1497
v ₄ (CH ₄)	1304	...	1296	1304	1303	...	1303	1298	...	1304	1304
v ₂ (H ₂ CO)	1246	1249
v ₄ (CH ₂ OH)	1192	...	1167	1168	1193	1165	...	1162	1194
v ₉ (HOCH ₂ CH ₂ OH)	1094	...	1070	1080	1094	913	...	1089	1087
v ₇ (HOCH ₂ CHO)	1062	1062

Notes. The numbers in parenthesis are the deconvoluted peak numbers as shown in Figure 1C and 1D.

Table 3. Deconvoluted peak positions of the carbonyl absorption bands in methanol and methanol-carbon monoxide ices (Figure 1C and 1D) are compared with the assignments reported for the deconvoluted carbonyl bands observed in the irradiated methane-carbon monoxide isotopologue ices reported in reference 61. Here, RCHO = saturated aldehyde, RCOR' = saturated ketone, RCOCHCHR' = α,β -unsaturated aldehyde/ketone

Assignments	CH ₃ OH			CD ₃ OD			CH ₃ ¹⁸ OH		
	ν (cm ⁻¹)	assignments	Ref 61	ν (cm ⁻¹)	assignments	Ref 60	ν (cm ⁻¹)	assignments	Ref 60
ν_{14} (HOCH ₂ CHO)	1743	ν_{CO} of RCHO	1746	1711	ν_{CO} of CH ₃ CHO	1715	1713	ν_{CO} of RCHO	1717
ν_4 (H ₂ CO)	1726	ν_{CO} of CH ₃ CHO	1727	1676	1693	ν_{CO} of CH ₃ CHO	1694
ν_{14} (HCOOCH ₃)	1714	ν_{CO} of RCOR'	1717	1664	1682	ν_{CO} of RCOR'	1683
$2\nu_6$ (HOCH ₂ CHO)	1697	ν_{CO} of RCOCHCHR'	1701	1647	1666
Assignments	CH ₃ OH-CO			CD ₃ OD-CO			CH ₃ ¹⁸ OH-C ¹⁸ O		
	ν (cm ⁻¹)	assignments	Ref 61	ν (cm ⁻¹)	assignments	Ref 60	ν (cm ⁻¹)	assignments	Ref 60
ν_{14} (HOCH ₂ CHO)	1743	ν_{CO} of RCHO	1746	1714	ν_{CO} of CH ₃ CHO	1715	1715	ν_{CO} of RCHO	1717
ν_4 (H ₂ CO)	1726	ν_{CO} of CH ₃ CHO	1727	1686	1693	ν_{CO} of CH ₃ CHO	1694
ν_{14} (HCOOCH ₃)	1714	ν_{CO} of RCOR'	1717	1668	1680	ν_{CO} of RCOR'	1683
$2\nu_6$ (HOCH ₂ CHO)	1697	ν_{CO} of RCOCHCHR'	1701	1651	1662
Assignments	¹³ CH ₃ OH-CO			CH ₃ ¹⁸ OH-CO			CH ₃ OH-C ¹⁸ O		
	ν (cm ⁻¹)	assignments	Ref 61	ν (cm ⁻¹)	assignments	Ref 60	ν (cm ⁻¹)	assignments	Ref 60
ν_{14} (HOCH ₂ CHO)	...	ν_{CO} of RCHO	...	1708	ν_{CO} of RCHO	1717	1747	ν_{CO} of RCHO	1746
	1743		1746	1743		1746	1707		1717
ν_4 (H ₂ CO)	1692	ν_{CO} of CH ₃ CHO	...	1692	ν_{CO} of CH ₃ CHO	1694	1726	ν_{CO} of CH ₃ CHO	1727
	1724		1727	1724		1727	1695		1694
ν_{14} (HCOOCH ₃)	1678	ν_{CO} of RCOR'	...	1680	ν_{CO} of RCOR'	1683	1716	ν_{CO} of RCOR'	1717
	1710		1717	1714		1717	1684		1683

$2\nu_6$ (HOCH ₂ CHO)	1664 1654 1670	ν_{CO} of RCOCHCHR'	... 1675
----------------------------------	--------------------	-----	-----	--------------------	-----	-----	--------------------	-----------------------------------	-------------

Table 4A: Molecular formula and corresponding mass-to-charges (in amu unit) of the products identified in the irradiated methanol isotopologue ices (CH_3OH , CD_3OD , $\text{CH}_3^{18}\text{OH}$ and $^{13}\text{CH}_3\text{OH}$) during the TPD studies using ReTOF mass spectroscopy. Molecules are grouped into different classes based on the number of oxygen atoms present. The molecule labelled with * designates a fragment of methoxy methanol ($\text{CH}_3\text{OCH}_2\text{OH}$) and not a sublimating radical for further information please see section 3.2.1

CH_3OH		CD_3OD		$\text{CH}_3^{18}\text{OH}$		$^{13}\text{CH}_3\text{OH}$	
Formula	m/z	Formula	m/z	Formula	m/z	Formula	m/z
Products with single oxygen atom							
$\text{C}_2\text{H}_2\text{O}$	42	$\text{C}_2\text{D}_2\text{O}$	44	$\text{C}_2\text{H}_2^{18}\text{O}$	44	$^{13}\text{C}_2\text{H}_2\text{O}$	44
$\text{C}_2\text{H}_4\text{O}$	44	$\text{C}_2\text{D}_4\text{O}$	48	$\text{C}_2\text{H}_4^{18}\text{O}$	46	$^{13}\text{C}_2\text{H}_4\text{O}$	46
$\text{C}_2\text{H}_6\text{O}$	46	$\text{C}_2\text{D}_6\text{O}$	52	$\text{C}_2\text{H}_6^{18}\text{O}$	48	$^{13}\text{C}_2\text{H}_6\text{O}$	48
$\text{C}_3\text{H}_6\text{O}$	58	$\text{C}_3\text{D}_6\text{O}$	64	$\text{C}_3\text{H}_6^{18}\text{O}$	60	$^{13}\text{C}_3\text{H}_6\text{O}$	61
$\text{C}_3\text{H}_8\text{O}$	60	$\text{C}_3\text{D}_8\text{O}$	68	$\text{C}_3\text{H}_8^{18}\text{O}$	62	$^{13}\text{C}_3\text{H}_8\text{O}$	63
$\text{C}_4\text{H}_8\text{O}$	72	$\text{C}_4\text{D}_8\text{O}$	80	$\text{C}_4\text{H}_8^{18}\text{O}$	74	$^{13}\text{C}_4\text{H}_8\text{O}$	76
Products with two oxygen atoms							
$\text{C}_2\text{H}_4\text{O}_2$	60	$\text{C}_2\text{D}_4\text{O}_2$	64	$\text{C}_2\text{H}_4^{18}\text{O}_2$	64	$^{13}\text{C}_2\text{H}_4\text{O}_2$	62
$\text{C}_2\text{H}_5\text{O}_2^*$	61	$\text{C}_2\text{D}_5\text{O}_2$	66	$\text{C}_3\text{H}_5^{18}\text{O}_2$	65	$^{13}\text{C}_2\text{H}_5\text{O}_2$	63
$\text{C}_2\text{H}_6\text{O}_2$	62	$\text{C}_2\text{D}_6\text{O}_2$	68	$\text{C}_2\text{H}_6^{18}\text{O}_2$	66	$^{13}\text{C}_2\text{H}_6\text{O}_2$	64
$\text{C}_3\text{H}_4\text{O}_2$	72	$\text{C}_3\text{D}_4\text{O}_2$	76	$\text{C}_3\text{H}_4^{18}\text{O}_2$	76	$^{13}\text{C}_3\text{H}_4\text{O}_2$	75
$\text{C}_3\text{H}_6\text{O}_2$	74	$\text{C}_3\text{D}_6\text{O}_2$	80	$\text{C}_3\text{H}_6^{18}\text{O}_2$	78	$^{13}\text{C}_3\text{H}_6\text{O}_2$	77
$\text{C}_3\text{H}_8\text{O}_2$	76	$\text{C}_3\text{D}_8\text{O}_2$	84	$\text{C}_3\text{H}_8^{18}\text{O}_2$	80	$^{13}\text{C}_3\text{H}_8\text{O}_2$	79
$\text{C}_4\text{H}_8\text{O}_2$	88	$\text{C}_4\text{D}_8\text{O}_2$	96	$\text{C}_4\text{H}_8^{18}\text{O}_2$	92	$^{13}\text{C}_4\text{H}_8\text{O}_2$	92
Products with three oxygen atoms							
$\text{C}_3\text{H}_6\text{O}_3$	90	$\text{C}_3\text{D}_6\text{O}_3$	96	$\text{C}_3\text{H}_6^{18}\text{O}_3$	96	$^{13}\text{C}_3\text{H}_6\text{O}_3$	93
$\text{C}_3\text{H}_8\text{O}_3$	92	$\text{C}_3\text{D}_8\text{O}_3$	100	$\text{C}_3\text{H}_8^{18}\text{O}_3$	98	$^{13}\text{C}_3\text{H}_8\text{O}_3$	95

Table 4B: Molecular formula and corresponding mass-to-charges (m/z in amu unit) of the products identified in the irradiated mixed methanol-carbon monoxide isotopologue ices ($\text{CH}_3\text{OH-CO}$, $\text{CD}_3\text{OD-CO}$, $\text{CH}_3^{18}\text{OH-C}^{18}\text{O}$, $^{13}\text{CH}_3\text{OH-CO}$, $\text{CD}_3\text{OD-}^{13}\text{CO}$, $\text{CH}_3^{18}\text{OH-CO}$ and $\text{CH}_3\text{OH-C}^{18}\text{O}$) during the TPD studies using ReTOF mass spectroscopy. Molecules with similar grouped into different classes based on the number of oxygen atoms present. In mixed isotopic ices ($^{13}\text{CH}_3\text{OH-CO}$, $\text{CD}_3\text{OD-}^{13}\text{CO}$, $\text{CH}_3^{18}\text{OH-CO}$ and $\text{CH}_3\text{OH-C}^{18}\text{O}$), observed molecules are shown in bold letters.

$\text{CH}_3\text{OH-CO}$		$\text{CD}_3\text{OD-CO}$		$\text{CH}_3^{18}\text{OH-C}^{18}\text{O}$		$^{13}\text{CH}_3\text{OH-CO}$		$\text{CD}_3\text{OD-}^{13}\text{CO}$		$\text{CH}_3^{18}\text{OH-CO}$		$\text{CH}_3\text{OH-C}^{18}\text{O}$	
Formula	m/z	Formula	m/z	Formula	m/z	Formula	m/z	Formula	m/z	Formula	m/z	Formula	m/z
Products with single oxygen atom													
$\text{C}_2\text{H}_2\text{O}$	42	$\text{C}_2\text{D}_2\text{O}$	44	$\text{C}_2\text{H}_2^{18}\text{O}$	44	$\text{C}_2\text{H}_2\text{O}$	42	$^{13}\text{C}_2\text{D}_2\text{O}$	46	$\text{C}_2\text{H}_2\text{O}$	42	$\text{C}_2\text{H}_2^{18}\text{O}$	44
						$^{13}\text{CCH}_2\text{O}$	43	$^{13}\text{CCD}_2\text{O}$	45	$\text{C}_2\text{H}_2^{18}\text{O}$	44	$\text{C}_2\text{H}_2\text{O}$	42
						$^{13}\text{C}_2\text{H}_2\text{O}$	44	$\text{C}_2\text{D}_2\text{O}$	44				
$\text{C}_2\text{H}_4\text{O}$	44	$\text{C}_2\text{D}_4\text{O}$	48	$\text{C}_2\text{H}_4^{18}\text{O}$	46	$\text{C}_2\text{H}_4\text{O}$	44	$^{13}\text{C}_2\text{D}_4\text{O}$	50	$\text{C}_2\text{H}_4\text{O}$	44	$\text{C}_2\text{H}_4^{18}\text{O}$	46
						$^{13}\text{CCH}_4\text{O}$	45	$^{13}\text{CCD}_4\text{O}$	49	$\text{C}_2\text{H}_4^{18}\text{O}$	46	$\text{C}_2\text{H}_4\text{O}$	44
						$^{13}\text{C}_2\text{H}_4\text{O}$	46	$\text{C}_2\text{D}_4\text{O}$	48				
$\text{C}_2\text{H}_6\text{O}$	46	$\text{C}_2\text{D}_6\text{O}$	52	$\text{C}_2\text{H}_6^{18}\text{O}$	48	$\text{C}_2\text{H}_6\text{O}$	46	$^{13}\text{C}_2\text{D}_6\text{O}$	54	$\text{C}_2\text{H}_4\text{O}$	46	$\text{C}_2\text{H}_6^{18}\text{O}$	48
						$^{13}\text{CCH}_6\text{O}$	47	$^{13}\text{CCD}_6\text{O}$	53	$\text{C}_2\text{H}_6^{18}\text{O}$	48	$\text{C}_2\text{H}_6\text{O}$	46
						$^{13}\text{C}_2\text{H}_6\text{O}$	48	$\text{C}_2\text{D}_6\text{O}$	52				
$\text{C}_3\text{H}_4\text{O}$	56	$\text{C}_3\text{D}_4\text{O}$	60	$\text{C}_3\text{H}_4^{18}\text{O}$	58	$\text{C}_3\text{H}_4\text{O}$	56	$^{13}\text{C}_3\text{D}_4\text{O}$	63	$\text{C}_3\text{H}_4\text{O}$	56	$\text{C}_3\text{H}_4^{18}\text{O}$	58
						$^{13}\text{CC}_2\text{H}_4\text{O}$	57	$^{13}\text{C}_2\text{CD}_4\text{O}$	62	$\text{C}_3\text{H}_4^{18}\text{O}$	58	$\text{C}_3\text{H}_4\text{O}$	56
						$^{13}\text{C}_2\text{CH}_4\text{O}$	58	$^{13}\text{CC}_2\text{D}_4\text{O}$	61				
						$^{13}\text{C}_3\text{H}_4\text{O}$	59	$\text{C}_3\text{D}_4\text{O}$	60				
$\text{C}_3\text{H}_6\text{O}$	58	$\text{C}_3\text{D}_6\text{O}$	64	$\text{C}_3\text{H}_6^{18}\text{O}$	60	$\text{C}_3\text{H}_6\text{O}$	58	$^{13}\text{C}_3\text{D}_6\text{O}$	67	$\text{C}_3\text{H}_6\text{O}$	58	$\text{C}_3\text{H}_6^{18}\text{O}$	60
						$^{13}\text{CC}_2\text{H}_6\text{O}$	59	$^{13}\text{C}_2\text{CD}_6\text{O}$	66	$\text{C}_3\text{H}_6^{18}\text{O}$	60	$\text{C}_3\text{H}_6\text{O}$	58
						$^{13}\text{C}_2\text{CH}_6\text{O}$	60	$^{13}\text{CC}_2\text{D}_6\text{O}$	65				
						$^{13}\text{C}_3\text{H}_6\text{O}$	61	$\text{C}_3\text{D}_6\text{O}$	64				
$\text{C}_3\text{H}_8\text{O}$	60	$\text{C}_3\text{D}_8\text{O}$	68	$\text{C}_3\text{H}_8^{18}\text{O}$	62	$\text{C}_3\text{H}_8\text{O}$	60	$^{13}\text{C}_3\text{D}_8\text{O}$	71	$\text{C}_3\text{H}_8\text{O}$	60	$\text{C}_3\text{H}_8^{18}\text{O}$	62
						$^{13}\text{CC}_2\text{H}_8\text{O}$	61	$^{13}\text{C}_2\text{CD}_8\text{O}$	70	$\text{C}_3\text{H}_8^{18}\text{O}$	62	$\text{C}_3\text{H}_8\text{O}$	60
						$^{13}\text{C}_2\text{CH}_8\text{O}$	62	$^{13}\text{CC}_2\text{D}_8\text{O}$	69				
						$^{13}\text{C}_3\text{H}_8\text{O}$	63	$\text{C}_3\text{D}_8\text{O}$	68				
$\text{C}_4\text{H}_8\text{O}$	72	$\text{C}_4\text{D}_8\text{O}$	80	$\text{C}_4\text{H}_8^{18}\text{O}$	74	$\text{C}_4\text{H}_8\text{O}$	72	$^{13}\text{C}_4\text{D}_8\text{O}$	84	$\text{C}_4\text{H}_8\text{O}$	72	$\text{C}_4\text{H}_8^{18}\text{O}$	74
						$^{13}\text{CC}_4\text{H}_8\text{O}$	73	$^{13}\text{C}_3\text{CD}_8\text{O}$	83	$\text{C}_4\text{H}_8^{18}\text{O}$	74	$\text{C}_4\text{H}_8\text{O}$	72

					$^{13}\text{C}_2\text{C}_2\text{H}_8\text{O}$	74	$^{13}\text{C}_2\text{C}_2\text{D}_8\text{O}$	82					
					$^{13}\text{C}_3\text{CH}_8\text{O}$	75	$^{13}\text{CC}_3\text{D}_8\text{O}$	81					
					$^{13}\text{C}_4\text{H}_8\text{O}$	76	$\text{C}_4\text{D}_8\text{O}$	80					
$\text{C}_4\text{H}_{10}\text{O}$	74	$\text{C}_4\text{D}_{10}\text{O}$	84	$\text{C}_4\text{H}_{10}^{18}\text{O}$	76	$\text{C}_4\text{H}_{10}\text{O}$	74	$^{13}\text{C}_4\text{D}_{10}\text{O}$	88	$\text{C}_4\text{H}_{10}\text{O}$	74	$\text{C}_4\text{H}_{10}^{18}\text{O}$	76
						$^{13}\text{CC}_4\text{H}_{10}\text{O}$	75	$^{13}\text{C}_3\text{CD}_{10}\text{O}$	87	$\text{C}_4\text{H}_{10}^{18}\text{O}$	76	$\text{C}_4\text{H}_{10}\text{O}$	74
						$^{13}\text{C}_2\text{C}_2\text{H}_{10}\text{O}$	76	$^{13}\text{C}_2\text{C}_2\text{D}_{10}\text{O}$	86				
						$^{13}\text{C}_3\text{CH}_{10}\text{O}$	77	$^{13}\text{CC}_3\text{D}_{10}\text{O}$	85				
						$^{13}\text{C}_4\text{H}_{10}\text{O}$	78	$\text{C}_4\text{D}_{10}\text{O}$	84				
Products with two oxygen atoms													
$\text{C}_2\text{H}_2\text{O}_2$	58	$\text{C}_2\text{D}_2\text{O}_2$	60	$\text{C}_2\text{H}_2^{18}\text{O}_2$	62	$\text{C}_2\text{H}_2\text{O}_2$	58	$^{13}\text{C}_2\text{D}_2\text{O}_2$	62	$\text{C}_2\text{H}_2\text{O}_2$	58	$\text{C}_2\text{H}_2^{18}\text{O}_2$	62
						$^{13}\text{CCH}_2\text{O}_2$	59	$^{13}\text{CCD}_2\text{O}_2$	61	$\text{C}_2\text{H}_2^{18}\text{OO}$	60	$\text{C}_2\text{H}_2^{18}\text{OO}$	60
						$^{13}\text{C}_2\text{H}_2\text{O}_2$	60	$\text{C}_2\text{D}_2\text{O}_2$	60	$\text{C}_2\text{H}_2^{18}\text{O}_2$	62	$\text{C}_2\text{H}_2\text{O}_2$	58
$\text{C}_2\text{H}_4\text{O}_2$	60	$\text{C}_2\text{D}_4\text{O}_2$	64	$\text{C}_2\text{H}_4^{18}\text{O}_2$	64	$\text{C}_2\text{H}_4\text{O}_2$	60	$^{13}\text{C}_2\text{D}_4\text{O}_2$	66	$\text{C}_2\text{H}_4\text{O}_2$	60	$\text{C}_2\text{H}_4^{18}\text{O}_2$	64
						$^{13}\text{CCH}_4\text{O}_2$	61	$^{13}\text{CCD}_4\text{O}_2$	65	$\text{C}_2\text{H}_4^{18}\text{OO}$	62	$\text{C}_2\text{H}_4^{18}\text{OO}$	62
						$^{13}\text{C}_2\text{H}_4\text{O}_2$	62	$\text{C}_2\text{D}_4\text{O}_2$	64	$\text{C}_2\text{H}_4^{18}\text{O}_2$	64	$\text{C}_2\text{H}_4\text{O}_2$	60
$\text{C}_2\text{H}_5\text{O}_2$	61	$\text{C}_2\text{D}_5\text{O}_2$	66	$\text{C}_2\text{H}_5^{18}\text{O}_2$	65	$\text{C}_2\text{H}_5\text{O}_2$	61	$^{13}\text{C}_2\text{D}_5\text{O}_2$	68	$\text{C}_2\text{H}_5\text{O}_2$	61	$\text{C}_2\text{H}_5^{18}\text{O}_2$	65
						$^{13}\text{CCH}_5\text{O}_2$	62	$^{13}\text{CCD}_5\text{O}_2$	67	$\text{C}_2\text{H}_5^{18}\text{OO}$	63	$\text{C}_2\text{H}_5^{18}\text{OO}$	63
						$^{13}\text{C}_2\text{H}_5\text{O}_2$	63	$\text{C}_2\text{D}_5\text{O}_2$	66	$\text{C}_2\text{H}_5^{18}\text{O}_2$	65	$\text{C}_2\text{H}_5\text{O}_2$	61
$\text{C}_2\text{H}_6\text{O}_2$	62	$\text{C}_2\text{D}_6\text{O}_2$	68	$\text{C}_2\text{H}_6^{18}\text{O}_2$	66	$\text{C}_2\text{H}_6\text{O}_2$	62	$^{13}\text{C}_2\text{D}_6\text{O}_2$	70	$\text{C}_2\text{H}_6\text{O}_2$	62	$\text{C}_2\text{H}_6^{18}\text{O}_2$	66
						$^{13}\text{CCH}_6\text{O}_2$	63	$^{13}\text{CCD}_6\text{O}_2$	69	$\text{C}_2\text{H}_6^{18}\text{OO}$	64	$\text{C}_2\text{H}_6^{18}\text{OO}$	64
						$^{13}\text{C}_2\text{H}_6\text{O}_2$	64	$\text{C}_2\text{D}_6\text{O}_2$	68	$\text{C}_2\text{H}_6^{18}\text{O}_2$	66	$\text{C}_2\text{H}_6\text{O}_2$	62
$\text{C}_3\text{H}_4\text{O}_2$	72	$\text{C}_3\text{D}_4\text{O}_2$	76	$\text{C}_3\text{H}_4^{18}\text{O}_2$	76	$\text{C}_3\text{H}_4\text{O}_2$	72	$^{13}\text{C}_3\text{D}_4\text{O}_2$	79	$\text{C}_3\text{H}_4\text{O}_2$	72	$\text{C}_3\text{H}_4^{18}\text{O}_2$	76
						$^{13}\text{CC}_2\text{H}_4\text{O}_2$	73	$^{13}\text{C}_2\text{CD}_4\text{O}_2$	78	$\text{C}_3\text{H}_4^{18}\text{OO}$	74	$\text{C}_3\text{H}_4^{18}\text{OO}$	74
						$^{13}\text{C}_2\text{CH}_4\text{O}_2$	74	$^{13}\text{CC}_2\text{D}_4\text{O}_2$	77	$\text{C}_3\text{H}_4^{18}\text{O}_2$	76	$\text{C}_3\text{H}_4\text{O}_2$	72
						$^{13}\text{C}_3\text{H}_4\text{O}_2$	75	$\text{C}_3\text{D}_4\text{O}_2$	76				
$\text{C}_3\text{H}_6\text{O}_2$	74	$\text{C}_3\text{D}_6\text{O}_2$	80	$\text{C}_3\text{H}_6^{18}\text{O}_2$	78	$\text{C}_3\text{H}_6\text{O}_2$	74	$^{13}\text{C}_3\text{D}_6\text{O}_2$	83	$\text{C}_3\text{H}_6\text{O}_2$	74	$\text{C}_3\text{H}_6^{18}\text{O}_2$	78
						$^{13}\text{CC}_2\text{H}_6\text{O}_2$	75	$^{13}\text{C}_2\text{CD}_6\text{O}_2$	82	$\text{C}_3\text{H}_6^{18}\text{OO}$	76	$\text{C}_3\text{H}_6^{18}\text{OO}$	76
						$^{13}\text{C}_2\text{CH}_6\text{O}_2$	76	$^{13}\text{CC}_2\text{D}_6\text{O}_2$	81	$\text{C}_3\text{H}_6^{18}\text{O}_2$	78	$\text{C}_3\text{H}_6\text{O}_2$	74
						$^{13}\text{C}_3\text{H}_6\text{O}_2$	77	$\text{C}_3\text{D}_6\text{O}_2$	80				
$\text{C}_3\text{H}_8\text{O}_2$	76	$\text{C}_3\text{D}_8\text{O}_2$	84	$\text{C}_3\text{H}_8^{18}\text{O}_2$	80	$\text{C}_3\text{H}_8\text{O}_2$	76	$^{13}\text{C}_3\text{D}_8\text{O}_2$	87	$\text{C}_3\text{H}_8\text{O}_2$	76	$\text{C}_3\text{H}_8^{18}\text{O}_2$	80
						$^{13}\text{CC}_2\text{H}_8\text{O}_2$	77	$^{13}\text{C}_2\text{CD}_8\text{O}_2$	86	$\text{C}_3\text{H}_8^{18}\text{OO}$	78	$\text{C}_3\text{H}_8^{18}\text{OO}$	78
						$^{13}\text{C}_2\text{CH}_8\text{O}_2$	78	$^{13}\text{CC}_2\text{D}_8\text{O}_2$	85	$\text{C}_3\text{H}_8^{18}\text{O}_2$	80	$\text{C}_3\text{H}_8\text{O}_2$	76
						$^{13}\text{C}_3\text{H}_8\text{O}_2$	79	$\text{C}_3\text{D}_8\text{O}_2$	84				

C ₄ H ₆ O ₂	86	C ₄ D ₆ O ₂	92	C ₄ H ₆ ¹⁸ O ₂	90	C ₄ H ₆ O ₂	86	¹³ C ₄ D ₆ O ₂	96	C₄H₆O₂	86	C₄H₆¹⁸O₂	90
						¹³ CC ₃ H ₆ O ₂	87	¹³ C ₃ CD ₆ O ₂	95	C ₄ H ₆ ¹⁸ OO	88	C ₄ H ₆ ¹⁸ OO	88
						¹³C₂C₂H₆O₂	88	¹³C₂C₂D₆O₂	94	C ₄ H ₆ ¹⁸ O ₂	90	C ₄ H ₆ O ₂	86
						¹³ C ₃ CH ₆ O ₂	89	¹³ CC ₃ D ₆ O ₂	93				
						¹³ C ₄ H ₆ O ₂	90	C ₄ D ₆ O ₂	92				
C ₄ H ₈ O ₂	88	C ₄ D ₈ O ₂	96	C ₄ H ₈ ¹⁸ O ₂	92	C ₄ H ₈ O ₂	88	¹³ C ₄ D ₈ O ₂	100	C ₄ H ₈ O ₂	88	C ₄ H ₈ ¹⁸ O ₂	92
						¹³ CC ₃ H ₈ O ₂	89	¹³ C ₃ CD ₈ O ₂	99	C₄H₈¹⁸OO	90	C₄H₈¹⁸OO	90
						¹³ C ₂ C ₂ H ₈ O ₂	90	¹³ C ₂ C ₂ D ₈ O ₂	98	C ₄ H ₈ ¹⁸ O ₂	92	C ₄ H ₈ O ₂	88
						¹³C₃CH₈O₂	91	¹³CC₃D₈O₂	97				
						¹³ C ₄ H ₈ O ₂	92	C ₄ D ₈ O ₂	96				
Products with three oxygen atoms													
C ₃ H ₄ O ₃	88	C ₃ D ₄ O ₃	92	C ₃ H ₄ ¹⁸ O ₃	94	C ₃ H ₄ O ₃	88	¹³ C ₃ D ₄ O ₃	95	C ₃ H ₄ O ₃	88	C ₃ H ₄ ¹⁸ O ₃	94
						¹³CC₂H₄O₃	89	¹³C₂CD₄O₃	94	C₃H₄¹⁸OO₂	90	C₃H₄¹⁸O₂O	92
						¹³ C ₂ CH ₄ O ₃	90	¹³ CC ₂ D ₄ O ₃	93	C ₃ H ₄ ¹⁸ O ₂ O	92	C ₃ H ₄ ¹⁸ OO ₂	90
						¹³ C ₃ H ₄ O ₃	91	C ₃ D ₄ O ₃	92	C ₃ H ₄ ¹⁸ O ₃	94	C ₃ H ₄ O ₃	88
C ₃ H ₆ O ₃	90	C ₃ D ₆ O ₃	96	C ₃ H ₆ ¹⁸ O ₃	96	C ₃ H ₆ O ₃	90	¹³ C ₃ D ₆ O ₃	99	C ₃ H ₆ O ₃	90	C ₃ H ₆ ¹⁸ O ₃	96
						¹³ CC ₂ H ₆ O ₃	91	¹³ C ₂ CD ₆ O ₃	98	C ₃ H ₆ ¹⁸ OO ₂	92	C ₃ H ₆ ¹⁸ O ₂ O	94
						¹³C₂CH₆O₃	92	¹³CC₂D₆O₃	97	C₃H₆¹⁸O₂O	94	C₃H₆¹⁸OO₂	92
						¹³ C ₃ H ₆ O ₃	93	C ₃ D ₆ O ₃	96	C ₃ H ₆ ¹⁸ O ₃	96	C ₃ H ₆ O ₃	90
C ₄ H ₆ O ₃	102	C ₄ D ₆ O ₃	108	C ₄ H ₆ ¹⁸ O ₃	108	C ₄ H ₆ O ₃	102	¹³ C ₄ D ₆ O ₃	112	C ₄ H ₆ O ₃	102	C ₄ H ₆ ¹⁸ O ₃	108
						¹³ CC ₃ H ₆ O ₃	103	¹³ C ₃ CD ₆ O ₃	111	C₄H₆¹⁸OO₂	104	C₄H₆¹⁸O₂O	106
						¹³C₂C₂H₆O₃	104	¹³C₂C₂D₆O₃	110	C ₄ H ₆ ¹⁸ O ₂ O	106	C ₄ H ₆ ¹⁸ OO ₂	104
						¹³ C ₃ CH ₆ O ₃	105	¹³ CC ₃ D ₆ O ₃	109	C ₄ H ₆ ¹⁸ O ₃	108	C ₄ H ₆ O ₃	102
						¹³ C ₄ H ₆ O ₃	106	C ₄ D ₆ O ₃	108				
C ₄ H ₈ O ₃	104	C ₄ D ₈ O ₃	112	C ₄ H ₈ ¹⁸ O ₃	110	C ₄ H ₈ O ₃	104	¹³ C ₄ D ₈ O ₃	116	C ₄ H ₈ O ₃	104	C ₄ H ₈ ¹⁸ O ₃	110
						¹³ CC ₃ H ₈ O ₃	105	¹³ C ₃ CD ₈ O ₃	115	C ₄ H ₈ ¹⁸ OO ₂	106	C ₄ H ₈ ¹⁸ O ₂ O	108
						¹³ C ₂ C ₂ H ₈ O ₃	106	¹³ C ₂ C ₂ D ₈ O ₃	114	C₄H₈¹⁸O₂O	108	C₄H₈¹⁸OO₂	106
						¹³C₃CH₈O₃	107	¹³CC₃D₈O₃	113	C ₄ H ₈ ¹⁸ O ₃	110	C ₄ H ₈ O ₃	104
						¹³ C ₄ H ₈ O ₃	108	C ₄ D ₈ O ₃	112				
Products with four oxygen atoms													
C ₄ H ₄ O ₄	116	C ₄ D ₄ O ₄	120	C ₄ H ₄ ¹⁸ O ₄	124	C ₄ H ₄ O ₄	116	¹³ C ₄ D ₄ O ₄	124	C ₄ H ₄ O ₄	116	C ₄ H ₄ ¹⁸ O ₄	124
						¹³CC₃H₄O₄	117	¹³C₃CD₄O₄	123	C₄H₄¹⁸OO₃	118	C₄H₄¹⁸O₃O	122

				$^{13}\text{C}_2\text{C}_2\text{H}_4\text{O}_4$	118	$^{13}\text{C}_2\text{C}_2\text{D}_4\text{O}_4$	122	$\text{C}_4\text{H}_4^{18}\text{O}_2\text{O}_2$	120	$\text{C}_4\text{H}_4^{18}\text{O}_2\text{O}_2$	120
				$^{13}\text{C}_3\text{CH}_4\text{O}_4$	119	$^{13}\text{CC}_3\text{D}_4\text{O}_4$	121	$\text{C}_4\text{H}_4^{18}\text{O}_3\text{O}$	122	$\text{C}_4\text{H}_4^{18}\text{OO}_3$	118
				$^{13}\text{C}_4\text{H}_4\text{O}_4$	122	$\text{C}_4\text{D}_4\text{O}_4$	120	$\text{C}_4\text{H}_4^{18}\text{O}_4$	124	$\text{C}_4\text{H}_4\text{O}_4$	116
$\text{C}_4\text{H}_6\text{O}_4$	118	$\text{C}_4\text{D}_6\text{O}_4$	124	$\text{C}_4\text{H}_6^{18}\text{O}_4$	126	$\text{C}_4\text{H}_6\text{O}_4$	118	$^{13}\text{C}_4\text{D}_6\text{O}_4$	128	$\text{C}_4\text{H}_6\text{O}_4$	118
				$^{13}\text{CC}_3\text{H}_6\text{O}_4$	119	$^{13}\text{C}_3\text{CD}_6\text{O}_4$	127	$\text{C}_4\text{H}_6^{18}\text{OO}_3$	120	$\text{C}_4\text{H}_6^{18}\text{O}_3\text{O}$	124
				$^{13}\text{C}_2\text{C}_2\text{H}_6\text{O}_4$	120	$^{13}\text{C}_2\text{C}_2\text{D}_6\text{O}_4$	126	$\text{C}_4\text{H}_6^{18}\text{O}_2\text{O}_2$	122	$\text{C}_4\text{H}_6^{18}\text{O}_2\text{O}_2$	122
				$^{13}\text{C}_3\text{CH}_6\text{O}_4$	121	$^{13}\text{CC}_3\text{D}_6\text{O}_4$	125	$\text{C}_4\text{H}_6^{18}\text{O}_3\text{O}$	124	$\text{C}_4\text{H}_6^{18}\text{OO}_3$	120
				$^{13}\text{C}_4\text{H}_6\text{O}_4$	122	$\text{C}_4\text{D}_6\text{O}_4$	124	$\text{C}_4\text{H}_6^{18}\text{O}_4$	126	$\text{C}_4\text{H}_6\text{O}_4$	118
$\text{C}_4\text{H}_8\text{O}_4$	120	$\text{C}_4\text{D}_8\text{O}_4$	128	$\text{C}_4\text{H}_8^{18}\text{O}_4$	128	$\text{C}_4\text{H}_8\text{O}_4$	120	$^{13}\text{C}_4\text{D}_8\text{O}_4$	132	$\text{C}_4\text{H}_8^{18}\text{O}_4$	128
				$^{13}\text{CC}_3\text{H}_8\text{O}_4$	121	$^{13}\text{C}_3\text{CD}_8\text{O}_4$	131	$\text{C}_4\text{H}_8^{18}\text{OO}_3$	122	$\text{C}_4\text{H}_8^{18}\text{O}_3\text{O}$	126
				$^{13}\text{C}_2\text{C}_2\text{H}_8\text{O}_4$	122	$^{13}\text{C}_2\text{C}_2\text{D}_8\text{O}_4$	130	$\text{C}_4\text{H}_8^{18}\text{O}_2\text{O}_2$	124	$\text{C}_4\text{H}_8^{18}\text{O}_2\text{O}_2$	124
				$^{13}\text{C}_3\text{CH}_8\text{O}_4$	123	$^{13}\text{CC}_3\text{D}_8\text{O}_4$	129	$\text{C}_4\text{H}_8^{18}\text{O}_3\text{O}$	126	$\text{C}_4\text{H}_8^{18}\text{OO}_3$	122
				$^{13}\text{C}_4\text{H}_8\text{O}_4$	124	$\text{C}_4\text{D}_6\text{O}_8$	128	$\text{C}_4\text{H}_8^{18}\text{O}_4$	128	$\text{C}_4\text{H}_8\text{O}_4$	120
$\text{C}_5\text{H}_6\text{O}_4$	130	$\text{C}_5\text{D}_6\text{O}_4$	136	$\text{C}_5\text{H}_6^{18}\text{O}_4$	138	$\text{C}_5\text{H}_6\text{O}_4$	130	$^{13}\text{C}_5\text{D}_6\text{O}_4$	141	$\text{C}_5\text{H}_6^{18}\text{O}_4$	138
				$^{13}\text{CC}_4\text{H}_6\text{O}_4$	131	$^{13}\text{C}_4\text{CD}_6\text{O}_4$	140	$\text{C}_5\text{H}_6^{18}\text{OO}_3$	132	$\text{C}_5\text{H}_6^{18}\text{O}_3\text{O}$	136
				$^{13}\text{C}_2\text{C}_3\text{H}_6\text{O}_4$	132	$^{13}\text{C}_3\text{C}_2\text{D}_6\text{O}_4$	139	$\text{C}_5\text{H}_6^{18}\text{O}_2\text{O}_2$	134	$\text{C}_5\text{H}_6^{18}\text{O}_2\text{O}_2$	134
				$^{13}\text{C}_3\text{C}_2\text{H}_6\text{O}_4$	133	$^{13}\text{C}_2\text{C}_3\text{D}_6\text{O}_4$	138	$\text{C}_5\text{H}_6^{18}\text{O}_3\text{O}$	136	$\text{C}_5\text{H}_6^{18}\text{OO}_3$	132
				$^{13}\text{C}_4\text{CH}_6\text{O}_4$	134	$^{13}\text{CC}_4\text{D}_6\text{O}_4$	137	$\text{C}_5\text{H}_6^{18}\text{O}_4$	138	$\text{C}_5\text{H}_6\text{O}_4$	130
				$^{13}\text{C}_5\text{H}_6\text{O}_4$	135	$\text{C}_5\text{D}_6\text{O}_4$	136				
$\text{C}_5\text{H}_8\text{O}_4$	132	$\text{C}_5\text{D}_8\text{O}_4$	140	$\text{C}_5\text{H}_8^{18}\text{O}_4$	140	$\text{C}_5\text{H}_8\text{O}_4$	132	$^{13}\text{C}_5\text{D}_8\text{O}_4$	145	$\text{C}_5\text{H}_8^{18}\text{O}_4$	140
				$^{13}\text{CC}_4\text{H}_8\text{O}_4$	133	$^{13}\text{C}_4\text{CD}_8\text{O}_4$	144	$\text{C}_5\text{H}_8^{18}\text{OO}_3$	134	$\text{C}_5\text{H}_8^{18}\text{O}_3\text{O}$	138
				$^{13}\text{C}_2\text{C}_3\text{H}_8\text{O}_4$	134	$^{13}\text{C}_3\text{C}_2\text{D}_8\text{O}_4$	143	$\text{C}_5\text{H}_8^{18}\text{O}_2\text{O}_2$	136	$\text{C}_5\text{H}_8^{18}\text{O}_2\text{O}_2$	136
				$^{13}\text{C}_3\text{C}_2\text{H}_8\text{O}_4$	135	$^{13}\text{C}_2\text{C}_3\text{D}_8\text{O}_4$	142	$\text{C}_5\text{H}_8^{18}\text{O}_3\text{O}$	138	$\text{C}_5\text{H}_8^{18}\text{OO}_3$	134
				$^{13}\text{C}_4\text{CH}_8\text{O}_4$	136	$^{13}\text{CC}_4\text{D}_8\text{O}_4$	141	$\text{C}_5\text{H}_8^{18}\text{O}_4$	140	$\text{C}_5\text{H}_8\text{O}_4$	132
				$^{13}\text{C}_5\text{H}_8\text{O}_4$	137	$\text{C}_5\text{D}_8\text{O}_4$	140				
Products with five oxygen atoms											
$\text{C}_5\text{H}_6\text{O}_5$	146	$\text{C}_5\text{D}_6\text{O}_5$	152	$\text{C}_5\text{H}_6^{18}\text{O}_5$	156	$\text{C}_5\text{H}_6\text{O}_5$	146	$^{13}\text{C}_5\text{D}_6\text{O}_5$	157	$\text{C}_5\text{H}_6^{18}\text{O}_5$	156
				$^{13}\text{CC}_4\text{H}_6\text{O}_5$	147	$^{13}\text{C}_4\text{CD}_6\text{O}_5$	156	$\text{C}_5\text{H}_6^{18}\text{OO}_4$	148	$\text{C}_5\text{H}_6^{18}\text{O}_4\text{O}$	154
				$^{13}\text{C}_2\text{C}_3\text{H}_6\text{O}_5$	148	$^{13}\text{C}_3\text{C}_2\text{D}_6\text{O}_5$	155	$\text{C}_5\text{H}_6^{18}\text{O}_2\text{O}_3$	150	$\text{C}_5\text{H}_6^{18}\text{O}_3\text{O}_2$	152
				$^{13}\text{C}_3\text{C}_2\text{H}_6\text{O}_5$	149	$^{13}\text{C}_2\text{C}_3\text{D}_6\text{O}_5$	154	$\text{C}_5\text{H}_6^{18}\text{O}_3\text{O}_2$	152	$\text{C}_5\text{H}_6^{18}\text{O}_2\text{O}_3$	150
				$^{13}\text{C}_4\text{CH}_6\text{O}_5$	150	$^{13}\text{CC}_4\text{D}_6\text{O}_5$	153	$\text{C}_5\text{H}_6^{18}\text{O}_4\text{O}$	154	$\text{C}_5\text{H}_6^{18}\text{OO}_4$	148
				$^{13}\text{C}_5\text{H}_6\text{O}_5$	151	$\text{C}_5\text{D}_6\text{O}_5$	152	$\text{C}_5\text{H}_6^{18}\text{O}_5$	156	$\text{C}_5\text{H}_6\text{O}_5$	146
$\text{C}_5\text{H}_8\text{O}_5$	148	$\text{C}_5\text{D}_8\text{O}_5$	156	$\text{C}_5\text{H}_8^{18}\text{O}_5$	158	$\text{C}_5\text{H}_8\text{O}_5$	148	$^{13}\text{C}_5\text{D}_8\text{O}_5$	161	$\text{C}_5\text{H}_8^{18}\text{O}_5$	158

$^{13}\text{C}_4\text{H}_8\text{O}_5$	149	$^{13}\text{C}_4\text{CD}_8\text{O}_5$	160	$\text{C}_5\text{H}_8^{18}\text{OO}_4$	150	$\text{C}_5\text{H}_8^{18}\text{O}_4\text{O}$	156
$^{13}\text{C}_2\text{C}_3\text{H}_8\text{O}_5$	150	$^{13}\text{C}_3\text{C}_2\text{D}_8\text{O}_5$	159	$\text{C}_5\text{H}_8^{18}\text{O}_2\text{O}_3$	152	$\text{C}_5\text{H}_8^{18}\text{O}_3\text{O}_2$	154
$^{13}\text{C}_3\text{C}_2\text{H}_8\text{O}_5$	151	$^{13}\text{C}_2\text{C}_3\text{D}_8\text{O}_5$	158	$\text{C}_5\text{H}_8^{18}\text{O}_3\text{O}_2$	154	$\text{C}_5\text{H}_8^{18}\text{O}_2\text{O}_3$	152
$^{13}\text{C}_4\text{CH}_8\text{O}_5$	152	$^{13}\text{CC}_4\text{D}_8\text{O}_5$	157	$\text{C}_5\text{H}_8^{18}\text{O}_4\text{O}$	156	$\text{C}_5\text{H}_8^{18}\text{OO}_4$	150
$^{13}\text{C}_5\text{H}_8\text{O}_5$	153	$\text{C}_5\text{D}_8\text{O}_5$	156	$\text{C}_5\text{H}_8^{18}\text{O}_5$	158	$\text{C}_5\text{H}_8\text{O}_5$	148

Table 5. List isotopomers of the products C₂H₂O, C₂H₄O and C₂H₆O together with their mass-to-charge ratios formulated via (i) "2 CH₃OH" (ii) "1 CH₃OH + 1 CO" and (iii) "2 CO" pathways in mixed isotopic ices of ¹³CH₃OH-CO, CD₃OD-¹³CO, CH₃¹⁸OH-CO and CH₃OH-C¹⁸O ices. The mass-to-charge ratios shown in bold for CD₃OD-¹³CO ice depict distinctiveness.

Ices	"2 CH ₃ OH"		"1 CH ₃ OH + 1 CO"		"2 CO"	
	Formula	m/z (amu)	Formula	m/z (amu)	Formula	m/z (amu)
C ₂ H ₂ O						
¹³ CH ₃ OH-CO	H ₂ ¹³ C ¹³ CO	44	H ₂ ¹³ CCO	43	H ₂ CCO	42
CD₃OD-¹³CO	D₂CCO	44	D₂C¹³CO	45	D₂¹³C¹³CO	46
CH ₃ ¹⁸ OH-CO	H ₂ CC ¹⁸ O	44	H ₂ CCO	42	H ₂ CCO	42
CH ₃ OH-C ¹⁸ O	H ₂ CCO	42	H ₂ CC ¹⁸ O	44	H ₂ CC ¹⁸ O	44
C ₂ H ₄ O						
¹³ CH ₃ OH-CO	¹³ CH ₃ ¹³ CHO	46	¹³ CH ₃ CHO	45	CH ₃ CHO	44
CD₃OD-¹³CO	CD₃CDO	48	CD₃¹³CDO	49	¹³CD₃¹³CDO	50
CH ₃ ¹⁸ OH-CO	CH ₃ CH ¹⁸ O	46	CH ₃ CHO	44	CH ₃ CHO	44
CH ₃ OH-C ¹⁸ O	CH ₃ CHO	44	CH ₃ CH ¹⁸ O	46	CH ₃ CH ¹⁸ O	46
C ₂ H ₆ O						
¹³ CH ₃ OH-CO	¹³ C ₂ H ₅ OH	48	¹³ CCH ₅ OH	47	C ₂ H ₅ OH	46
CD₃OD-¹³CO	C₂D₅OD	52	C¹³CD₅OD	53	¹³C₂D₅OD	54
CH ₃ ¹⁸ OH-CO	C ₂ H ₅ ¹⁸ OH	48	C ₂ H ₅ OH	46	C ₂ H ₅ OH	46

$\text{CH}_3\text{OH-C}^{18}\text{O}$	$\text{C}_2\text{H}_5\text{OH}$	46	$\text{C}_2\text{H}_5^{18}\text{OH}$	48	$\text{C}_2\text{H}_5^{18}\text{OH}$	48
---------------------------------------	---------------------------------	----	--------------------------------------	----	--------------------------------------	----